



HORIZON 2020

HORIZON 2020 RESEARCH AND INNOVATION FRAMEWORK PROGRAMME OF THE EUROPEAN ATOMIC ENERGY COMMUNITY

Nuclear Fission and Radiation Protection 2018 (NFRP-2018-4)

Project acronym: **SANDA**

Project full title: **Solving Challenges in Nuclear Data for the Safety of European Nuclear facilities**

Grant Agreement no.: **H2020 Grant Agreement number: 847552**

Workpackage N°: **WP4**

Identification N°: **D4.5**

Type of document: **Deliverable**

Title: **REPORT ON THE PROCESSING AND SENSITIVITY ANALYSIS**

Dissemination Level: **PU**

Reference:

Status: **VERSION 1**

Comments:

	Name	Partner	Date	Signature
Prepared by:	O. Cabellos	UPM	June 26, 2023	
WP leader:	D. A. Rochman	PSI		
IP Co-ordinator:	E. González	CIEMAT		

SANDA Project D4.5: Report on the processing and sensitivity analysis

O. Cabellos¹, V. Bécares², M. Estienne³, M. Fallot³, L. Giot³, A. Laureau³

¹Universidad Politécnica de Madrid (UPM), José Gutiérrez Abascal, 2, 28006 Madrid (Spain)

²CIEMAT, Avenida Complutense, 40, 28040 Madrid (Spain)

³CNRS/Subatech, 4 rue Alfred Kastler, 44307 Nantes (France)

Contact: oscar.cabellos@upm.es, Tel: +34 910 67 71 21

Contents

1.	Introduction.....	2
2.	Processing, verification and Benchmarking of nuclear data libraries.....	3
2.1.	Processing with FRENDY code and criticality Benchmarking using MCNP.....	3
2.2.	Processing with NJOY2016 code.....	10
2.2.1.	Benchmarking with criticality using MCNP.....	10
2.2.2.	Benchmarking with PU-SOL-THERM-034 case.....	17
2.2.3.	Benchmarking with reaction rates in critical systems using MCNP.....	19
2.3.	Benchmarking at room and elevated temperatures: KRITZ Benchmarks.....	23
2.3.1.	KRITZ 1-3.....	23
2.3.2.	KRITZ-4.....	25
2.4.	Processing with AMPX code.....	28
2.4.1.	Processing JEFF-3.3 neutron data library with AMPX code.....	30
2.4.2.	Benchmarking AMPX processing with criticality systems using KENO code.....	31
2.5.	Processing the unresolved resonances with the AMPX and NJOY codes.....	35
2.6.	Review of NJOY code: LRF7 option for reconstruction of angular distributions.....	40
2.7.	Processing covariances.....	41
2.8.	Uncertainty quantification JEFF-3.3 outliers.....	43
3.	Sensitivity analysis and uncertainty propagation.....	45
3.1.	For fission yields on decay heat calculations.....	45
3.2.	Impact of recent TAGS data on reactor antineutrino calculations.....	47
3.3.	For fission yields on reactor antineutrino calculations.....	49
3.4.	For shielding applications on pulsed spheres.....	51
3.5.	For transmission experiments.....	57
3.6.	For burnup calculations.....	61
3.7.	For reaction rates.....	68
3.8.	For criticality Benchmarks: PST34 criticality benchmarks.....	69
4.	Summary and conclusions.....	72
5.	Acknowledgements.....	74
6.	References.....	75
	Appendix 1. Presentations/Contributions related to AMPX Processing.....	79
	Appendix 2. Presentations/Contributions related to Review of Processing Tools.....	80
	Appendix 3. Presentations/Contributions related to Processing and Verification.....	81
	Appendix 4. Presentations/Contributions related to SA and UQ.....	82
	Appendix 5. Presentations/Contributions related to Processing Covariances.....	83

1. Introduction

This Deliverable includes the different steps in the nuclear data pipeline on checking, processing, verification and benchmarking of evaluated nuclear data files.

Nuclear data processing is the procedure devoted to the conversion of evaluated nuclear data into libraries for specific final applications such as neutron transport or inventory calculations. Computational codes are specifically dedicated to nuclear data processing. The Deliverable will focus on the review of processing tools, processing and verification of evaluated nuclear data files and covariances, in different nuclear applications: criticality, shielding, transmission and burnup calculations.

A review of current processing codes used in this work is summarized in the following list:

- FREN DY, (FRom Evaluated Nuclear Data librarY to any application) [**FREN DY, 2017**] is a nuclear data processing system developed by JAEA.
- NJOY [**NJOY, 2016**] which is a comprehensive system for generating application libraries, developed at Los Alamos National Laboratory (LANL).

In 2021, two versions of NJOY were currently managed and distributed:

- NJOY2016 is the legacy Fortran version which is deprecated. Although, it was stated that no active development would be done on NJOY2016 (only bug fixes), currently is the recommended NJOY version by LANL team.
- NJOY21 is a new version—written in C++—and backwards compatible with NJOY2016. NJOY21 is the future of NJOY.

NJOY is freely available under the BSD 3-clause license. Both NJOY2016 and NJOY21 are free to use. NJOY is the most popular processing code within the nuclear data community.

- AMPX [**AMPX, 2016**] is the modular processing code of SCALE Code System that takes basic cross section data in Evaluated Nuclear Data File (ENDF) format to provide both multigroup (MG) or continuous energy (CE) libraries for their use by the neutron transport codes included within SCALE [**SCALE, 2020**].

As a continuation of the work done in CHANDA/FP7 and in consonance with efforts done by OECD-NEA, this Deliverable includes a processing nuclear data route for AMPX in order to process state-of-the-art nuclear data. Best processing parameters will be identified and input decks for processing CE libraries with the AMPX system will be generated.

Additionally, JEFF-3.3 and different beta-versions of JEFF-4.0 are processed and tested using the same criticality validation suite.

The second part of this task will concern the sensitivity calculations and uncertainty propagation based on the processed files.

2. Processing, verification and Benchmarking of nuclear data libraries

2.1. Processing with FRENDY code and criticality Benchmarking using MCNP

FRENDY (FRom Evaluated Nuclear Data librarY to any application) is a nuclear data processing system developed by JAEA. <https://www.oecd-nea.org/tools/abstract/detail/nea-1907/>. FRENDY is released under the BSD license: https://rpg.jaea.go.jp/main/en/program_frendy/

In the framework of JEFF-P&V Working Group, the UPM has performed a comparison between the FRENDY-1.01.007 and NJOY-2016.46 codes for the JEFF-3.3 nuclear data library. As a result of this work, feedback and suggested updates in several JEFF-3.3 evaluations were submitted to the JEFF Coordination Group [JEFF-JENDL, 2019], [JEFFDOC-1987, 2019], [IAEA/TM/Processing, 2019].

An interesting capability of FRENDY is the possibility to use NJOY inputs (see **Figure 1**). This capability may be use for an easy integration of FRENDY in processing pipelines.

```
reconr
 20 21 /
 'pendf ' /
 9228
0.001 0.0 0.01 5.0000000000000004e-08 /
0 /
broadr
 20 21 22 /
 9228 1 0 0 0.0 /
0.001 1000000.0 0.01 5.0000000000000004e-08 /
293.6
0 /
purr
 20 22 25 /
 9228 1 3 16 64 1 /
293.6
1.0E+10 100.0 10.0 /
0 /
acer
 20 25 0 55 56 /
1 1 1 .33 /
'Lib----JEFF-3.3 Process: FRENDY ' /
 9228 293.6 /
1 1 /
/
stop
```

Figure 1. An example of NJOY/FRENDY Input for 235U processing.

An exception is the generation of thermal ACE file using THERMR module.

Figure 2 is an example for the H in H₂O.

- FRENDY uses NJOY99 option in THERMR
- NJOY2012/2016 uses the input “iform” for the output format for inelastic distributions:
 - iform=0; E-mu-E' ordering (MF6 special)
 - iform=1; E-mu-E' ordering (MF6/Law7)

<pre> moder 30 -31 reconr -31 -32 'pendf tape for h-1 from jeff33 '/' 125 1/ 0.001 0.0/ '1-h-1 from jeff33 '/' 0/ broadr -31 -32 -33 125 1 0 0 0.0 / .001/ 293.6 0/ thermr 34 -33 -35 1 125 16 1 2 0 2 222 2 / 293.6 0.001 10.0 / acer -31 -35 0 60 61 2 1 1 .33 / 'H(H2O)-JEFF33 and TSL-JEFF311/' 125 293.6 'lw00 '/' 1001 0 0 / 222 64 0 0 1 10.0 0 / moder -32 70 stop </pre>	<pre> moder 30 -31 reconr -31 -32 'pendf tape for h-1 from jeff33 '/' 125 1/ 0.001 0.0/ '1-h-1 from jeff33 '/' 0/ broadr -31 -32 -33 125 1 0 0 0.0 / .001/ 293.6 0/ thermr 34 -33 -35 1 125 16 1 2 0 2 222 2 / 293.6 0.001 10.0 / acer -31 -35 0 60 61 2 1 1 .33 / 'H(H2O)-JEFF33 and TSL-JEFF311/' 125 293.6 'lw00 '/' 1001 0 0 / 222 64 0 0 1 10.0 0 / moder -32 70 stop </pre>
---	---

Figure 2. An example (H in H₂O) of NJOY and FRENDY processing of thermal ACE files.

The following is a list of Warnings/Errors found in P&V activities using FRENDY code in JEFF-3.3 evaluation:

- <Error Message> ...MF = 1, MT = 1: The order of X data list in Tab1 record is not appropriate (X[i] < X[i-1])<Error Message>

```
[cabellos@nodo0 r_1-H-2g]$ diff 1-H-2g.jeff33 1-H-2g.jeff33.original
133c133
< 1.450000+7 8.024095-1 1.475000+7 7.716093-1 1.500000+7 7.612092-1 128 3 1 31
---
> 1.400000+7 8.024095-1 1.475000+7 7.716093-1 1.500000+7 7.612092-1 128 3 1 31
172c172
< 1.450000+7 6.364000-1 1.475000+7 6.047000-1 1.500000+7 5.941000-1 128 3 2 31
---
> 1.400000+7 6.364000-1 1.475000+7 6.047000-1 1.500000+7 5.941000-1 128 3 2 31
211c211
< 1.450000+7 1.660095-1 1.475000+7 1.669093-1 1.500000+7 1.671092-1 128 3 3 31
---
> 1.400000+7 1.660095-1 1.475000+7 1.669093-1 1.500000+7 1.671092-1 128 3 3 31
238c238
< 1.450000+7 1.660000-1 1.475000+7 1.669000-1 1.500000+7 1.671000-1 128 3 16 19
---
> 1.400000+7 1.660000-1 1.475000+7 1.669000-1 1.500000+7 1.671000-1 128 3 16 19
277c277
< 1.450000+7 9.500000-6 1.475000+7 9.298823-6 1.500000+7 9.235346-6 128 3102 31
---
> 1.400000+7 9.500000-6 1.475000+7 9.298823-6 1.500000+7 9.235346-6 128 3102 31
```

- <Error Message> ...MF = 6, MT = 102: The mass (AWR) is different

```
[cabellos@nodo0 r_26-Fe-54g]$ diff 26-Fe-54g.jeff33 26-Fe-54g.jeff33.original
26192c26192
< 2.605400+4 5.347625+1 0 3 1 02625 6102 1
---
> 2.605600+4 5.545440+1 0 3 1 02625 6102 1
```

- <Error Message> ...MF = 6, MT = 102: The mass (AWR) is different

```
[cabellos@nodo0 r_26-Fe-58g]$ diff 26-Fe-58g.jeff33 26-Fe-58g.jeff33.original
23826c23826
< 2.605800+4 5.743561+1 0 3 1 02637 6102 1
---
> 2.605800+4 6.743560+0 0 3 1 02637 6102 1
```

- <Error Message> ...MF = 1, MT = 91: The order of X data list in Tab1 record is not appropriate (X[i] < X[i-1])

```
[cabellos@nodo0 r_72-Hf-178g]$ diff 72-Hf-178g.jeff33 72-Hf-178g.jeff33.original
1968c1968
< 1.562810+6 0.000000+0 1.600000+6 0.000000+0 1.700000+6 0.000000-07237 3 91 4
---
> 1.562810+6 0.000000+0 1.800000+6 0.000000+0 1.700000+6 0.000000-07237 3 91 4
```

- <Error Message> ...MF = 6, MT = 102: The material data (ZA) is different

```
[cabellos@nodo0 r_64-Gd-155g]$ diff 64-Gd-155g.jeff33 64-Gd-155g.jeff33.original
2544c2544
< 6.415500+4 1.535920+2 0 2 1 06434 6102 1
---
> 6.155500+4 1.535920+2 0 2 1 06434 6102 1
```

- <Error Message> ...MF=01, MT=451 line no is smaller than NWD+NXC+4

```
[cabellos@nodo0 r_95-Am-243g]$ diff 95-Am-243g.jeff33 95-Am-243g.jeff33.original
29c29
< 23/11/2016 P. Leconte on behalf of CEA Reverted MF=1/5, MT=455 9549 1451 28
---
> 23/11/2016 P. Leconte on behalf of CEA Reverted MF=1/5, MT=455 9543 1451 28
```

In close collaboration with FRENDY’s developers, JEFF-3.3 has been processed in ACE format and successfully tested using the NEA (extended Mosteller) benchmark criticality suite consisting of 123 cases (see Tables 1, 2, 3 and 4). In a few cases, differences more than three times the statistical uncertainty were found [JEFD0C-1987, 2019]. Calculations performed with MCNP-6.1 and 5×10^7 histories (statistical uncertainty ≤ 11 pcm)

Table 1. HEU cases.

#	CASE	FRENDY 1.01.007		NJOY 2016.46		Diff. in pcm
		keff	Δ keff-stat	keff	Δ keff-stat	
1	heu-comp-inter-003-case7	1.00294	0.00011	1.00291	0.00011	3
2	heu-met-fast-001	1.00008	0.00008	1.00001	0.00009	7
3	heu-met-fast-003-case10	1.00524	0.00010	1.00493	0.00009	31
4	heu-met-fast-003-case11	1.00996	0.00010	1.00986	0.00009	10
5	heu-met-fast-003-case12	1.00537	0.00009	1.00538	0.00010	-1
6	heu-met-fast-003-case1	0.99574	0.00009	0.99596	0.00009	-22
7	heu-met-fast-003-case2	0.99507	0.00009	0.99528	0.00009	-21
8	heu-met-fast-003-case3	0.99999	0.00009	0.99998	0.00009	1
9	heu-met-fast-003-case4	0.99826	0.00009	0.99835	0.00009	-9
10	heu-met-fast-003-case5	1.00241	0.00009	1.00276	0.00009	-35
11	heu-met-fast-003-case6	1.00300	0.00010	1.00329	0.00009	-29
12	heu-met-fast-003-case7	1.00366	0.00010	1.00389	0.00009	-23
13	heu-met-fast-003-case8	1.00143	0.00009	1.00148	0.00009	-5
14	heu-met-fast-003-case9	1.00160	0.00009	1.00175	0.00009	-15
15	heu-met-fast-004-case1	0.99831	0.00011	0.99831	0.00011	0
16	heu-met-fast-008	0.99577	0.00008	0.99593	0.00009	-16
17	heu-met-fast-009-case1	0.99625	0.00009	0.99623	0.00009	2
18	heu-met-fast-009-case2	0.99499	0.00009	0.99510	0.00009	-11
19	heu-met-fast-011	0.99816	0.00011	0.99808	0.00011	8
20	heu-met-fast-012	0.99823	0.00009	0.99819	0.00008	4
21	heu-met-fast-013	0.99553	0.00009	0.99546	0.00009	7
22	heu-met-fast-014	0.99809	0.00008	0.99818	0.00009	-9
23	heu-met-fast-015	0.99443	0.00008	0.99444	0.00009	-1
24	heu-met-fast-018-case2	0.99997	0.00008	0.99981	0.00008	16
25	heu-met-fast-019-case2	1.00650	0.00009	1.00653	0.00009	-3
26	heu-met-fast-020-case2	1.00086	0.00010	1.00071	0.00010	15
27	heu-met-fast-021-case2	0.99651	0.00009	0.99659	0.00009	-8
28	heu-met-fast-022-case2	0.99727	0.00009	0.99724	0.00008	3
29	heu-met-fast-026-case9	0.98996	0.00010	0.98985	0.00010	11
30	heu-met-fast-028	1.00418	0.00009	1.00421	0.00009	-3
31	heu-met-fast-73	1.00727	0.00009	1.00713	0.00009	14
32	heu-met-inter-006-case1	0.99677	0.00011	0.99654	0.00010	23
33	heu-met-inter-006-case2	0.99855	0.00011	0.99859	0.00011	-4
34	heu-met-inter-006-case3	0.99902	0.00010	0.99891	0.00010	11
35	heu-met-inter-006-case4	1.00140	0.00011	1.00145	0.00011	-5
36	heu-sol-therm-004	0.99406	0.00013	0.99410	0.00012	-4
37	heu-sol-therm-013-case1	0.99802	0.00008	0.99802	0.00008	0
38	heu-sol-therm-013-case2	0.99680	0.00009	0.99711	0.00008	-31
39	heu-sol-therm-013-case3	0.99362	0.00009	0.99368	0.00009	-6
40	heu-sol-therm-013-case4	0.99507	0.00009	0.99503	0.00009	4
41	heu-sol-therm-032	0.99746	0.00005	0.99732	0.00005	14

NOTE: $2*\Delta\sigma_{stat} > \text{Diff. (FRENDY-NJOY)} > 3*\Delta\sigma_{stat}$; $\text{Diff. (FRENDY-NJOY)} > 3*\Delta\sigma_{stat}$

Table 2. IEU-MIX cases.

#	CASE	FRENDY 1.01.007		NJOY 2016.46		Diff. in pcm
		keff	Δ keff-stat	keff	Δ keff-stat	
42	ieu-comp-therm-002-CASE_3	1.00149	0.00010	1.00140	0.00010	9
43	ieu-met-fast-001-case1	1.00016	0.00009	1.00009	0.00009	7
44	ieu-met-fast-001-case2	1.00029	0.00009	1.00024	0.00009	5
45	ieu-met-fast-001-case3	0.99999	0.00009	1.00012	0.00009	-13
46	ieu-met-fast-001-case4	1.00055	0.00009	1.00031	0.00009	24
47	ieu-met-fast-002	0.99628	0.00008	0.99645	0.00008	-17
48	ieu-met-fast-003-case2	1.00123	0.00009	1.00131	0.00009	-8
49	ieu-met-fast-004-case2	1.00550	0.00008	1.00555	0.00009	-5
50	ieu-met-fast-005-case2	0.99981	0.00009	0.99982	0.00009	-1
51	ieu-met-fast-006-case2	0.99387	0.00009	0.99381	0.00009	6
52	ieu-met-fast-007-case1	1.00485	0.00008	1.00507	0.00008	-22
53	ieu-comp-ther-008-CASE_1	1.00246	0.00009	1.00221	0.00010	25
54	ieu-comp-therm-008-CASE_11	1.00251	0.00009	1.00263	0.00009	-12
55	ieu-comp-therm-008-CASE_2	1.00205	0.00010	1.00198	0.00009	7
56	ieu-comp-therm-008-CASE_5	1.00164	0.00009	1.00161	0.00009	3
57	ieu-comp-therm-008-CASE_7	1.00139	0.00009	1.00126	0.00009	13
58	ieu-comp-therm-008-CASE_8	1.00098	0.00010	1.00093	0.00009	5
59	ieu-sol-therm-002-case1	0.99918	0.00008	0.99915	0.00008	3
60	ieu-sol-therm-002-case2	0.99563	0.00009	0.99573	0.00009	-10
61	ieu-sol-therm-007-CASE14	0.99508	0.00010	0.99532	0.00009	-24
62	ieu-sol-therm-007-CASE30	0.99728	0.00010	0.99723	0.00010	5
63	ieu-sol-therm-007-CASE32	0.99567	0.00010	0.99588	0.00009	-21
64	ieu-sol-therm-007-CASE36	0.99822	0.00009	0.99811	0.00009	11
65	ieu-sol-therm-007-CASE49	0.99693	0.00009	0.99694	0.00008	-1
66	mix-comp-therm-002-case-pnl30	1.00082	0.00011	1.00094	0.00010	-12
67	mix-comp-therm-002-case-pnl31	1.00343	0.00011	1.00334	0.00012	9
68	mix-comp-therm-002-case-pnl32	1.00082	0.00011	1.00101	0.00010	-19
69	mix-comp-therm-002-case-pnl33	1.00577	0.00011	1.00586	0.00011	-9
70	mix-comp-therm-002-case-pnl34	1.00134	0.00010	1.00152	0.00011	-18
71	mix-comp-therm-002-case-pnl35	1.00412	0.00010	1.00402	0.00010	10
72	mix-met-fast-001-CASE_1	0.99897	0.00009	0.99889	0.00008	8
73	mix-met-fast-003	1.00014	0.00009	1.00055	0.00008	-41
74	mix-met-fast-008-case7	1.02625	0.00006	1.02618	0.00005	7

NOTE: $2*\Delta\sigma_{stat} > \text{Diff. (FRENDY-NJOY)} > 3*\Delta\sigma_{stat}$; $\text{Diff. (FRENDY-NJOY)} > 3*\Delta\sigma_{stat}$

Table 3. PU cases.

#	CASE	FRENDY 1.01.007		NJOY 2016.46		Diff. in pcm
		keff	Δ keff-stat	keff	Δ keff-stat	
75	pu-comp-inter-001	0.99833	0.00008	0.99833	0.00007	0
76	pu-met-fast-001-CASE_1	0.99925	0.00008	0.99929	0.00008	-4
77	pu-met-fast-002-CASE_1	1.00148	0.00008	1.00117	0.00009	31
78	pu-met-fast-003-case103	0.99672	0.00009	0.99671	0.00010	1
79	pu-met-fast-005-CASE_1	1.00132	0.00009	1.00129	0.00010	3
80	pu-met-fast-006	1.00322	0.00010	1.00341	0.00010	-19
81	pu-met-fast-008-case2	0.99656	0.00009	0.99655	0.00009	1
82	pu-met-fast-009-CASE_1	0.99882	0.00009	0.99894	0.00009	-12
83	pu-met-fast-010-CASE_1	1.00039	0.00009	1.00037	0.00009	2
84	pu-met-fast-011-CASE_1	0.99984	0.00011	0.99982	0.00011	2
85	pu-met-fast-018-CASE_1	0.99820	0.00009	0.99833	0.00009	-13
86	pu-met-fast-019	1.00008	0.00009	1.00022	0.00009	-14
87	pu-met-fast-020	0.99924	0.00009	0.99921	0.00009	3
88	pu-met-fast-021-case1	1.00415	0.00009	1.00401	0.00009	14
89	pu-met-fast-021-case2	0.99318	0.00009	0.99291	0.00010	27
90	pu-met-fast-022	0.99782	0.00008	0.9979	0.00008	-8
91	pu-met-fast-023	0.99917	0.00009	0.99926	0.00008	-9
92	pu-met-fast-024	1.00145	0.00009	1.00164	0.00010	-19
93	pu-met-fast-025	0.99671	0.00009	0.99667	0.00009	4
94	pu-met-fast-026	0.99853	0.00009	0.99848	0.00009	5
95	pu-sol-therm-009-case3a	1.01367	0.00006	1.01397	0.00005	-30
96	pu-sol-therm-009	1.00999	0.00006	1.00999	0.00006	0
97	pu-sol-therm-011-CASE_1.18	0.99059	0.00012	0.99066	0.00011	-7
98	pu-sol-therm-011-CASE_5.16	1.00240	0.00013	1.00236	0.00013	4
99	pu-sol-therm-011-CASE_6.18	0.99625	0.00012	0.99649	0.00012	-24
100	pu-sol-therm-018-case_9	1.00026	0.00010	1.00057	0.00010	-31
101	pu-sol-therm-021-case_1.t9a	1.00146	0.00013	1.00163	0.00012	-17
102	pu-sol-therm-021-CASE_3.T9A	1.00241	0.00015	1.00231	0.00014	10
103	pu-sol-therm-034-case_01	0.99576	0.00013	0.99595	0.00013	-19

NOTE: $2 * \Delta\sigma_{stat} > \text{Diff. (FRENDY-NJOY)} > 3 * \Delta\sigma_{stat}$; $\text{Diff. (FRENDY-NJOY)} > 3 * \Delta\sigma_{stat}$

Table 4. SPEC and U233 cases.

#	CASE	FRENDY 1.01.007		NJOY 2016.46		Diff. in pcm
		keff	Δ keff-stat	keff	Δ keff-stat	
104	spec-met-fast-008	0.99422	0.00008	0.99431	0.00008	-9
105	u233-comp-therm-001-case3	1.00365	0.00015	1.00342	0.00015	23
106	u233-comp-therm-001-case6	1.00379	0.00012	1.00386	0.00013	-7
107	u233-met-fast-001	1.00099	0.00008	1.00102	0.00008	-3
108	u233-met-fast-002-CASE_1	0.99982	0.00008	0.99992	0.00008	-10
109	u233-met-fast-002-CASE_2	1.00137	0.00009	1.00123	0.00008	14
110	u233-met-fast-003-CASE_1	1.00085	0.00008	1.00078	0.00009	7
111	u233-met-fast-003-CASE_2	1.00097	0.00009	1.00091	0.00009	6
112	u233-met-fast-004-CASE_1	1.00024	0.00009	1.00018	0.00009	6
113	u233-met-fast-004-CASE_2	0.99834	0.00009	0.99821	0.00009	13
114	u233-met-fast-005-CASE_1	0.99733	0.00009	0.99721	0.00009	12
115	u233-met-fast-005-CASE_2	0.99631	0.00010	0.99634	0.00009	-3
116	u233-met-fast-006	1.00330	0.00010	1.00333	0.00010	-3
117	u233-sol-inter-001-case1	0.98527	0.00016	0.98513	0.00015	14
118	u233-sol-therm-001-case1	1.00232	0.00008	1.00254	0.00008	-22
119	u233-sol-therm-001-case2	1.00216	0.00008	1.00229	0.00008	-13
120	u233-sol-therm-001-case3	1.00182	0.00008	1.00181	0.00008	1
121	u233-sol-therm-001-case4	1.00179	0.00008	1.00184	0.00008	-5
122	u233-sol-therm-001-case5	1.00113	0.00009	1.00122	0.00009	-9
123	u233-sol-therm-008	1.00199	0.00006	1.00212	0.00005	-13

NOTE: $2 * \Delta\sigma_{stat} > \text{Diff. (FRENDY-NJOY)} > 3 * \Delta\sigma_{stat}$; $\text{Diff. (FRENDY-NJOY)} > 3 * \Delta\sigma_{stat}$

2.2. Processing with NJOY2016 code

UPM has been collaborating with NEA/Data Bank and helping JEFF evaluators [JEF-CG/Nov. 2020], [JEF/DOC-2041] processing with NJOY2016.57 the new evaluation JEFF-4.0T0. The last contribution to JEFF project is the processing and benchmarking of the beta release named as JEFF-4.0T2.2 [JEF/DOC-2224], [JEF/DOC-2239].

2.2.1. Benchmarking with criticality using MCNP

Table 5 shows the performance of JEFF-3.3, JEFF-4.0T0 and JEFF-4.0T2.2 nuclear data evaluations with the Extended (123) Criticality Mosteller's suite.

Table 5. *Reduced-chi squared values in the Extended (123) Criticality Mosteller's suite*

	JEFF-3.3	JEFF-4.0T0	JEFF-4.0T2,2
PU	3.05	3.13	4.15
HEU	2.64	6.76	9.08
IEU	3.33	4.29	2.75
LEU	2.14	2.60	2.79
U233	1.55	2.35	2.37
MIX	0.91	0.88	0.70
SPEC (C/E) DEXP=0.00340	0.99173	0.99479	.99408
ALL	2.25	3.80	6.74

As an example, several issues were identified in this work for the JEFF-4.0T0 and reported to JEFF/CG:

- W evaluation by KIT: potential problems PMF5-001 and UMF4-001 due to inelastic cross-section (see **Figure 3**)
- Ni evaluation by TENDL2019: potential problems in HMF3-012 due to elastic and inelastic cross.sections (see **Figure 4**)
- Rh-103: potential issue in LMCT5-009 due to (n, gamma)
- Increase reactivity in LCTs (see **Figure 5**)

A summary of additional results for JEFF-4.0T0 are presented in the following DICE plots:

- PU-INTER (**Figure 6**), PU-THERM (**Figure 7**)
- HEU-INTER (**Figure 8**), HEU-THERM (**Figure 9**)
- IEU-FAST (**Figure 10**), IEU-THERM (**Figure 11**)
- U233-FAST (**Figure 12**), U233-INTER (**Figure 13**), U233-THERM (**Figure 14**)

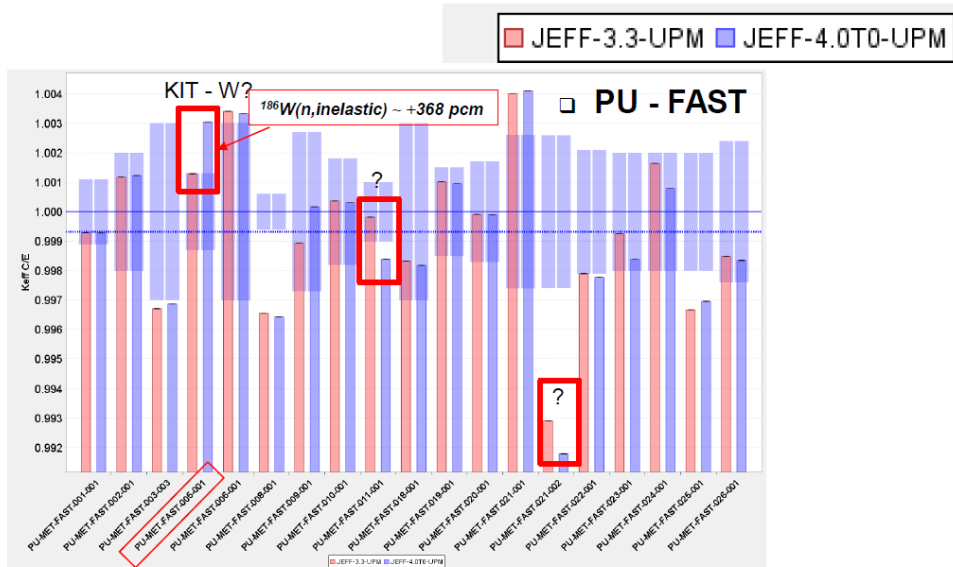


Figure 3. Comparison JEFF-3.3 and JEFF-4.0/T0 in PU cases

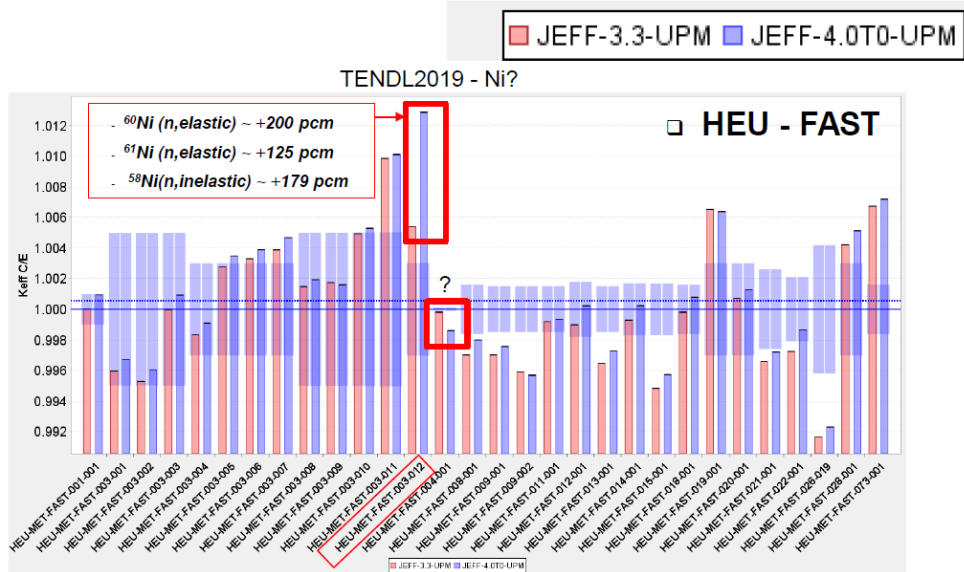


Figure 4. Comparison JEFF-3.3 and JEFF-4.0/T0 in HEU cases

JEFF-3.3-UPM JEFF-4.0T0-UPM

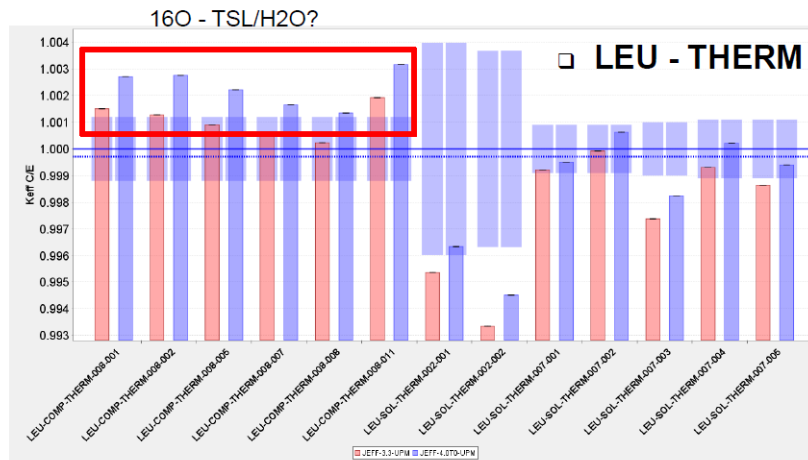


Figure 5. Comparison JEFF-3.3 and JEFF-4.0/T0 in LEU cases

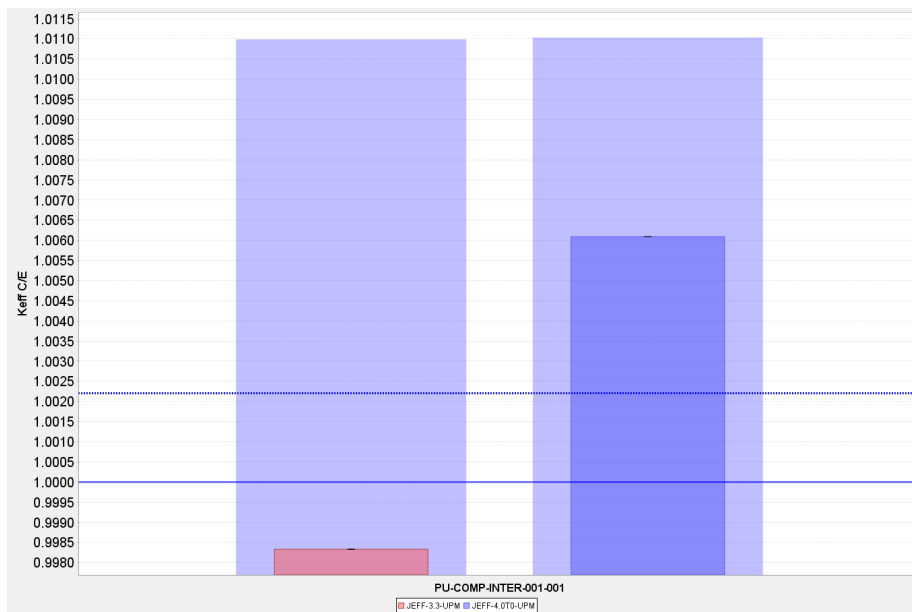


Figure 6. k_{eff} (C/E-1) values in PU-INTER Benchmarks within 123-Mosteller's suite

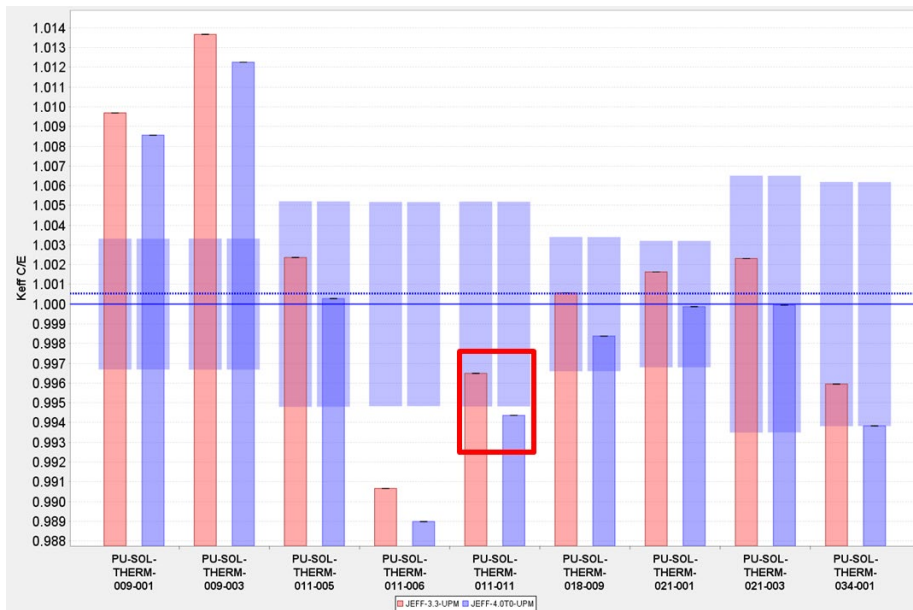


Figure 7. k_{eff} (C/E-1) values in PU-THERM Benchmarks within 123-Mosteller's suite

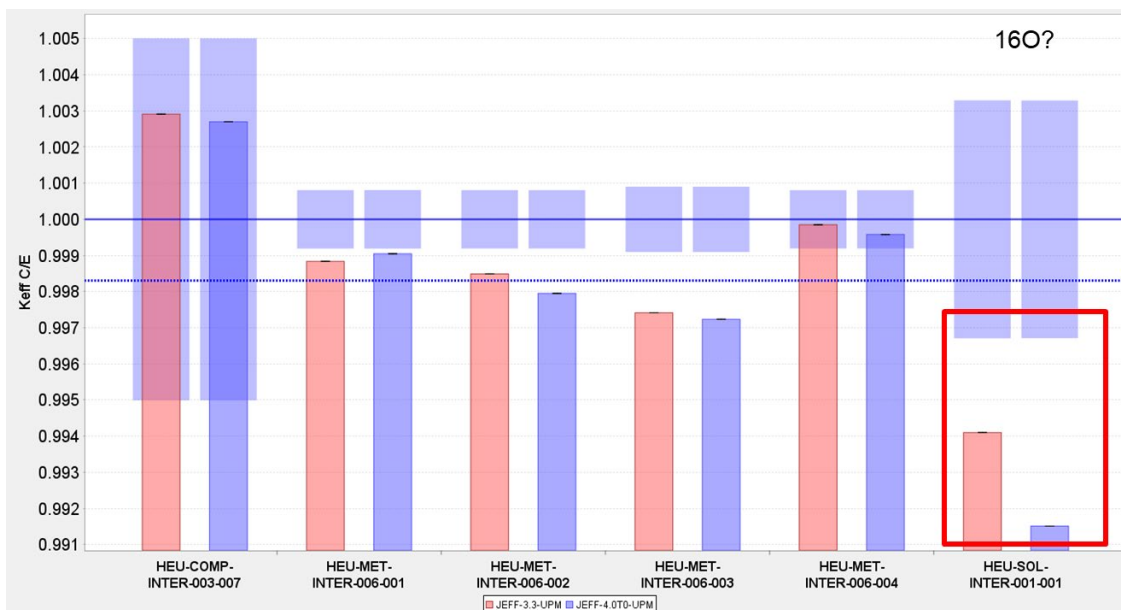


Figure 8. k_{eff} (C/E-1) values in HEU-INTER Benchmarks within 123-Mosteller's suite

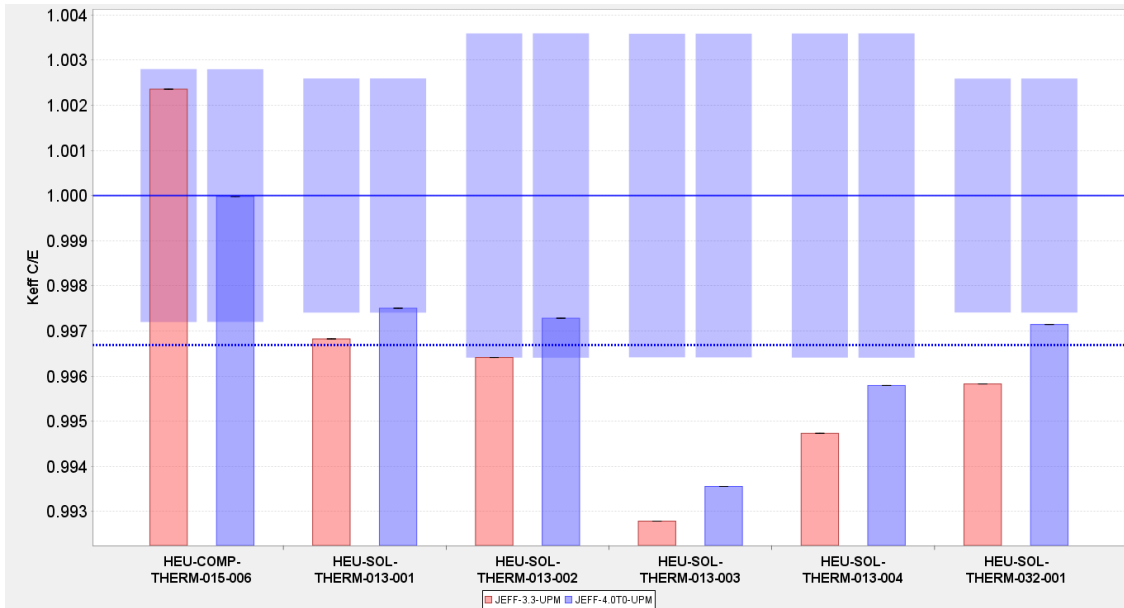


Figure 9. k_{eff} ($C/E-1$) values in HEU-THERM Benchmarks within 123-Mosteller's suite

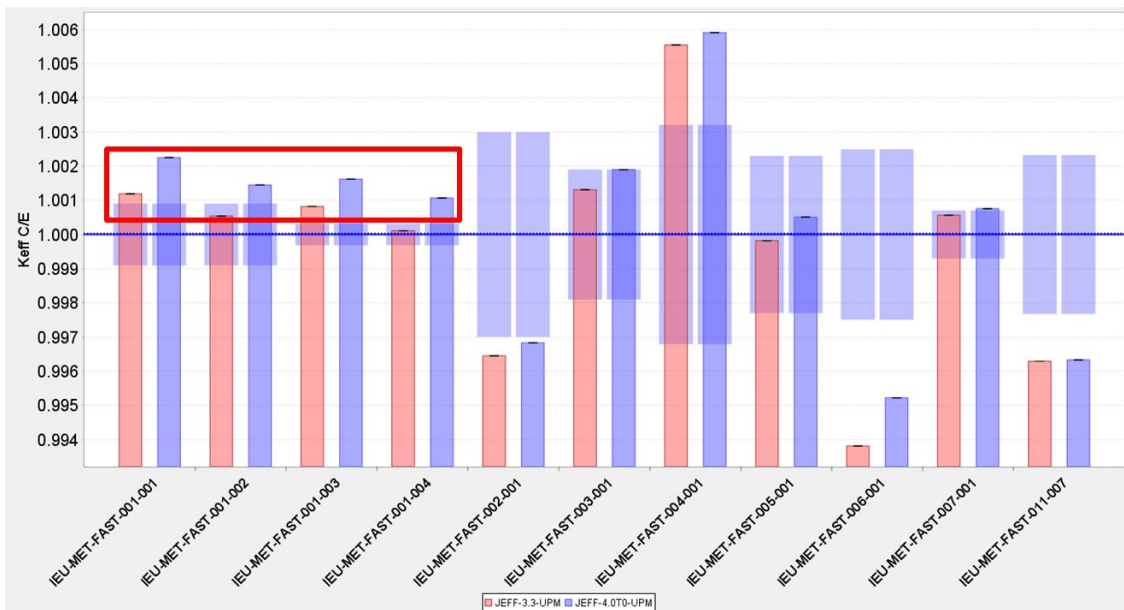


Figure 10. k_{eff} ($C/E-1$) values in IEU-FAST Benchmarks within 123-Mosteller's suite

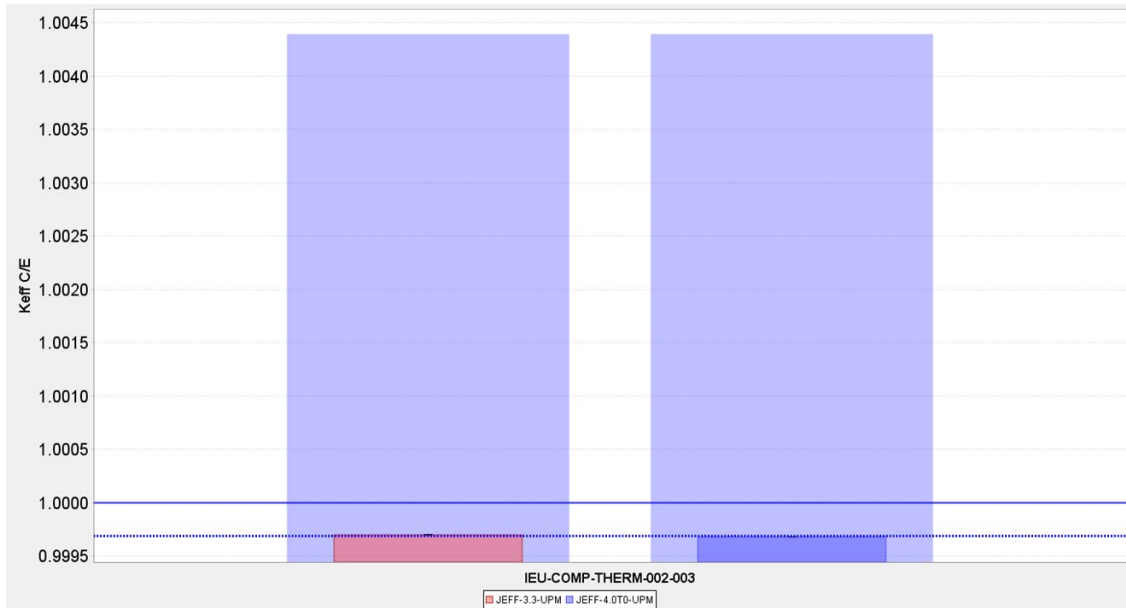


Figure 11. k_{eff} (C/E-1) values in IEU-THERM Benchmarks within 123-Mosteller's suite

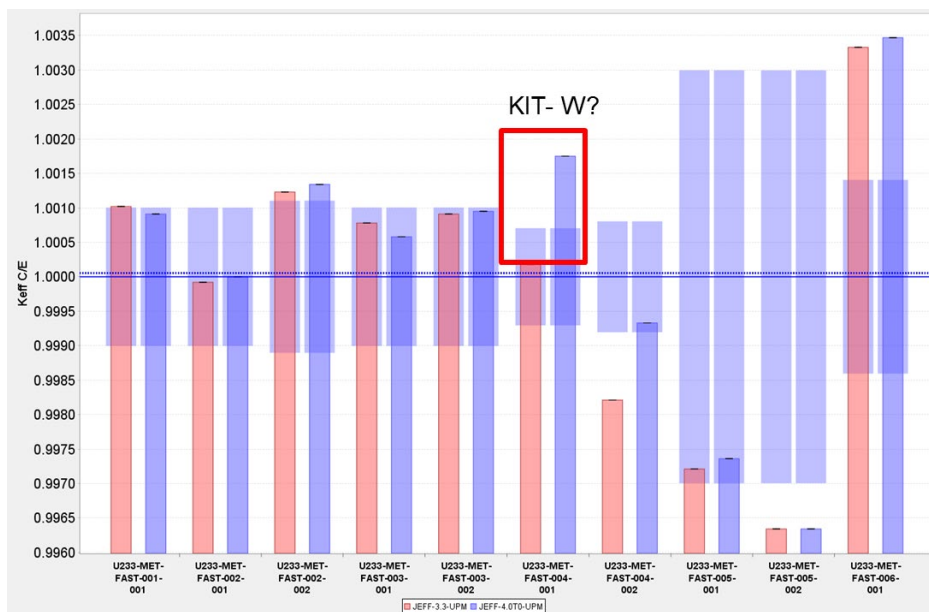


Figure 12. k_{eff} (C/E-1) values in U233-FAST Benchmarks within 123-Mosteller's suite

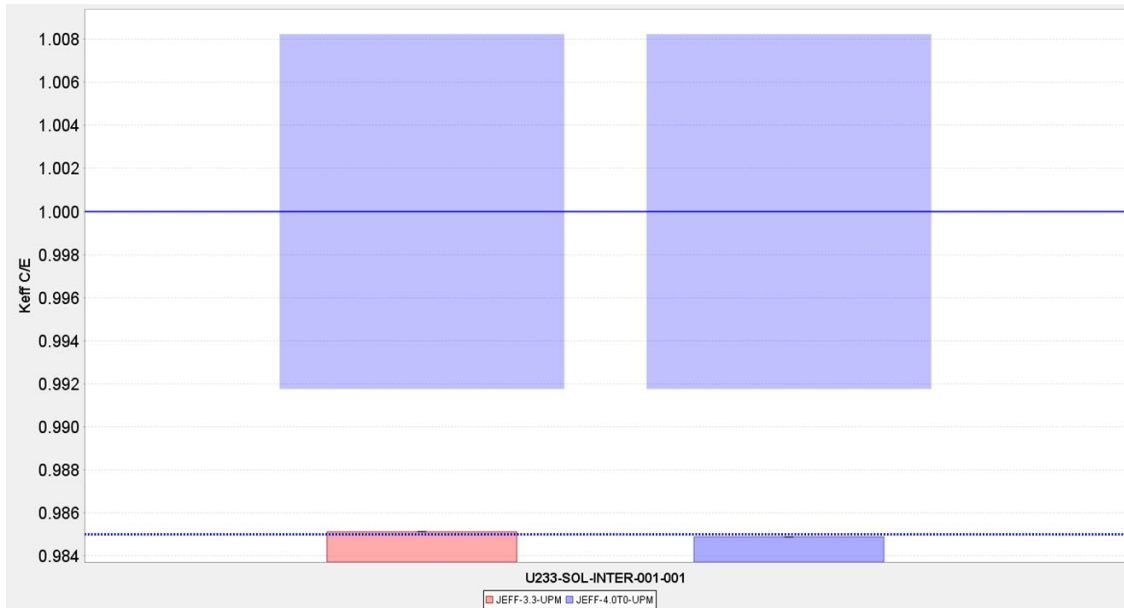


Figure 13. *keff (C/E-1) values in U233-INTER Benchmarks within 123-Mosteller's suite*

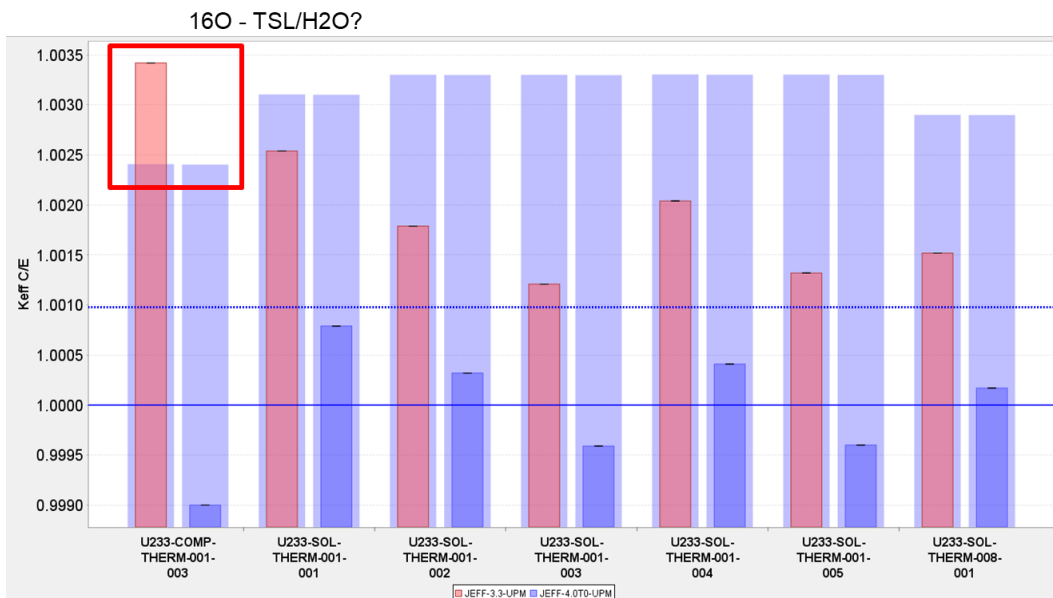


Figure 14. *keff (C/E-1) values in U233-THERM Benchmarks within 123-Mosteller's suite*

Additionally, several issues were identified in this work for the JEFF-4.0T2.2 and reported to JEFF/CG in April 2023 [JEF/DOC-2239]:

- Pu239 in PSTs
- W in PMF5-1
- Ni58 in HMF3-12
- Cu63 in HMI6
- O16 in HIS-1
- U235 in LSTs
- U233 in USTs and UMFs

2.2.2. Benchmarking with PU-SOL-THERM-034 case

In this section, we study the PU-SOL-THERM-034 benchmarks, that is, 15 cases consisting of a plutonium nitrate solution with gadolinium in a water-reflected cylinder with a 24-inch diameter compiled as a part of the International Criticality Safety Benchmark. **Figure 15** shows the 361 PST benchmarks used in the Steven Van der Marck (NRG)' suite published in the [Plompen, 2020]. The PST34 set is highlighted in the **Figure 16**. The unique PST34 case in the 123-Mosteller's suite is PST34-001 [JEFDOC-2015].

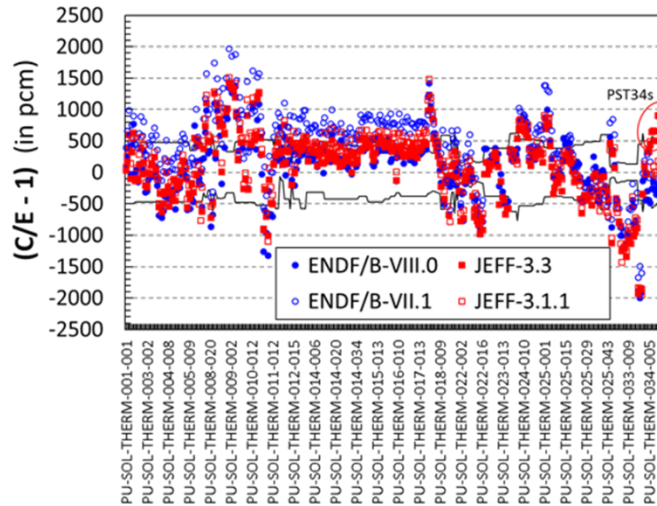


Figure 15. $(C/E-1)$ values in pcm for PU-SOL-THERM benchmarks (361)¹

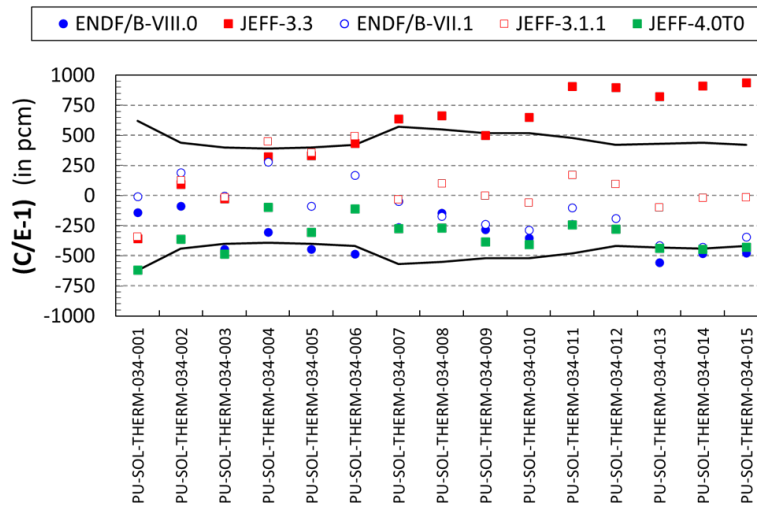


Figure 16. $(C/E-1)$ values in pcm for PU-SOL-THERM 034 benchmarks (15)

To identify the differences in keff results between JEFF-3.3 and ENDF/B-VIII.0 a sensitivity analysis is performed with NDaST. Results are shown in **Table 6**. Thus, we conclude that the most important contributors to the difference are: 239Pu, 160 and TSL-H2O.

¹ NOTE: keff-values... by courtesy of Steven van der Marck

Table 6. Differences between base library (JEFF-3.3) and updated with ENDF/B-VIII.0 isotopes. Calculations with MCNP6.1.

PST Benchmarks	Pu239	O16	TSL-H2O	Pu240	Cr52	Fe56	Gd157	Gd155	...	All E80 isotopes
PST-034-001	61	-176	227	-25	-13	46	0	0		80
PST-034-002	5	-145	-10	6	-2	23	-25	-17		-200
PST-034-003	-33	-157	-195	-10	-2	38	-16	-17		-404
PST-034-004	-81	-133	-380	-27	-10	-7	-47	-54		-629
PST-034-005	-85	-86	-474	28	28	48	27	16		-732
PST-034-006	-118	-106	-578	-8	-7	-20	-53	-3		-902
PST-034-007	-466	-165	-143	-25	-8	0	-42	-39		-749
PST-034-008	-482	-151	-159	9	21	25	-25	22		-803
PST-034-009	-506	-138	-198	13	5	47	9	32		-861
PST-034-010	-560	-135	-257	29	11	9	-33	14		-1008
PST-034-011	-621	-156	-295	-5	-3	12	-13	8		-1092
PST-034-012	-732	-154	-329	-24	-25	-4	-72	1		-1233
PST-034-013	-731	-138	-339	23	34	-4	-23	13		-1301
PST-034-014	-793	-154	-364	-10	3	14	-75	-16		-1341
PST-034-015	-802	-108	-398	11	16	30	-18	40		-1393

In the last years, this benchmark has been extensively used by the nuclear data evaluation community to test different beta evaluations within the JEFF project. An example of this work is shown in **Figure 17** where different evaluation of IRSN (L. Leal’s team) are shown:

- 239Pu (versions “December 9, 2020” and “December 4, 2020”)
- 16O (“16O-AngJENDL”)
- TSL/H in H2O (“Sab_Vaibhab”)

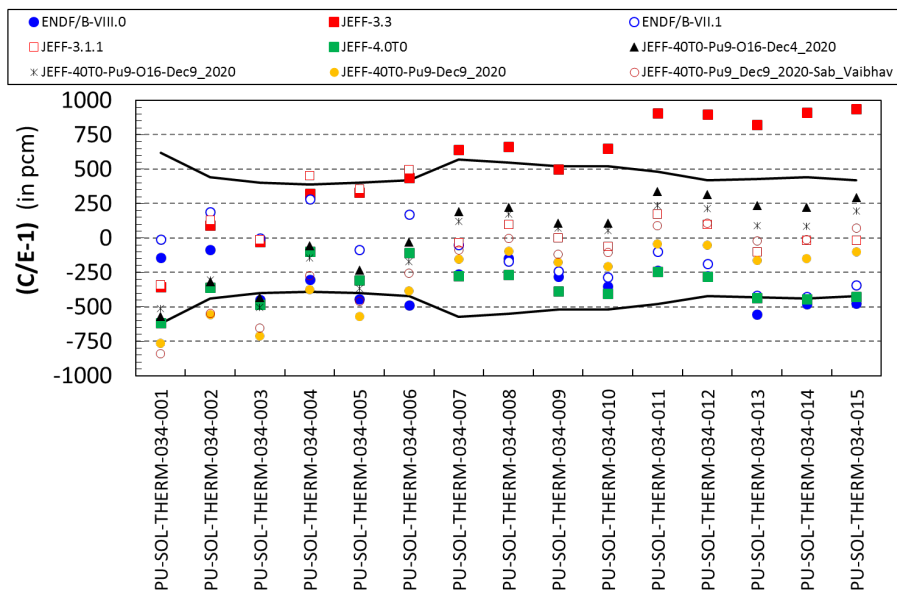


Figure 17. Testing different evaluations for the PU-SOL-THERM 034 benchmarks (15)

2.2.3. Benchmarking with reaction rates in critical systems using MCNP

Additional integral data for validation/testing nuclear data are the reaction rates in critical assemblies. Some useful references with such information are in:

- *Updated Results of LANL Integral Experiments (CIELO paper), NDS 118 (2014) 1–25*
- *Integral Data Testing/Reaction Rates in Critical Assemblies (ENDF/B-VIII.0 paper) Nuclear Data Sheets 148 (2018) 1–142*
- *IAEA Compilation of Nuclear Data Experiments for Radiation Characterisation - CoNDERC Project – <https://www-nds.iaea.org/conderc/> (see **Table 7**).*

(See MCNP inputs by courtesy of Skip Kahler at CONDERC website (April 30, 2019))

Table 7. A List (12) of ICSBEP and IRPhEP Benchmarks with reaction rate exp. data

ICSBEP or IRPhEP	Comment
HEU-MET-FAST-001	Godiva. CAUTION: The ICSBEP Handbook description is for the original (spherical, or Godiva-I) assembly which ceased operation in 1954, but the experimental data are said to come from a 1959 measurement. The 1959 “Godiva” assembly, Godiva-II, was a cylindrical assembly with a dome top. Further research is needed to determine the applicable model for these data.
IEU-MET-FAST-007 ²	
HEU-MET-FAST-028	
PU-MET-FAST-001	
PU-MET-FAST-002	
PU-MET-FAST-006,	
PU-MET-FAST-008	
LEU-COMP-THERM-008	
LEU-COMP-THERM-055	
U233-MET-FAST-001,	
U233-MET-FAST-006	
FUND-IPPE-FR-MULTRRR-001	

Therefore, reaction rates can give us some additional trends of nuclear data that allow us to identify potential issues in the nuclear data. **Table 8** gives a summary of C/E reactions rates for Big-10. This calculation is performed with MCNP-6.1 using CoNDERC input for JEFF-3.3 and ENDF/B-VIII.0 [JEFD0C-1991].

Table 8. Calculation of reactions rates for IEU-MET-FAST-007: Big-10

Quantity	C/E	
	JEFF-3.3	ENDF/B-VIII.0
$^{233}\text{U}(n,f) / ^{235}\text{U}(n,f)$	0.98	0.98
$^{238}\text{U}(n,f) / ^{235}\text{U}(n,f)$	0.90	0.96
$^{238}\text{U}(n,2n)^{237}\text{U} / ^{235}\text{U}(n,f)$	0.92	0.93

² IEU-MET-FAST-007/Big-10 is a large cylindrical assembly consisting of uranium metal plates of various enrichments. Measurements were made in the center of a large 10% enriched region

$^{238}\text{U}(n,g) / ^{235}\text{U}(n,f)$	0.92	0.96
$^{237}\text{Np}(n,f) / ^{235}\text{U}(n,f)$	0.95	0.97
$^{239}\text{Pu}(n,f) / ^{235}\text{U}(n,f)$	0.98	0.98
$^{45}\text{Sc}(n,g) / ^{235}\text{U}(n,f)$	1.04	1.10
$^{55}\text{Mn}(n,g) / ^{235}\text{U}(n,f)$	1.26	1.22
$^{59}\text{Co}(n, g) / ^{235}\text{U}(n,f)$	0.93	0.91
$^{63}\text{Cu}(n,g) / ^{235}\text{U}(n,f)$	1.15	1.08
$^{89}\text{Y}(n,2n)^{88}\text{Y} / ^{235}\text{U}(n,f)$	0.35	0.24
$^{89}\text{Y}(n, g) / ^{235}\text{U}(n,f)$	1.07	1.06
$^{153}\text{Eu}(n, g) / ^{235}\text{U}(n,f)$	1.01	1.04
$^{169}\text{Tm}(n,2n)^{168}\text{Tm} / ^{235}\text{U}(n,f)$	0.76	0.69
$^{169}\text{Tm}(n, g) / ^{235}\text{U}(n,f)$	1.12	1.16
$^{176}\text{Lu}(n, g) / ^{235}\text{U}(n,f)$	0.92	0.87
$^{181}\text{Ta}(n, g) / ^{235}\text{U}(n,f)$	0.85	0.92
$^{180}\text{W}(n,g) / ^{235}\text{U}(n,f)$	0.58	0.75
$^{184}\text{W}(n,g) / ^{235}\text{U}(n,f)$	0.87	1.07
$^{186}\text{W}(n, g) / ^{235}\text{U}(n,f)$	0.99	0.92
$^{193}\text{Ir}(n, g) / ^{235}\text{U}(n,f)$	1.10	1.09
$^{197}\text{Au}(n,2n)^{196}\text{Au} / ^{235}\text{U}(n,f)$	1.00	0.87
$^{197}\text{Au}(n, g) / ^{235}\text{U}(n,f)$	1.00	0.99
$^{241}\text{Am}(n,g) / ^{235}\text{U}(n,f)$	1.52	1.46
$^6\text{Li}(n,\alpha) / ^{235}\text{U}(n,f)$	0.94	0.94
$^{10}\text{B}(n,\alpha) / ^{235}\text{U}(n,f)$	0.94	0.93
$^{10}\text{B}(n,\alpha) / ^{235}\text{U}(n,f)$	0.95	0.97
$^{27}\text{Al}(n,p)^{27}\text{Mg} / ^{235}\text{U}(n,f)$	1.03	1.08
$^{27}\text{Al}(n,\alpha) / ^{235}\text{U}(n,f)$	0.99	0.98
$^{46}\text{Ti}(n,p)^{46}\text{Sc} / ^{235}\text{U}(n,f)$	0.91	0.86
$^{47}\text{Ti}(n,p)^{47}\text{Sc} / ^{235}\text{U}(n,f)$	0.88	0.98
$^{48}\text{Ti}(n,p)^{48}\text{Sc} / ^{235}\text{U}(n,f)$	0.89	1.05
$^{54}\text{Fe}(n,p)^{54}\text{Mn} / ^{235}\text{U}(n,f)$	0.80	0.93
$^{56}\text{Fe}(n,p)^{56}\text{Mn} / ^{235}\text{U}(n,f)$	1.23	1.28
$^{59}\text{Co}(n,2n)^{58}\text{Co} / ^{235}\text{U}(n,f)$	0.72	0.54
$^{59}\text{Co}(n,p)^{59}\text{Fe} / ^{235}\text{U}(n,f)$	0.92	0.96
$^{58}\text{Ni}(n,p)^{58}\text{Co} / ^{235}\text{U}(n,f)$	0.90	0.93

Table 9 shows a good performance in keff for both JEFF-3.3 and ENDF/B-VIII.0. This good agreement in keff with very different cross-section may indicate compensating effects in different cross-sections (^{235}U and ^{238}U).

Table 9 also shows reaction rates values with an underestimation of F8/F5 and C8/F5 for JEFF-3.3 that may be attributed to $^{238}\text{U}(n,\gamma)$ URR evaluation.

It is well known that ^{238}U -JEFF-3.3 “retains the evaluation present in the JEFF-3.2 library, which dates from JEFF-2.2..... In this respect, the JEFF-3.3 evaluation does not follow the result from the evaluation of the standards. [Plompen, 2020]”.

Table 9. Calculation of k_{eff} and reactions rates for IEU-MET-FAST-007: Big-10

Quantity	$\Delta E_{\text{exp}}/E$	C/E	
		JEFF-3.3	ENDF/B-VIII.0
$^{238}\text{U}(n,f) / ^{235}\text{U}(n,f)$	± 0.02	0.90	0.96
$^{238}\text{U}(n,g) / ^{235}\text{U}(n,f)$	± 0.03	0.92	0.96
K-eff (detailed model)	± 70 (pcm)	1.00041	0.99979
K-eff (Improved simplified model)	± 80 (pcm)	0.99997	0.99951

These compensating effects between nuclear data ^{235}U - ^{238}U can be clearly seen in **Figure 18** for criticality (k_{eff}). This Figure provides some indications from Big-10 on ^{235}U - ^{238}U evaluation. In this case, the $^{238}\text{U}(n,\gamma)$ specifically in the URR is compensated with the $^{238}\text{U}(n,n')$, $^{238}\text{U}(n,\text{fission})$ and $^{235}\text{U}(n,\gamma)$ [JEFDOC-2015].

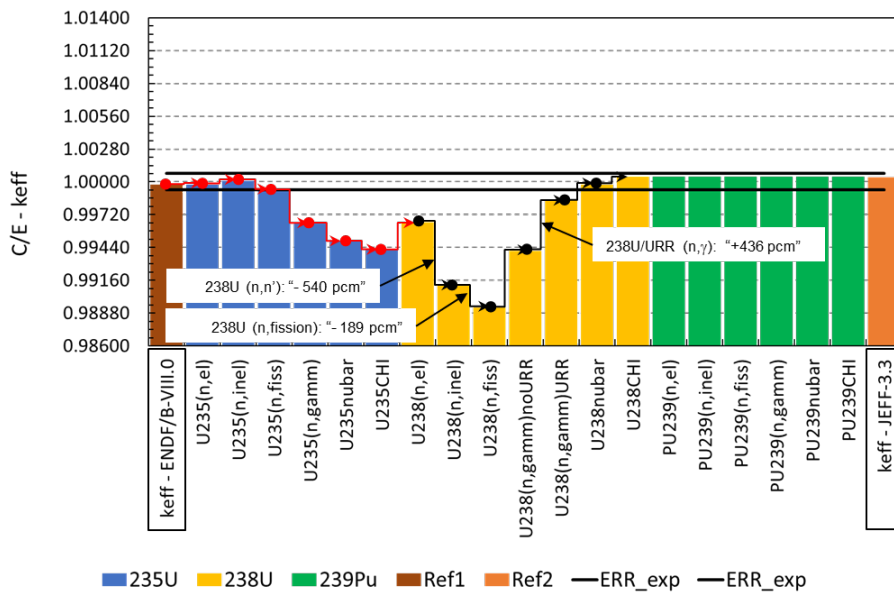


Figure 18. Changes in criticality for Big-10 when individual cross-section channels are substituted between ENDF/B-VIII.0 and JEFF-3.3. Perturbations in k_{eff} calculated with NDaST code.

However, the compensating effects between nuclear data ^{235}U - ^{238}U is not recovered in the reaction rates for F28/F25 as it can be seen in **Figure 19**. In this case, the $^{238}\text{U}(n,\gamma)$, $^{238}\text{U}(n,n')$, and $^{238}\text{U}(n,\text{fission})$ is not compensated with the ^{235}U [JEFDOC-2015].

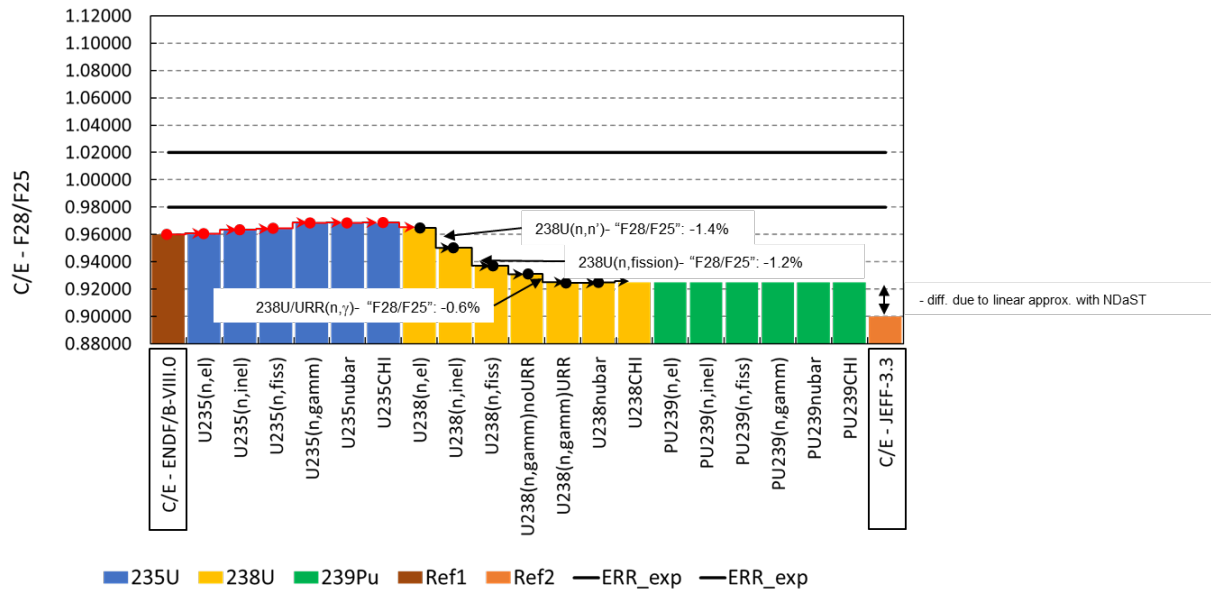


Figure 19. Changes in F28/F25 for Big-10 when individual cross-section channels are substituted between ENDF/B-VIII.0 and JEFF-3.3. Perturbations in keff calculated with NDaST code.

2.3. Benchmarking at room and elevated temperatures: KRITZ Benchmarks

The main objective of this work is:

- To extend Benchmarking for nuclear data validation: IRPhEP Handbook
- Looking for Benchmarks more sensitivity to capture reaction: $^{238}\text{U}(n,\gamma)$ and $^{239}\text{Pu}(n,\gamma)$
- Benchmarking at room and elevated temperatures
- Testing our AMPX processing capabilities
- Benchmarking at room and elevated temperatures for JEFF-3.3 and ENDF/B-VIII.0

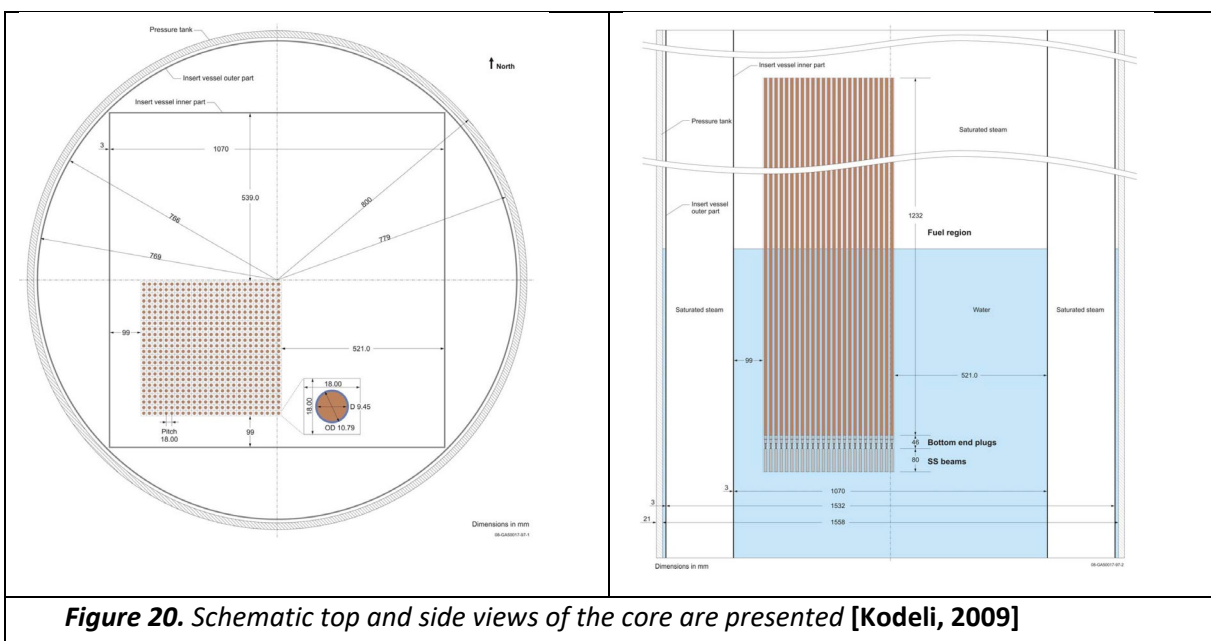
In this section, we study light-water reactor lattices at KRITZ reactor in Studsvik (Sweden). Criticality at room and elevated temperatures.

2.3.1. KRITZ 1-3

A summary of KRITZ1-3 Benchmarks is shown in **Table 10**. A schematic view is also shown in **Figure 20**.

Table 10. Summary of benchmarks

Core	Fuel type	Array size	Cold pitch (cm)	Temp (°C)	Boron (ppm)
KRITZ-2:19 KRITZ-LWR-RESR-001	MOX fuel pins 1.50wt% PuO ₂ in fuel 91.41 at% Pu ²³⁹ Clad Zircaloy	25x24	1.635	21.1 235.9	4.8 5.2
KRITZ-2:1 KRITZ-LWR-RESR-002	UO ₂ fuel pins 1.86wt% U ₂₃₅ Clad Zircaloy	44x44	1.800	19.7 248.5	217.9 26.2
KRITZ-2:13 KRITZ-LWR-RESR-003	UO ₂ fuel pins 1.86wt% Clad Zircaloy	44x40	1.485	22.1 243.0	451.9 280.1



Calculations are performed with MCNP-6.1 with three different evaluations: JEFF-3.3, JEFF-3.1.1 and ENDF/B-VIII.0. **Table 11** shows results for the KRITZ-1 where large biases are found specially for JEFF-3.3 at high temperature.

Table 11. Summary of KRITZ-2:19 (KRITZ-LWR-RESR-001)

	KRITZ2:19 at 21.1°C (cold)		KRITZ2:19 at 235.9 °C (hot)		KRITZ2:19 at 21.1°C	KRITZ2:19 at 235.9 °C	$\Delta C/E(C-H)$
	keff	$\Delta keff$	keff	$\Delta keff$	(C/E-1) in pcm	(C/E-1) in pcm	
Benchmark model	1.00770	0.00300	1.00550	0.00270	-	-	
MCNP6.1-JEFF-3.3	0.99993	0.00008	0.99553	0.00008	-771	-992	-220
MCNP6.1-JEFF-3.1.1	1.00029	0.00007	1.00022	0.00008	-735	-525	210
MCNP6.1-ENDFB80	0.99945	0.00007	0.99888	0.00008	-819	-658	160
MONK10B-JEFF-3.1.2 (JEFDOC-1998, T. Ware)	1.00090	0.00020	1.00060	0.00020	-675	-487	187
MONK10B-JEFF-3.3 (JEFDOC-1998, T. Ware)	1.00030	0.00020	0.99540	0.00020	-734	-1004	-270
MONK10B-JEFF-3.3+Pu9E80 (JEFDOC-2250, T. Ware)	1.00290	0.00020	1.00170	0.00020	-476	-378	98

Table 12 shows results for the KRITZ-2 where for JEFF-3.3 lower biases are found. For JEFF-3.3, the biases are different are at cold and hot temperatures.

Table 12. Summary of KRITZ-2:1 (KRITZ-LWR-RESR-002)

	KRITZ2:1 at 19.7°C		KRITZ2:1 at 248.5 °C		KRITZ2:1 at 19.7°C	KRITZ2:1 at 248.5 °C	$\Delta C/E(C-H)$
	keff	$\Delta keff$	keff	$\Delta keff$	(C/E-1) in pcm	(C/E-1) in pcm	
Benchmark model	1.00250	0.00200	1.00240	0.00280	-	-	
MCNP6.1-JEFF-3.3	1.00076	0.00008	1.00294	0.00008	-174	54	227
MCNP6.1-JEFF-3.1.1	0.99834	0.00008	0.99910	0.00008	-415	-329	86
MCNP6.1-ENDFB80	0.99812	0.00008	0.99958	0.00008	-437	-281	156

Table 13 shows results for the KRITZ-3 where for JEFF-3.3 lower biases are found. For JEFF-3.3 the biases are similar at cold and hot temperatures.

Table 13. Summary of KRITZ-2:13 (KRITZ-LWR-RESR-003)

	KRITZ2:13 at 22.1°C		KRITZ2:13 at 243.0 °C		KRITZ2:13 at 22.1°C	KRITZ2:13 at 243.0 °C	$\Delta C/E(C-H)$
	keff	$\Delta keff$	keff	$\Delta keff$	(C/E-1) in pcm	(C/E-1) in pcm	
Benchmark model	1.00130	0.00100	1.00190	0.00200	-	-	
MCNP6.1-JEFF-3.3	1.00201	0.00008	1.00261	0.00008	71	71	0
MCNP6.1-JEFF-3.1.1	1.00056	0.00008	0.99875	0.00007	-74	-314	-240
MCNP6.1-ENDFB80	1.00062	0.00008	0.99952	0.00008	-68	-238	-170

2.3.2. KRITZ-4

The description of this Benchmarks is included in the IRPhE database: “KRITZ-LWR-RESR-004 Evaluation Report. 2019 Rev.0”. It contains 37 criticality measurements at room and elevated temperatures (critical water heights of active fuel covered by water), with UO2 fuels 1.35wt% in 235U.

Four different sets of measurements are given:

- 9 cases with array 39x39 fuel rods at 41° C - 226° C. Boron=0.8 ppm
- 4 cases with array 46x46 fuel rods at 90° C - 246° C. Boron=46.3 ppm
- 11 cases with array 46x46 fuel rods at 22° C - 205° C. Boron=175 ppm
- 13 cases with array 39x39 fuel rods at 20° C - 244° C. Boron=0.2 ppm

An extensive work of this Benchmarks has been performed within the nuclear criticality safety community [Mennerdahl, 2020] concluding that:

- there are correlations between measurements were very strong, $ck > 0.95$
- a priory uncertainty due to nuclear data uncertainties ~ 600 pcm
- the totally dominating nuclear data adjustment is 238U (n, γ)

A summary of results are shown in **Figure 21, Figure 22, Figure 23 and Figure 24.**

❑ UPM calculations [JEFDOC-2091]:

- KRITZ4 simple models and calculations with KENO-VI/SCALE6.2.3
- Processed ND libraries JEFF-3.3 and JEFF-3.1.1 with APMX/SCALE6.3b11 code
- On-the-fly doppler broadening (DBX=2)

❑ MORET calculations (included in IRPhE Report)

(as reported in “KRITZ-LWR-RESR-004 Evaluation Report. 2019 Rev.0”)

- KRITZ4 simple models and calculations with MORET5.D.1
- Processed ND libraries JEFF-3.3 and ENDF/B-VIII.0 with GAIA1.1.1 tool
- TSLs available in ENDF files

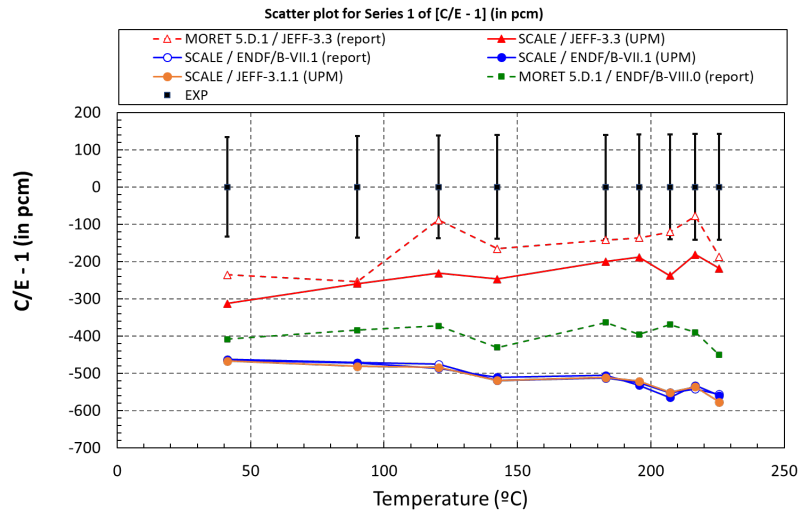


Figure 21. C/E for KRITZ4/Series1.

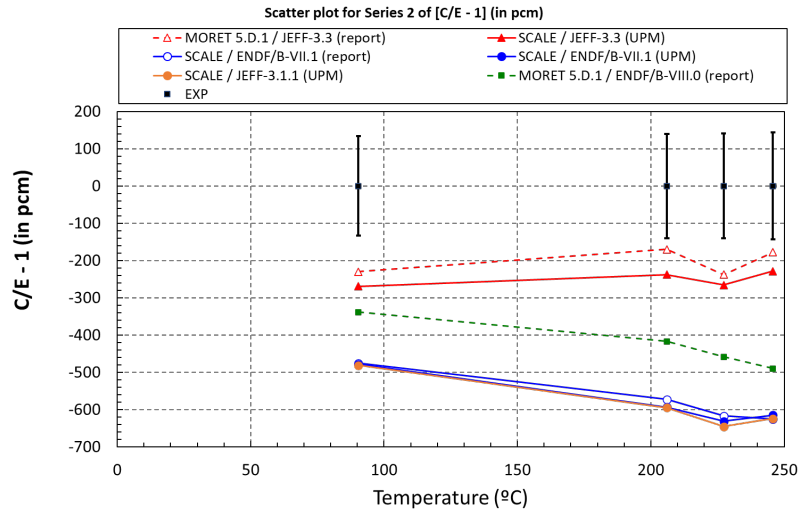


Figure 22. C/E for KRITZ4/Series2

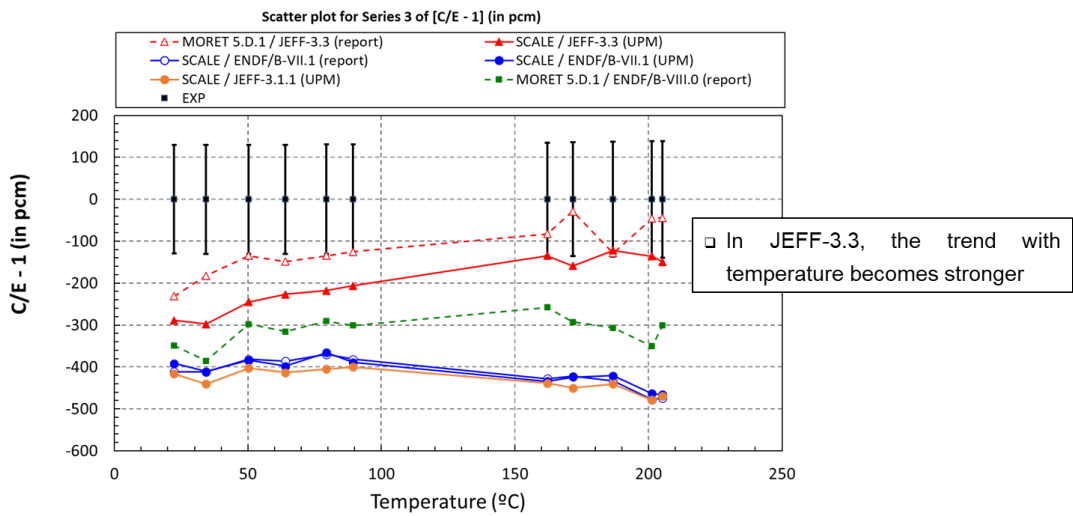


Figure 23. C/E for KRITZ4/Series3

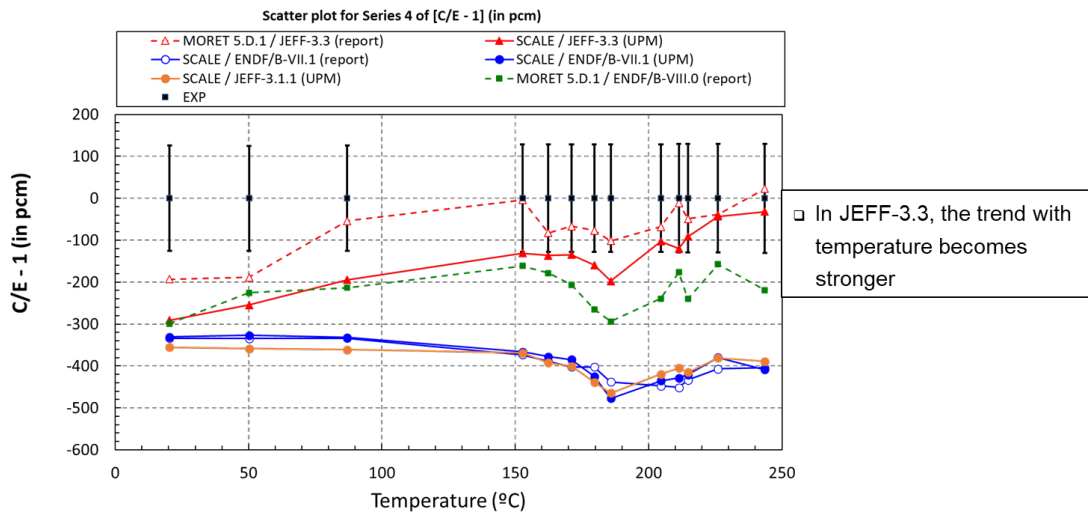


Figure 24. C/E for KRITZ4/Series4

As a conclusion, one can summarize the following:

- Calculations with different codes (by different organizations) show consistent trends in the results
- Results for detailed and simple models appear to be consistent (see IRPhE Report)
 - ENDF/B-VII.1 and JEFF-3.1.1:
 - Larger biases from -600pcm to -400 pcm
 - Smaller biases for the most thermalized series of measurements
 - No strong trend with temperature is observed
 - ENDF/B-VIII.0 and JEFF-3.3
 - Smaller calculation biases, particularly for JEFF-3.3
 - The trend with temperature becomes stronger for series 4, in particular for JEFF-3.3
 - *This strong trend may indicate remaining nuclear data biases in JEFF-3.3*

2.4. Processing with AMPX code

Nuclear data processing is the procedure devoted to the conversion of evaluated nuclear data into libraries for specific final applications such as neutron transport or inventory calculations. Computational codes are specifically dedicated to nuclear data processing. AMPX [Wiarda, 2016] is the modular processing code of SCALE Code System that takes basic cross section data in Evaluated Nuclear Data File (ENDF) format to provide both multigroup (MG) or continuous energy (CE) libraries for their use by the neutron transport codes included within SCALE [Rearden, 2018].

The OECD Nuclear Energy Agency (NEA) Data Bank coordinates the Joint Evaluated Fission and Fusion (JEFF) nuclear data library project. In the last years, a new version of the JEFF library, namely JEFF-3.3 [Plompen, 2020], has been released with relevant updates in the neutron reaction and the thermal neutron scattering sub-libraries. The library is publicly released through the NEA in ENDF-6 format [Herman, 2012]. Thus, users should perform the nuclear data processing to produce a nuclear data set in an adequate format for the final application. Therefore, the use of JEFF nuclear data libraries within SCALE system is not straightforward so that the processing of the nuclear data library must be undertaken with AMPX.

Past efforts set the first milestones for the usage of JEFF libraries within SCALE [Diez, 2016]. As a continuation of that work, within the EU H2020 SANDA (Supplying Accurate Nuclear Data for energy and non-energy Applications) project, AMPX is being used for processing the JEFF-3.1.1 and JEFF-3.3 neutron library.

This section deals with the processing of JEFF-3.1.1 and JEFF-3.3 neutron data libraries into a CE library for its use with SCALE transport codes such as KENO-VI. Main aspects concerning the processing of CE and covariance libraries with AMPX are depicted. The CE library performance is also evaluated for a set of criticality benchmarks. This allows to identify the application domain of the generated library and those issues that require further development activities.

AMPX is the modular processing code of SCALE Code System, developed at Oak Ridge National Laboratory (ORNL). In this work, the CE library is generated using AMPX code available with SCALE6.3β11. This version incorporates relevant updates regarding the generation of probability tables for the unresolved resonance region (URR), affecting to intermediate and fast spectrum systems [Kim, 2019].

This section presents a brief summary about the processing of both CE libraries and covariance matrices.

(1) Continuous energy libraries

The generation of a CE library with AMPX is performed through a multi-step procedure based on the usage of different modules (see **Figure 25**).

Then, for each available isotope and starting from the ENDF-6 file the following procedure is applied:

- POLIDENT is firstly used to reconstruct point-wise CE cross sections at 0 K.
- Then, BROADEN performs the Doppler-broadening for those temperatures required by the user. The first stage is completed by TGEL, which ensures the consistency between partial and total reactions.
- For those isotopes that contain unresolved resonance parameters, PURM generates probability tables that describe the unresolved resonance region for each desired temperature.
- Y12 is applied to generate two-dimensional kinematics data for neutron scattering producing double-differential data and JAMAICAN converts the data into marginal probability distribution in exit energy.
- Finally, PLATINUM creates the final CE library by merging the data produced in previous steps.

- The thermal moderator data given by Thermal Scattering Libraries (TSL) must be combined with the proper evaluation in the higher energy range. Then, thermal moderators (such as H-1 in H₂O) are constructed by TSL data in thermal range (<10 eV) and data from neutron library for higher energies. Y12 and JAMAICAN are also used for processing the Thermal Scattering Libraries (TSL), combining the thermal moderator data with the proper evaluation in the higher energy range (>10 eV).

In the frame of the SANDA project, best processing parameters for each step are identified and inputs decks have been created for processing CE libraries with AMPX.

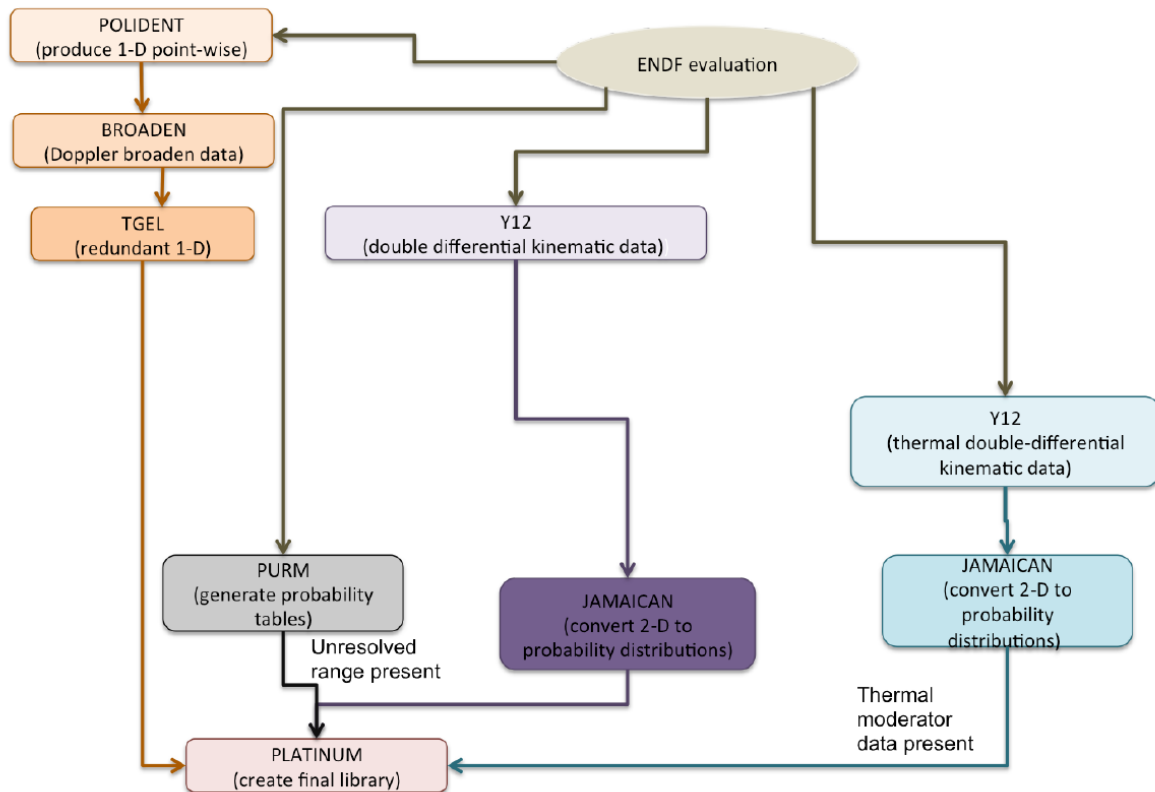


Figure 25. AMPX sequence for the generation of CE library [Wiarda, 2016].

(2) Covariance libraries

This work also deals with the processing of JEFF-3.3 covariance libraries.

AMPX is applied to generate COVERX-format covariances for average number of neutrons per fission (MF31), resonance parameters (MF32) and neutron cross-sections (MF33) and prompt fission spectrum (MF35).

PUFF is the module devoted to generating covariance libraries according to the group-averaged cross section data on the user-defined energy structure. Files produced by PUFF are then merged into a library that contains cross-reaction and cross-material covariance matrices (if present). Corrections are finally applied to the library by means of the COGNAC module.

AMPX sequence is shown in **Figure 26**.

In this work, two sets of covariance libraries are generated using a weighting function generically optimized for fast reactor analyses. The first covariance library is created for general purposes using a

33-energy group structure. Moreover, a 7-group structure covariance matrix is also created in the frame of the OECD/NEA WPEC Subgroup-46 [Hursin, 2022].

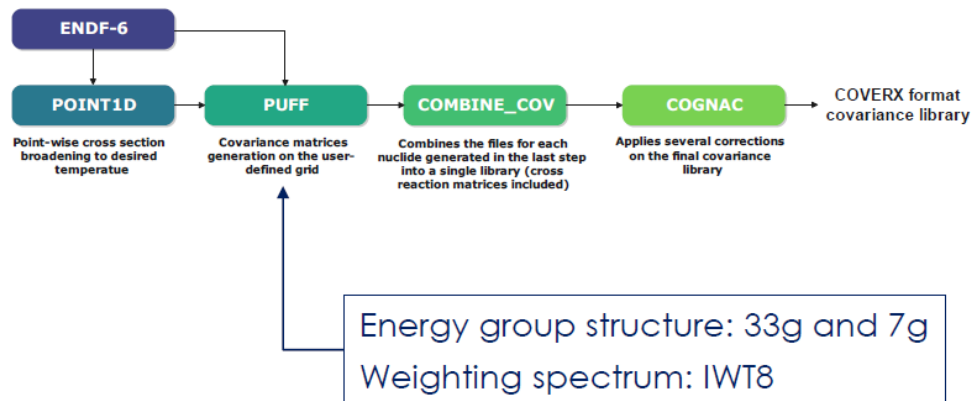


Figure 26. AMPX sequence for the generation of covariance library [Wiarda, 2016].

2.4.1. Processing JEFF-3.3 neutron data library with AMPX code

The latest release of the JEFF project, JEFF-3.3, is a thorough update of the neutron, decay data, fission yields, dpa and neutron activation libraries with TSLs for 20 compounds. It also includes new evaluations for the major nuclides U-235, U-238 and Pu-239 along with important updates for many other isotopes in terms of neutron cross sections. It is worth mentioning that JEFF-3.3 improvements targeted the needs for advanced reactors developments programs, including upgrades for both sodium and lead.

This work addresses the processing of JEFF-3.3 neutron data for 562 isotopes and 20 TSLs. The procedure detailed in **Subsection 2.1** is successfully applied for the processing of all the isotopes. Nonetheless, several issues are identified through the processing itself and via testing cases using a simple infinite dilution problem. The latter consists of very simple criticality calculations of an infinite dilution containing fissile material (U-235) in a solution, allowing to test all the nuclides included in the library by comparing results provided by KENO-VI and MCNP. **Figure 27** shows around 400 cases/isotopes with differences below 100 pcm.

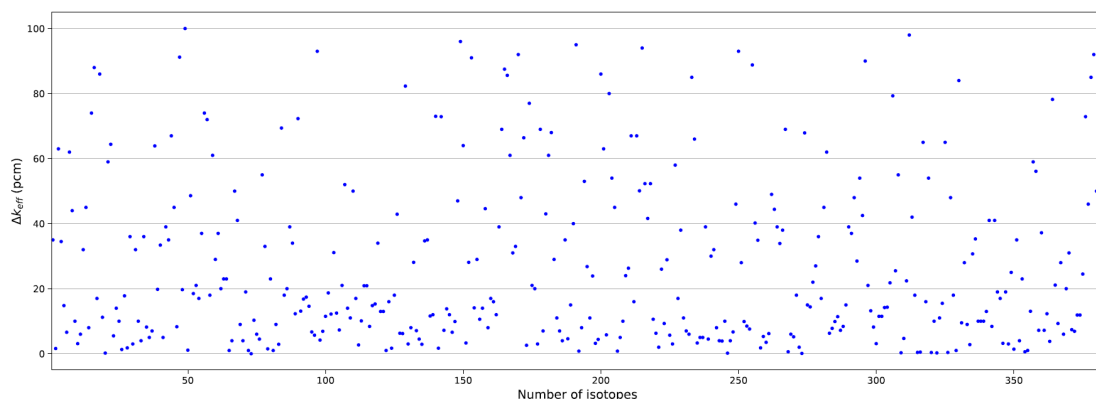


Figure 27. *Keff*-differences (in pcm) between KENO-VI and MCNP simple criticality calculations of an infinite dilution containing fissile material (U-235) in a solution

However, several isotopes show deviations dramatically higher, so they require additional checking activities.

The main outcomes of the testing phase are detailed below:

- Negative cross section values are found when reconstructing cross section from resonance parameters for 19 isotopes: Ag-108, Ar-40, As-74, As-77, Ce-137, Fe-54, Gd-151,152,157, Hg-203, La-137, Sc-46, Sr-90, Tb-158, Tl-202, V-49 and Yb-175
- The total resonance width given in the file differs from calculated for the same set of isotopes.
- The lower limit of the URR does not include some unresolved resonance parameters for U-239.
- Regarding TSL, data for H-1 in CaH₂, Ca in CaH₂ and Mg in Mg metal are not considered since they are not identified in SCALE.
- The infinite dilution calculation also reveals relevant issues concerning TSLs since it is observed that SCALE is not currently able to manage the following compounds: H-1 in H₂O ice, H-1 in Toluene, H-1 in Mesitylene, O-16 in Al₂O₃ and O-16 in D₂O.

This is due to the lack of available material identification for them. However, this can be solved in future iterations using the COMPOZ module to update the standard composition library.

- Additionally, certain metastable isotopes are not manageable by SCALE so that they do not pass this phase: Ag-106m, Co-62m, Eu-152m, Nb-94m and Xe-135m.

The rest of the isotopes are successfully processed, and they can be used in transport calculations. The performance of the library as a whole is evaluated in the next section.

2.4.2. Benchmarking AMPX processing with criticality systems using KENO code

In order to test the new cross section library, a comprehensive set of experiments from the International Handbook of Evaluated Criticality Safety Benchmark Experiments (ICSBEP) [ICSBEP, 2019] has been selected and evaluated. This analysis includes a comparison between KENO-VI and MCNP6.1, that use AMPX and NJOY-processed cross section data respectively. Results are presented in terms of C/E since experimental values are also considered and provided insight into the behaviour of the library itself.

A set of ICSBEP benchmarks is created aiming to cover a variety of fuel, moderators, reflectors, spectra and geometries, see **Table 14**. This set consists of 120 benchmarks, divided into 43 highly enriched uranium (HEU) cases, 10 intermediate-enriched uranium (IEU) cases, 14 low-enriched uranium (LEU) cases, 8 mixed uranium and plutonium (MIX) cases, 28 plutonium (PU) cases and 17 U-233 systems (U233). Of these, 71 corresponds to fast neutron spectra (FAST), 6 as for intermediate spectrum (INTER) and 43 for thermal spectrum (THERM). This set is mostly composed by cases included within ICSBEP database along with updated inputs provided by OECD/NEA, ensuring the consistency between KENO-VI and MCNP inputs. The latter has been widely used in previous works [JEFDOC-1904, 2017].

Table 14. Overview of selected ICSBEP benchmarks classified by the spectrum and fissile material.

<i>Fuel</i>	<i>Number of benchmarks</i>		
	<i>Fast</i>	<i>Intermediate</i>	<i>Thermal</i>
<i>HEU (43)</i>	32	6	5
<i>IEU (10)</i>	10	-	-
<i>LEU (14)</i>	-	-	14
<i>MIX (8)</i>	2	-	6
<i>PU (28)</i>	17	-	11
<i>U233 (17)</i>	10	-	7
Total	71	6	43

Multiplication factor calculations for the set of benchmarks using both KENO-VI and MCNP are presented from **Figure 28** to **Figure 31**.

- For HEU category (**Figure 28**) a good agreement can be observed between the values provided by KENO-VI and MCNP. Nonetheless, a dramatic deviation of around 900 pcm appears for the HMF009-001 benchmark. Further analyses reveals that this difference can be explained by the presence of Be-9. In fact, this behaviour is systematically found in subsequent cases and this also affects to Be-9 bound in Be metal.

This issue lies in the description of the (n,2n) reaction in the Be-9 ENDF-6 file provided by JEFF-3.3 evaluation. It is described by means of its partial reactions (i.e., MT875+ reaction channels), but the total reaction is not included. AMPX properly deals with these channels but an additional patch should be included to construct the (n,2n) description. This issue also affects to HCl003-007, for which a deviation of around 300 pcm is found.

The rest of cases presents discrepancies below 100 pcm except for HMF-003-009, HMF-003-011, HMF-011-001, HMI-006-003 and HMI-006-004. Deviations between 100 and 200 pcm are found for these cases suggesting that models shall be reviewed and updated.

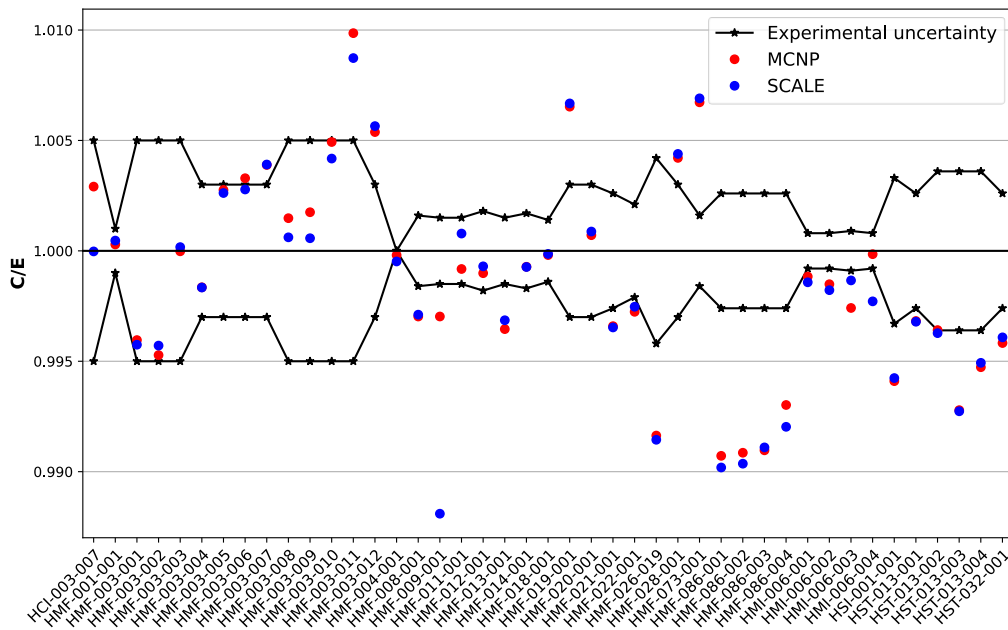


Figure 28. Eigenvalue comparison of calculations with selected experiments for HEU benchmarks.

- **Figure 29** shows results for IEU, LEU and MIX benchmarks. A very good agreement is obtained for IEU benchmarks since differences are lower than 30 pcm in each case. Nonetheless, only benchmarks with fast spectra are included in this case so that more configurations with different physical forms and spectra may be added to the study for a wider comparison.

Regarding LEU category, results are consistent between both codes considering that deviations are not larger than 60 pcm in all cases. This is also observed for MIX benchmarks, where a very good agreement is also obtained (deviations <60 pcm). However, it is worth mentioning that both MCT002-001 and -002 present differences of around 100 pcm because simplified models are used in SCALE while MCNP results are obtained with detailed models.

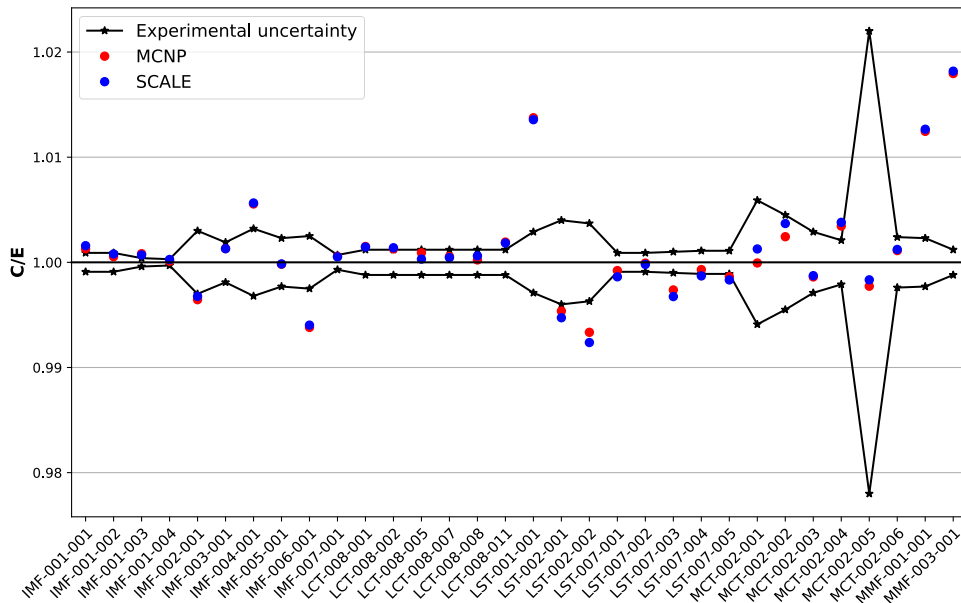


Figure 29. Eigenvalue comparison of calculations with selected experiments for IEU, LEU and MIX benchmarks.

- Results for PU benchmarks are presented in **Figure 30**. In general, both codes predict reasonably similar multiplication factors. The effect of the presence of Be-9 is again observed for PMF018-001, PMF019-001 and PMF021-001, showing differences larger than 2000 pcm. Apart from that, PMF005-001 presents deviations of around 150 pcm, even after updating the KENO-VI model. This benchmark may suggest that additional verification exercises are recommended for W isotopes.

This test is performed based on infinite dilution cases along with verification calculations for PMF-005-001. Firstly, infinite dilution tests show remarkable discrepancies between KENO-VI and MCNP for several W isotopes: W-182, 184 and 186. Concerning PMF-005-001, deviation between both codes is initially around 150 pcm but it is reduced up to 30 pcm when these nuclides are removed from the calculations. This behaviour is also confirmed for other cases such as HMF-003-009, that also contains these isotopes. Thus, further analyses are mandatory to solve this issue.

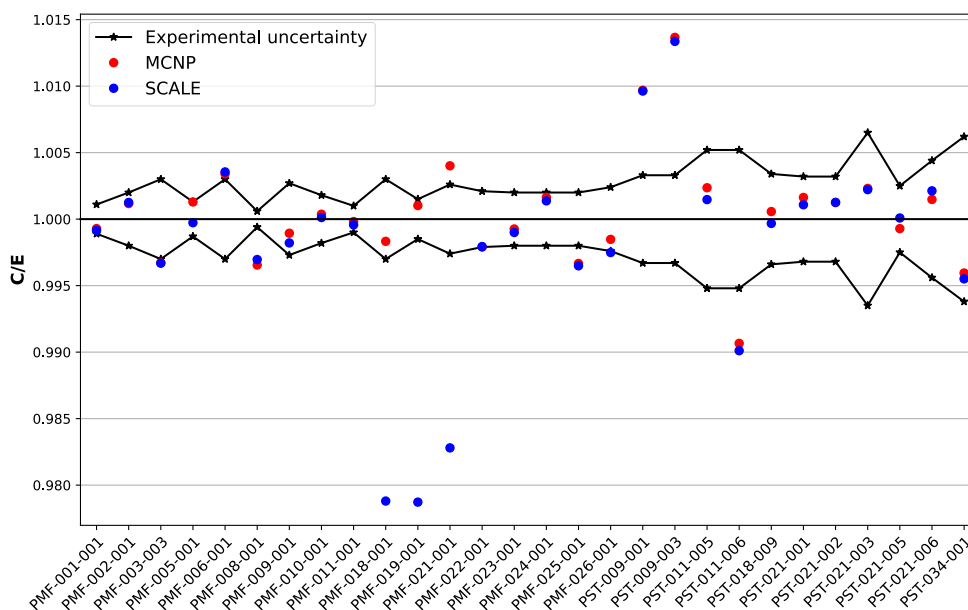


Figure 30. Eigenvalue comparison of calculations with selected experiments for PU benchmarks.

- Finally, U233 cases (**Figure 31**) are considered covering a wide range of physical forms. Deviations are consistent between KENO-VI and MCNP besides the fact that of Be-9 is involved in both UMF005-001 and -002. On the other hand, UMF004-001 and -002, for which differences of around 200 pcm are found between both codes, are also affected by W isotopes.

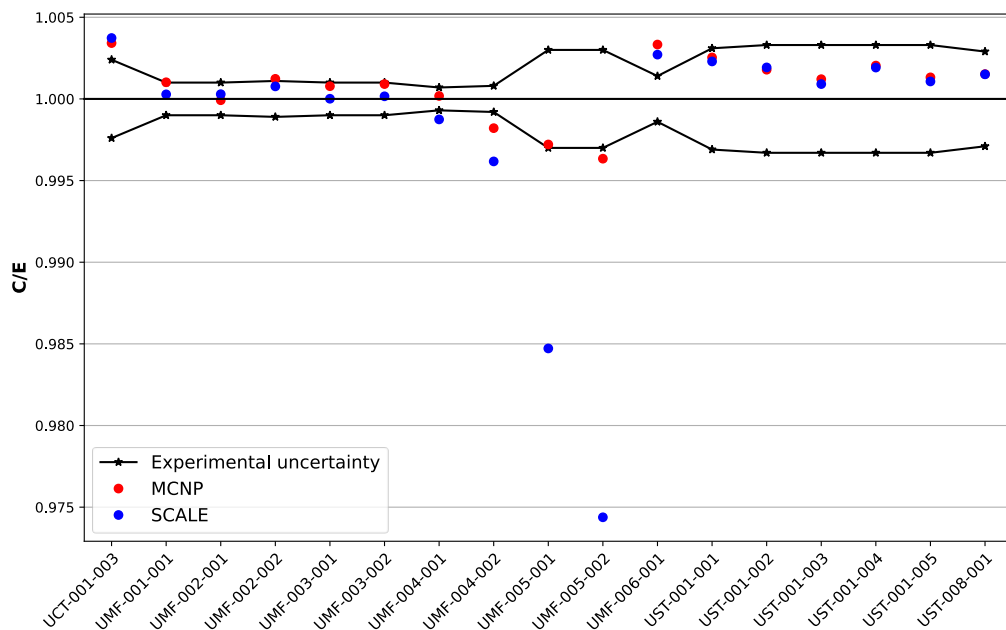


Figure 31. Eigenvalue comparison of calculations with selected experiments for U233 benchmarks.

In general, the AMPX-formatted JEFF-3.3 library shows a reasonably good performance. Results provided in this work are accompanied by extensive verification and validation activities carried out in the frame of the JEFF project:

- This library has been used to assess temperature trends observed for the IRPhE KRITZ (KRITZ-LWR-RESR-004) benchmarks [**JEFD0C-2091, 2021**]. This allowed to test the library at room and elevated temperatures, showing a good performance compared to benchmark results.
- Additionally, reactor physics calculations have been also performed for the SEFOR fast reactor, evaluating the associated Doppler reactivity effect [**JEFD0C-2097, 2021**].
- Benchmarking activities successfully support the performance of the processed JEFF-3.3 library, establishing a reference processing route for future releases. In fact, preliminary recent works have been carried out for the JEFF-4T1 testing library [**JEFD0C-2144, 2022**], paving the way towards an optimized interaction between the future JEFF-4 library and AMPX processing code.

2.5. Processing the unresolved resonances with the AMPX and NJOY codes

An alternative route for cross-validation of AMPX and NJOY has also been undertaken within the frame of SANDA T4.3 by directly comparing the processed cross sections provided by both codes. These results were already reported in [Bécares 2020a] and [Bécares 2020b], and the present chapter is a synthesis of these two documents. The comparison of the results produced by both codes is difficult, however, because they are provided in different formats for use with different transport codes. There is always the possibility, of course, of cross-validating both codes through transport calculations with different transport codes in benchmark systems, but in this way it is not possible to determine whether the observed differences are due to the processing or the transport code.

As stated above, the processing of a continuous energy neutron library consists of many steps, for the cross-validation exercise described in this section three have been considered:

- (1) Reconstructing the pointwise cross section from the evaluated nuclear data files (POLIDENT module in AMPX and RECONR module in NJOY).
- (2) Doppler-broadening the reconstructed data (BROADEN module in AMPX and BROADR module in NJOY).
- (3) Generating probability tables in the unresolved resonance range (PURM module in AMPX and PURR module in NJOY).

For steps (1) and (2), the cross-validation between AMPX and NJOY can be easily performed using the MAKPEN module of AMPX. With this module, AMPX output can be converted to the PENDF format used by NJOY and the results readily compared. An example for the case of ^{235}U fission cross section is shown in **Figure 32**. As it can be observed, no noticeable differences between the codes are apparent.

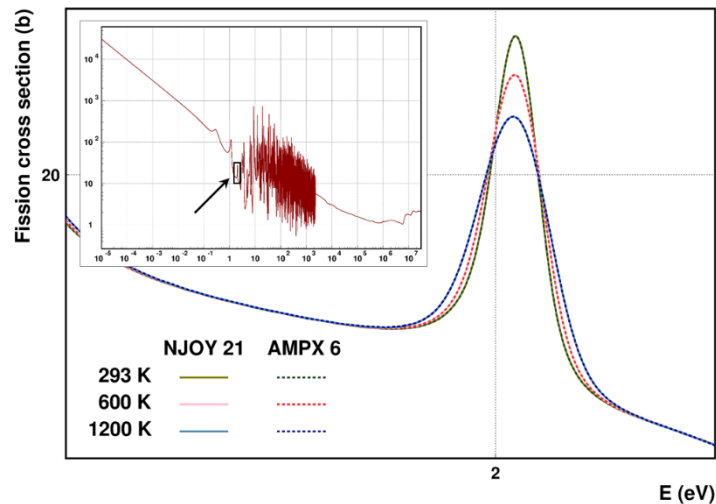


Figure 32. Cross-comparison between Doppler-broadened cross section with AMPX and NJOY (^{235}U fission cross section).

Concerning step (3), processing the unresolved resonance range (URR), the comparison between AMPX and NJOY is more complex because the MAKPEN module cannot convert URR AMPX output into the PENDF format. However, this step was of particular interest since it had been reported that results of criticality calculations in fast reactors using AMPX-processed data were significantly different from results obtained with other codes using NJOY processed data [Jiménez-Carrascosa 2019]. In this work, a normalization issue in the unresolved resonance range with AMPX 6.2.3 was given as an explanation for the differences. Hence, in order to directly compare AMPX and NJOY results in the unresolved resonance range, a subroutine (MAKPEN_URR) has been developed to rewrite AMPX-processed unresolved

resonance data in the PENDF format (MF=2/MT=152 and MF=2/MT=153 style). A second subroutine (MAKPEN_URR2) is used to add these files to an existing PENDF file containing the remaining nuclear data. In this way, AMPX-processed URR data can be directly compared with NJOY processed data and further converted by NJOY (ACER routine) into the ACE nuclear data format used by several neutron transport codes. A schematic of the workflow is presented in **Figure 33**. The procedure is described more detail in the following paragraphs.

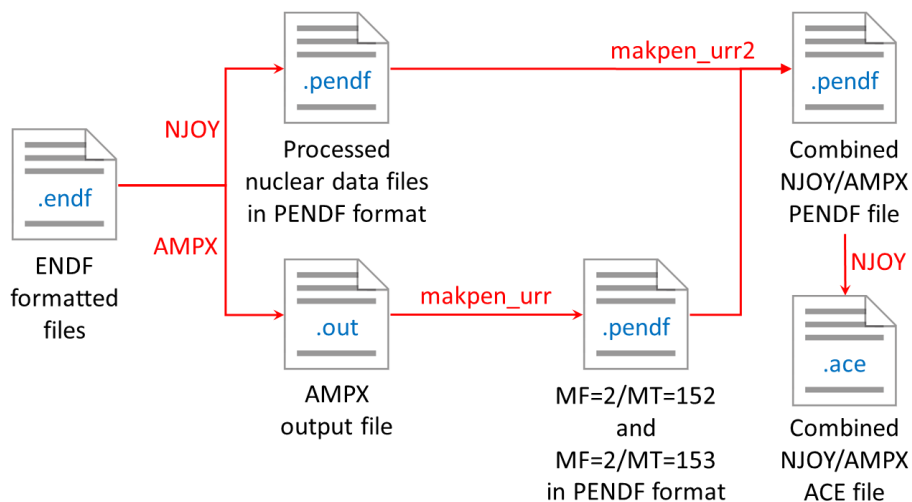


Figure 33. Workflow for converting AMPX-processed URR data to PENDF format and comparing them with NJOY.

Unresolved resonance range data are contained in file 2 (MF=2) of the ENDF format. This file contains statistical information about the unresolved resonances (probability distributions for the resonance density and width) and cannot be directly used by neutron transport codes. To take into account this information and produce effective cross sections usable by transport codes that take into account the unresolved resonance information two major methodologies exist:

(1) Self-shielded cross sections.

This methodology consists in taking into account the increased absorption in the resonances and the consequent decrease in the neutron flux to produce effective cross sections in the unresolved resonance range. The most common methodology to obtain these self-shielded cross is the Bondarenko method [Bondarenko 1964]. This method is applied by both AMPX and NJOY and therefore the self-shielded cross sections provided by the two codes can be expected to be the same or at least very similar. The value of the parameter σ_0 has been taken as 10^{10} in both codes.

In the case of NJOY, the Bondarenko cross sections are written in the PENDF formatted files under label MF=2/MT=152. It may be worth remarking that the UNRESR module of NJOY also produces Bondarenko cross sections (but not probability tables). Both NJOY PURR and AMPX PURM produce Bondarenko cross sections for the total, elastic scattering, fission and capture reactions. Additionally, NJOY produces a fifth value corresponding to the current-weighted (instead of flux-weighted) total cross section that is not produced by AMPX. However, this current-weighted cross section is not listed in the ACE format, so it has no relevance when these data are used by codes using this format.

In **Figure 34**, the values of the Bondarenko cross sections obtained with NJOY and AMPX (with either equiprobable and non-equiprobable probability values, see below) are presented for different isotopes of the JEFF-3.3 [Plompen 2020] libraries. Notice that AMPX and NJOY use different energy values. As expected (because, as stated before, both codes use the Bondarenko method) the difference between the two codes is virtually unnoticeable in most cases. Some differences can be observed, though, the largest being for ^{239}Pu in the 10-30 keV energy range, but even in this case the difference is always less than 3%.

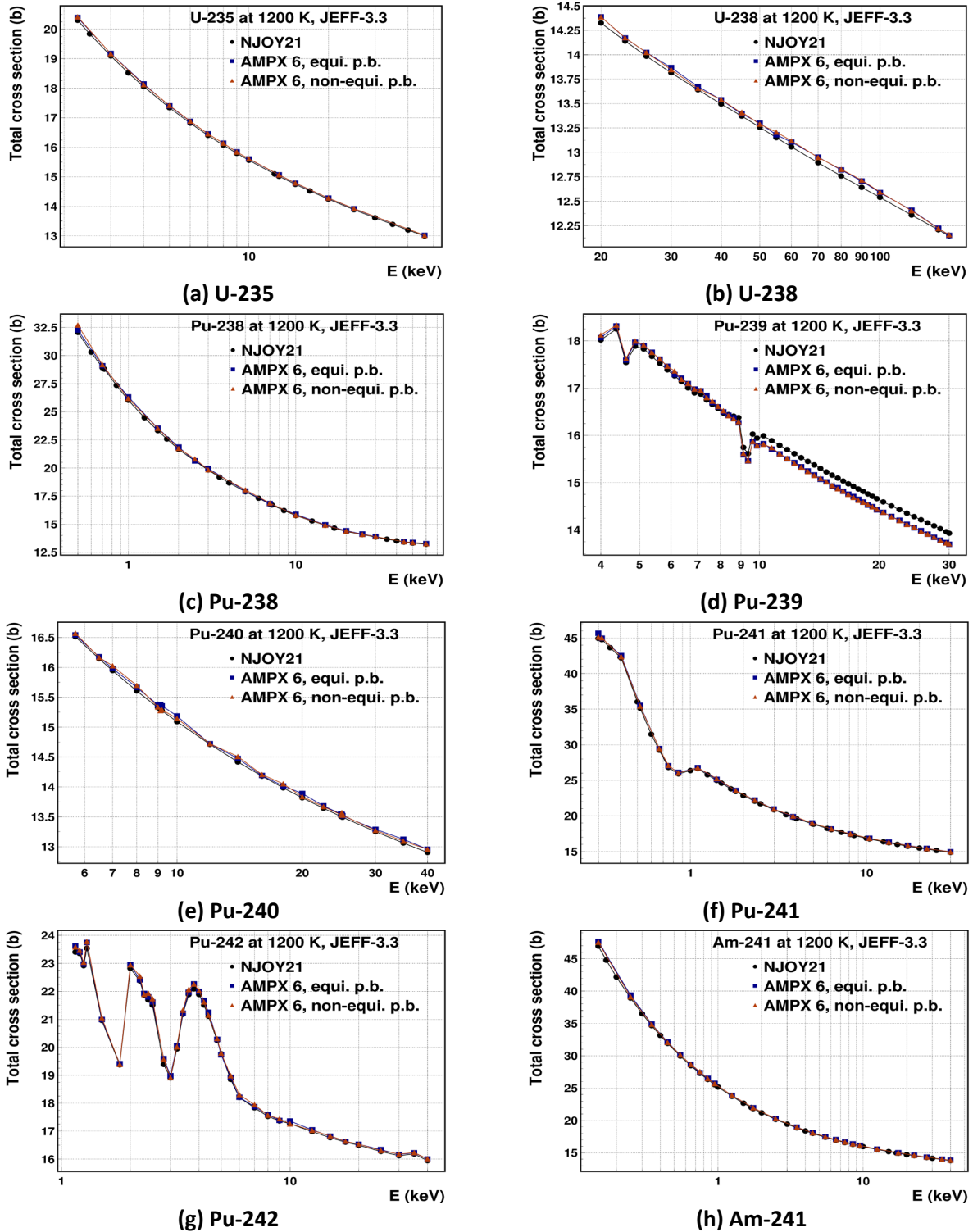


Figure 34. Bondarenko total cross sections vs. energy obtained with AMPX (with equidistant and non-equidistant probability bands) and NJOY. JEFF-3.3 library.

(2) Probability tables.

In addition to self-shielded cross sections, Monte Carlo codes usually also make use of probability tables in the unresolved resonance range. These probability tables contain a number of cross section values and the probability of the value of the cross section being less than this value. Both NJOY and AMPX produce probability tables for the most relevant cross sections (total, elastic scattering, fission and capture) but, contrary to the case of the Bondarenko cross sections, the procedures to obtain them are different [Dunn 2002] and hence the results provided can be expected to differ between the codes.

NJOY writes the probability tables in the PENDF format under the MF=2/MT=153 label. In addition to the reactions previously listed, NJOY also provides probability tables for the heat production, values that are not produced by AMPX. Hence, when AMPX results are written in the PENDF MF=2/MT=153 format, these values are written as zero. However, these values are not required for the criticality calculations. A feature shared by AMPX and NJOY is that the values of the different cross sections listed in the probability tables share the same probability values, i.e. the cross-section values are adjusted to correspond to the same set of probabilities for all nuclear reactions listed in the probability tables. On the other hand, one feature missing in NJOY that is present in AMPX is the capability to select equiprobable or non-equiprobable probability bands. In this work, the two options have been explored.

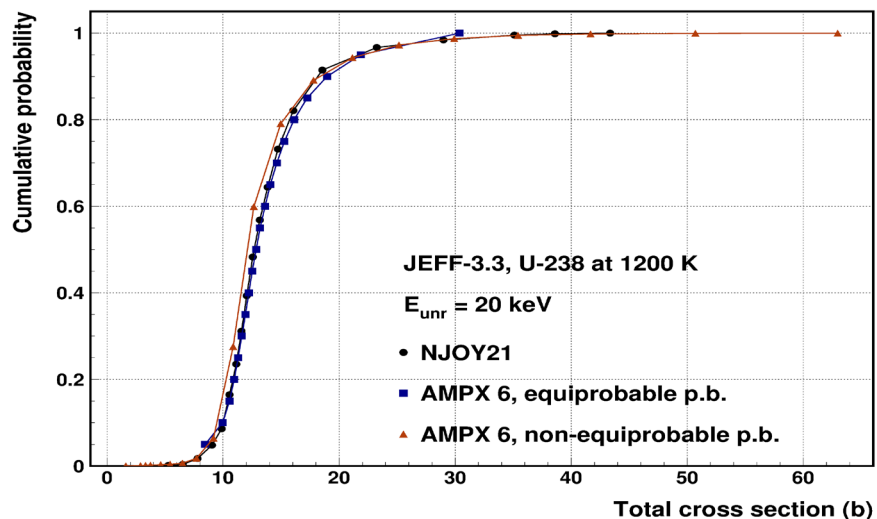
It should be mentioned as well that probability tables can be given in absolute or relative values. This is controlled by the LSSF option in the header of these data blocks. If LSSF=0, the values of the MF=2/MT=153 data block are absolute cross section values. If LSSF=1, the contents of the MF=2/MT=153 data block are relative values and have to be multiplied by the values of the cross sections in the MF=2/MT=152 block. In the case of the PENDF files produced from AMPX results, MF=2/MT=153 values are always written as relative cross section values (i.e. LSSF=1). In the ACE format, the equivalent parameter to LSSF is referred as IFF in [Conlin 2019].

Probability table processing results in a probability table for every energy value, cross section and isotope, which results in a large number of data and would be too extensive to include all them in this work. The temperature at which the cross section is processed also has to be taken into account. Hence, only two examples are presented in

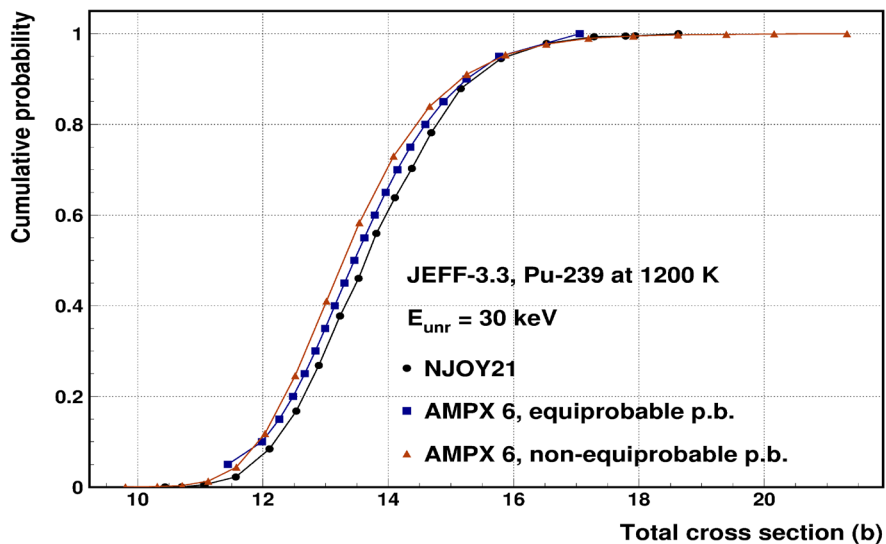
Figure 35, for two specific energies of ^{238}U and ^{239}Pu at 1200K, both taken from the JEFF-3.3 library. As AMPX and NJOY provide different values of the probability band limits, the cumulative probability is presented instead of the probability density in order to facilitate the comparison between the two codes. For the case of AMPX, the values obtained with both equiprobable and non-equiprobable probability bands are shown.

In general, although some differences between AMPX and NJOY can be observed, no major difference or general trend between the two codes is apparent concerning the probability tables, and a major difference is not to be expected between transport calculations performed with data produced with AMPX or NJOY.

In any case, and in view of the discrepancies reported in [Jiménez-Carrascosa 2019], the same calculations carried out in this work have been repeated using URR cross sections processed both with NJOY and AMPX, and both with the JEFF-3.3 and ENDF-VII.1 nuclear data libraries [Chadwick 2011]. The system consists of a simplified, two-dimensional model of an SFR (Sodium Fast Reactor) fuel rod, consisting of MOX fuel (at 1200 K), iron cladding and sodium coolant (both at 900 K). Reflecting conditions are applied at the model boundaries. The criticality constant of the system obtained calculated with MCNP 6.2 using URR data produced with NJOY, AMPX (both with equiprobable and non-equiprobable probability bands) and omitting the URR treatment are presented in **Table 15**. It can be observed the difference in the results due to the use of NJOY or AMPX to process URR data is rather small (~ 10 pcm), much smaller than omitting URR treatment in the calculation. Hence, the discrepancies observed in [Jiménez-Carrascosa 2019] seem not be due to any fundamental flaw in the way AMPX processes the unresolved resonances, it rather should lie in the way the transport codes use the processed data.



(a) U-238 at 1200K, $E_{unr}=20 \text{ keV}$



(b) Pu-239 at 1200K, $E_{unr}=30 \text{ keV}$

Figure 35. Two examples of cumulative probability vs. total cross section, extracted for the probability tables (JEFF-3.3).

Table 15. Criticality values obtained with NJOY and AMPX (equidistant and non-equidistant) probability tables and without probability tables treatment.

	ENDF-VII.1		JEFF-3.3	
	Result	Diff. (pcm)	Result	Diff. (pcm)
MCNP 6.2 + NJOY p. t.	1.31850± 0.00005	(ref)	1.32444± 0.00005	(ref)
MCNP 6.2 + AMPX p. t. (eq.)	1.31858± 0.00005	8 ± 7	1.32435± 0.00005	-9 ± 7
MCNP 6.2 + AMPX p. t. (non-eq.)	1.31866± 0.00005	16 ± 7	1.32458± 0.00005	14 ± 7
MCNP 6.2 (phys:n iunr=1)	1.31676± 0.00005	-174 ± 7	1.32278± 0.00004	-166 ± 6

2.6. Review of NJOY code: LRF7 option for reconstruction of angular distributions

This section presents the current status of processing activities on the reconstruction of the angular differential cross-sections (MF4) from resonance parameters (RPs) of the Reich-More Limited format (LRF=7) using NJOY code. NJOY2016 code is used for the reconstruction the angular differential cross-sections from resonance parameters using LRF7 formalism [JEF/DOC-2211, 2022], [IAEA/TM/Processing, 2022].

Firstly, a list of isotopes including LRF=7 in recent evaluations is given in **Table 16**.

Table 16. Evaluated files in recent evaluations using LRF=7

JEFF-3.3*	ENDF/B-VIII.0	JENDL-5.0
17-Cl-35	17-Cl-35	17-Cl-35
	20-Ca-40	26-Fe-54
	26-Fe-54	26-Fe-57
	26-Fe-57	
	29-Cu-63	
	29-Cu-65	
	74-W-182	
	74-W-183	
	74-W-184	
	74-W-186	

The LRF7 formalism is introduced to allow the inclusion of additional channels, *such as the inelastic channels, charged-particle channels, etc ...*, beyond the usual total, scattering, capture, and fission cross sections. Furthermore, LRF7 allows the reconstruction of the angular distribution of the outgoing particles relative to the incoming particles from the RPs [L.Leal, 2016].

The following **Figure 36** shows a comparison of EXFOR data and MF4 with and without reconstruction with LRF7.

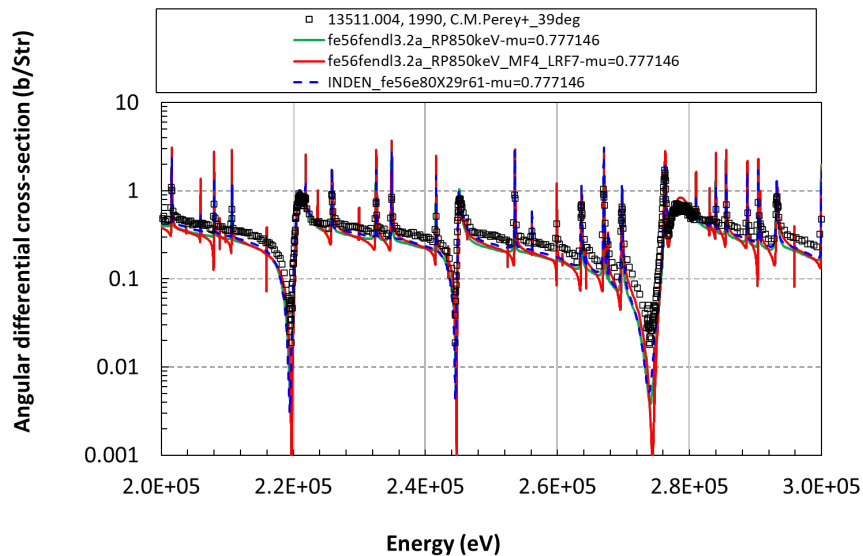


Figure 36. $^{56}\text{Fe}/\text{RPs-850keV}: 39 \text{ deg} / 200\text{keV} - 300\text{keV}$.

2.7. Processing covariances

This section is devoted to the procedure for processing covariance data which has been extensively presented in the following References: [JEFFDOC-2062], [JEFFDOC-2109], [SG46/CSEWG, November 2021], [SG46/Cov, December 2021], [SG46/TAR, December 2021], [ND2022/TAR, 2022].

This work is performed with NJOY2016.63 [NJOY, 2016], and it covers the processing of different nuclear data files:

- MF31: prompt a delayed neutron multiplicity
- MF32/MF33: cross-sections
- MF34: angular distributions
- MF35: Energy distributions

We have used and energy structure of 7 energy groups (see **Table 17**) - weighting IWT8 (for fast reactors). For energy distributions of prompt neutron fission spectra we have used an incident neutron energy (E_{in}) of 100keV.

Table 17. WPEC/SG46 Energy group structure- 7 energy groups

Group #	Lower Energy (eV)	Upper Energy (eV)	Comment
1	$2.23130 \cdot 10^6$	$1.96403 \cdot 10^7$	Above threshold fertile
2	$4.97871 \cdot 10^5$	$2.23130 \cdot 10^6$	Above threshold inelastic
3	$6.73795 \cdot 10^4$	$4.97871 \cdot 10^5$	Continuum to URR
4	$2.03468 \cdot 10^3$	$6.73795 \cdot 10^4$	URR
5	$2.26033 \cdot 10^1$	$2.03468 \cdot 10^3$	RRR
6	$5.40000 \cdot 10^{-1}$	$2.26033 \cdot 10^1$	EPITHERMAL
7	$1.40000 \cdot 10^{-5}$	$5.40000 \cdot 10^{-1}$	THERMAL

Covariances are generated in formats: BOXER, ERROR (and COVERX). An example of such covariances is presented for the isotopes: ^{10}B , ^{16}O , ^{52}Cr , ^{56}Fe , ^{58}Ni , $^{235,238}\text{U}$, $^{239,240,241}\text{Pu}$, $^{206,207,208}\text{Pb}$, ^{23}Na .

The processed covariances can be found at: <https://oecd-nea.org/download/wpec/sg46/materials/>

An example of NJOY input for processing MF33 is given in **Figure 37**. Correlations between different reactions can be also processed, see **Figure 38**.

```

groupr /
21 24 0 31/
  9237 1 0 8 0 1 1 1 /
'GENDF- 7g' /
300.0
1.E10
7 /
1.00000E-05
5.40000E-01
2.26033E+01
2.03468E+03
6.73795E+04
4.97871E+05
2.23130E+06
1.9640E+07 /
3/
3 18/
3 251/
3 452 nubar_t/
3 455 nubar_d/
3 456 nubar_p/
5 455 nubar_spc/
0/
errorr
21 0 31 77 /
  9237 1 2 1 1 1 /
1 300.0 /
0 33 /
7 /
1.00000E-05
5.40000E-01
2.26033E+01
2.03468E+03
6.73795E+04
4.97871E+05
2.23130E+06
1.9640E+07 /
covr
77 0 81 /
1/
/
/
  9237 0 0 0 /
viewr
81 82
covr
77 78 /
4 1
'LIB_JEFF33
'BOXER format'/
  9237 0 0 0 /
stop

```

Figure 37. Processed covariance data for $^{238}\text{U}(n,\gamma)$

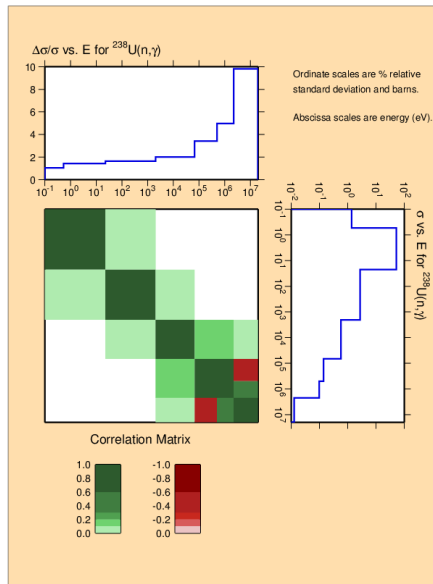
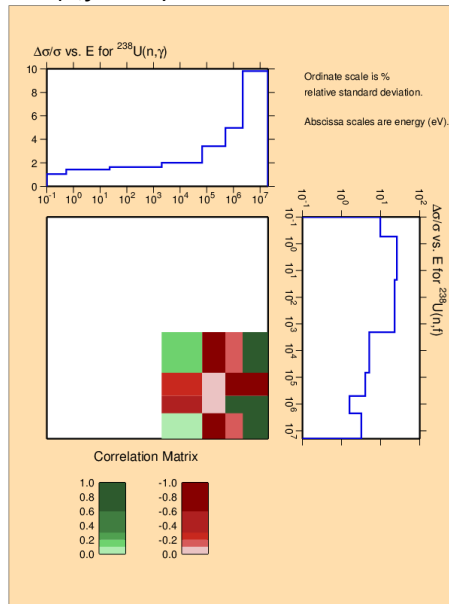


Figure 38. Processed covariance data for $^{238}\text{U}(n,\gamma)$ - $^{238}\text{U}(n,fission)$



This work has identified potential issues/problems in covariance data, see an example in **Table 18**.

Table 18. List of issues in JEFF-3.3 covariance data

ND Evaluation	Large processed uncertainties (> 100%)	Lack of ND covariances	Processed null
JEFF-3.3	B10(n,n') – g=2 U238(n,elasticP1) – g=6,7	No MF31 <ul style="list-style-type: none"> • Pu240 No MF33 <ul style="list-style-type: none"> • Pb206(n,p), Pb206(n,alpha) • Pb207(n,p), Pb207(n,alpha) • Pb208(n,p), Pb208(n,alpha) No MF34 <ul style="list-style-type: none"> • B10 • O16 • Na23 • Cr52 • U235 • Pu239, Pu240 No MF35 <ul style="list-style-type: none"> • Pu240 	Processed null values <ul style="list-style-type: none"> • B10(n,alpha) –g=1 • B10(n,n') - g=3-7 • Cr52(n,n') - g=3-7 • Ni58(n,alpha) – g=3-7 • Ni58(n,p) –g=3-7 • Fe56(n,alpha) –g=2-7 • U235(n,n') – g=5 • Ni58(n,elasticP1) –g=3-7 • Pu241(n, elasticP1) –g=6-7

2.8. Uncertainty quantification JEFF-3.3 outliers

The prediction of uncertainty in keff for some ICSBEP outliers identified in the JEFF-3.3. paper (Table 35, published in Eur. Phys. J. A (2020) 56:181) was carried out using the JEFF-3.3 covariance data. This work was presented in JEFF Meeting, April 2020. [JEFDOC-1991]

See **Table 19**, it shows a list of materials refers to non-actinide materials with C/E off by more than 3 experimental standard uncertainties.

Table 19. TABLE 35 presented in Ref-JEFF-3.3 paper [Plompen, 2020]

mat.	N	Cases
PE	2	lmt5-1 , pmf31-1
D ₂ O	1	hst20-5
Be&BeO	5	hmf9-2, hst46-1 , pmf21-2 , hmf38-1, hci4-1
C	3	hmf19-1, hmi6-3, hst46-1
F	2	hmf7-32 , hst20-5
Al	3	hmf70-1 , imf6-1, lmt5-1
concrete	1	hst7-1
S	1	hst46-1
Steel	4	hmf13, hmf7-1, lct34-17, hmi1-1
Cu	2	hmf73 , hmi6-1
Er	1	lmt5-1
Hf	1	lct29-8
W	2	umf4-2 , hmf70-1
Pb	5	hmf57-2, lct27-1 to -4,
Th	1	pmf8-1
Np	1	smf8-1

NOTE: Non-actinide materials (mat.) featuring in outliers of the NEA and IRSN suites. N is the number of cases. Bold are cases off by more than 3 experimental standard uncertainties.

Calculations performed with NDaST using JANIS Database for JEFF-3.3 covariances are shown in **Table 20**. These values show that “ND Uncertainty” is greater than “3* Exp. Uncert”, so there is still room for nuclear data improvement.

Table 20. Uncertainty in keff due to nuclear data in TABLE 35-JEFF-3.3 paper

#	Case	Benchmark	Exp. Uncert (pcm)	ND Uncertainty (pcm)	Contribution to keff Uncertainty ~ only diagonal terms (in pcm)	
1	Np	SMF8-1	338	1143	235U ~ 923pcm	237Np ~ 493pcm
2	Th	PMF8-1	115	677	239Pu ~ 647pcm	232Th ~ 317pcm
3	Pb	HMF57-2	232	1294	235U ~ 1130pcm	Pb ~ 223pcm
		LCT27-1	164	820	235U ~ 768pcm	Pb ~ 186pcm
		LCT27-2	137	817	235U ~ 769pcm	Pb ~ 164pcm
		LCT27-3	164	817	235U ~ 774pcm	Pb ~ 142pcm
		LCT27-4	165	807	235U ~ 768pcm	Pb ~ 116pcm
4	W	UMF4-2	80	*		
		HMF70-1	138	1619	235U ~ 1444pcm	W ~ 268pcm
5	Hf	LCT29-1	145	863	235U ~ 831pcm 238U ~ 156pcm	Hf ~ 22pcm
6	Er	LMT5-1	60	*		
7	S	HST46-1	290	*		
8	Concrete	HST7-1	381	1054	235U ~ 1036pcm	Fe ~ 108pcm
9	Cu	HMF73	164	1409	235U ~ 1188pcm	Cu ~ 499pcm
		HMI6-1	85	1346	235U ~ 1213pcm	Cu ~ 458pcm
10	Fe	HMF13	154	1291	235U ~ 1125pcm	Fe ~ 249pcm
		HMF7-1	240	1267	235U ~ 1134pcm	Fe ~ 0pcm
		LCT34-17	536	774	235U ~ 733pcm 238U ~ 162pcm	Fe ~ 23pcm
		HMI1-1	283	1748	235U ~ 1543pcm	Fe ~ 0pcm
11	Al	HMF70-1	138	1622	235U ~ 1444pcm	Al ~ 279pcm
		IMF6-1	247	1542	235U ~ 1229pcm 238U ~ 430pcm	Al ~ 391pcm
		LMT5-1	60	*		
12	F	HMF7-32	123	1277	235U ~ 1125pcm	F ~ 179pcm
		HST20-5	783	750	235U ~ 736pcm	F ~ 2pcm
13	C	HMF19-1	292	1259	235U ~ 1114pcm	
		HMI6-3	95	1458	235U ~ 1301pcm	
		HST46-1	290	*		
14	Be	PMF21-2	267	559	239Pu ~ 594pcm	
		HMF9-2	157	1268	235U ~ 1119pcm	
		HMF38-1	75	1531	235U ~ 1264pcm 238U ~ 342pcm	
		HCI4-1	413	1381	235U ~ 1436pcm	
		HST46-1	290	*		
15	D2O	HST20-5	783	4340	235U ~ 736pcm	D(n,el) ~ 4258pcm 16O(n,el) ~ 478pcm
16	PE	LMT5-1	60	*		
		PMF31-1	235	874	239Pu ~ 535pcm	2D(n,el) ~ 757pcm

NOTE: * No sensitivities in NDaST

3. Sensitivity analysis and uncertainty propagation

This work is focused on the sensitivity calculations in criticality, shielding, decay heat and spent nuclear fuel/burnup calculations.

3.1. For fission yields on decay heat calculations

Detailed studies of the impact of recent TAGS (Total Absorption Gamma Spectroscopy) measurements on the calculated Light Particles and Electromagnetic decay heat components of different fission-based systems were performed in [Nichols, 2023, plus deliverable decay data in SANDA]. To disentangle the impact of the decay data and fission yields libraries, some decay heat calculations were also carried out with the Serpent2 code [Leppänen, 2015] for systems with existing experimental decay-heat measurements on neutron pulse irradiations: ^{239}Pu thermal, ^{241}Pu thermal, ^{235}U thermal, ^{233}U fast, ^{237}Np fast and ^{238}U fast fission. Pulse irradiation decay-heat data for single-actinide targets were obtained from the IAEA CoNDRER database [CoNDRER, 2021].

For each fission-based systems, decay heat calculations were repeated with the same JEFF-3.3 decay data sub-library combined with three different fission-yield sub-libraries: ENDF/B-VIII.0, JEFF-3.3 and JENDL-5. Cases with some clear differences due to the choice of the fission-yields sub-libraries are shown on Figure 39 to Figure 42. For the electromagnetic component of ^{239}Pu and ^{241}Pu thermal fission, the adoption of the ENDF/VIII.0 and JEFF-3.3 fission-yield sub-libraries gives similar results and agrees reasonably well with the decay heat measurements, while the JENDL-5 fission-yield sub-library leads either to an under or overestimation in the 1-100s cooling range. At the opposite, the adoption of JENDL-5 leads to a significant improvement for the light particle decay heat of ^{238}U fast fission at cooling times between 1 and 10s. All three fission-yield sub-libraries give similar results for ^{237}Np fast fission at cooling times greater than 80s, while ENDF/B-VIII.0 deviates from JEFF-3.3 and JENDL-5 at shorter cooling times between 3 and 50s.

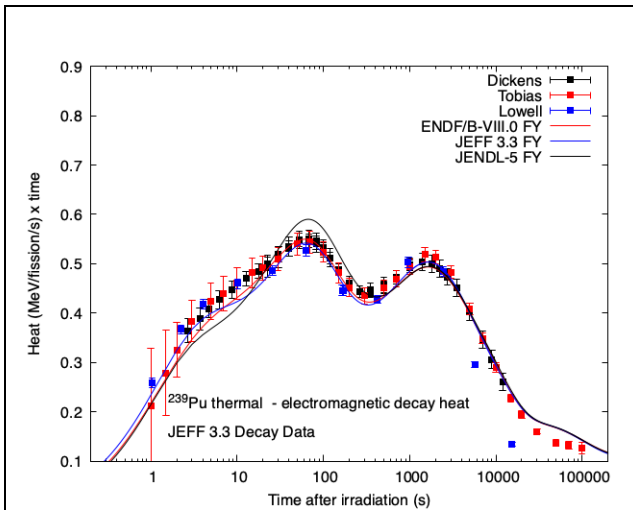


Figure 39. Comparison of electromagnetic decay heat of ^{239}Pu thermal fission obtained from the calculations with the JEFF-3.3. decay data sub-library and three fission-yield sub-libraries (ENDF/B-VIII.0, JEFF-3.3. and JENDL-5)

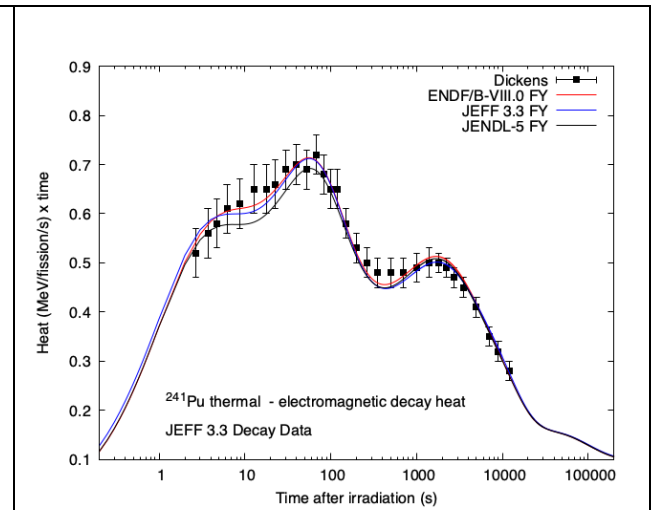
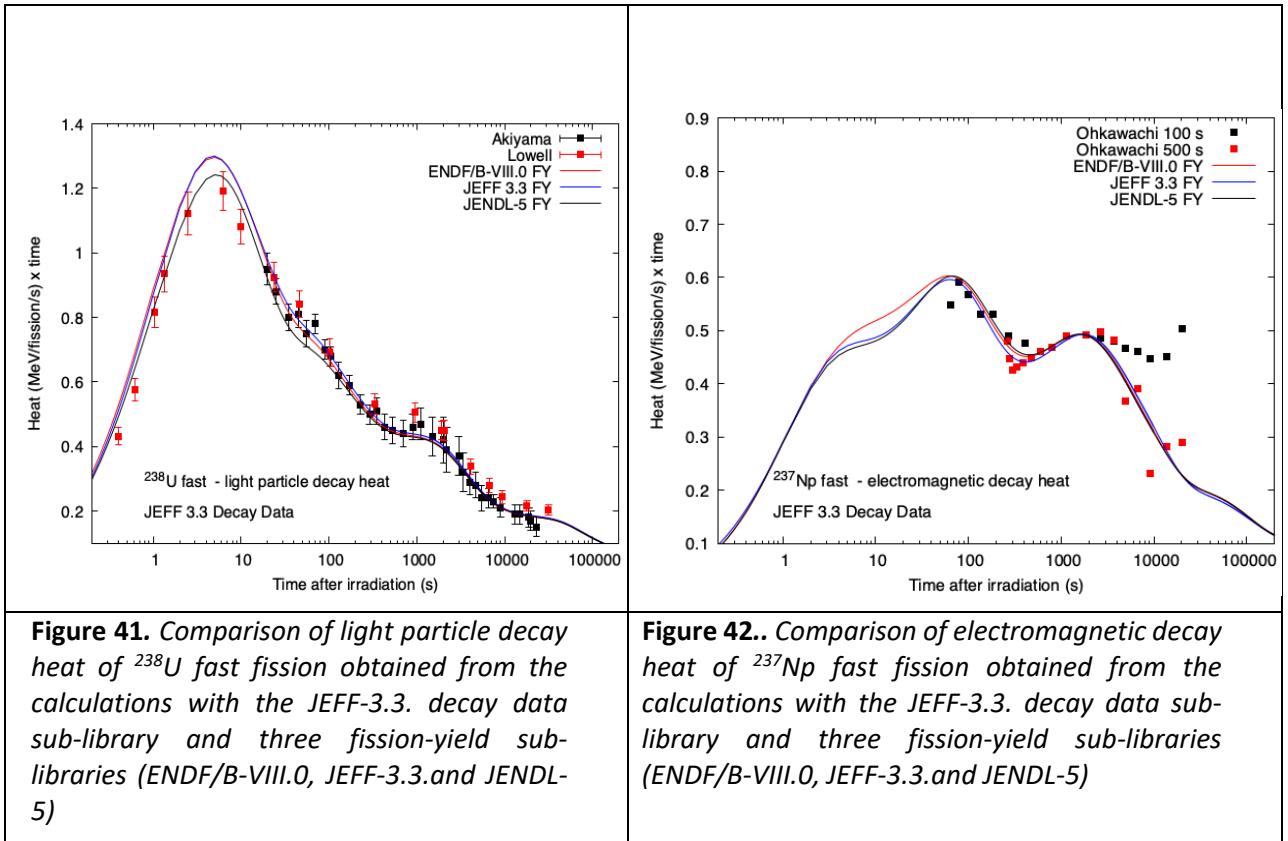


Figure 40. Comparison of electromagnetic decay heat of ^{241}Pu thermal fission obtained from the calculations with the JEFF-3.3. decay data sub-library and three fission-yield sub-libraries (ENDF/B-VIII.0, JEFF-3.3. and JENDL-5)



The COCODRILO code, based on the use of the Monte-Carlo method, is under development at SUBATECH to study the impact of fission yields on the uncertainty of decay heat for both thermal fission pulses. COCODRILO is a set of python scripts, which allows to read fission yields from JEFF or ENDF libraries at the ENDF-B6 format, to produce a number N of independent fission yields with Gaussian sampling or using available covariance matrices and which are then coupled to N depletion calculations.

For the moment, COCODRILO is coupled to the evolution code SERPENT2 but developments have been made in order to easily allow the use of other evolution codes such as OPENMC which is also foreseen in the future. An optimization of the scripts has been realized in order to reduce the computation time and the memory space needed at the IN2P3 computing center, associated with an automatic extraction and plotting of the results. An example is presented on **Figure 43** for the calculation of the ^{239}Pu decay heat with a sample of 10^3 independent fission yield files produced with a Gaussian sampling in the variances associated with the fission yields evaluation for JEFF3.1.1.

The code is currently under development to take into account different covariance matrices for fission yields and then to be applied to the case of thermal fission pulse cases of ^{235}U and ^{239}Pu (part of the PhD thesis of Y. Molla 2021-2024, Subatech).

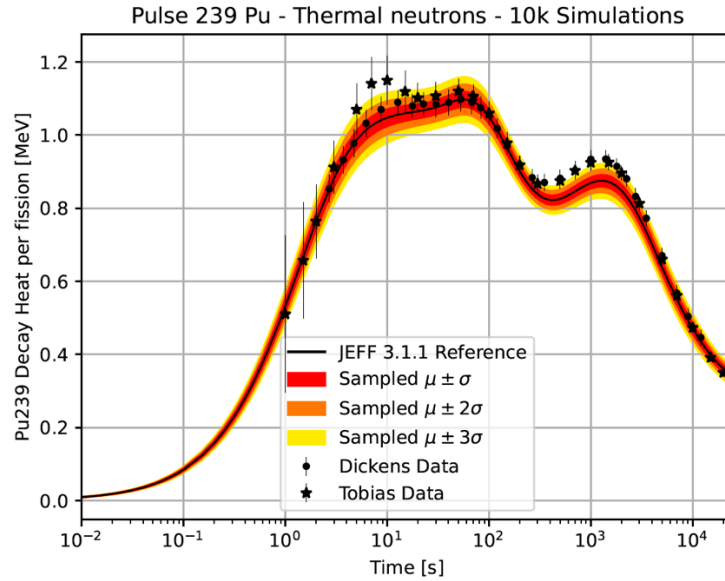


Figure 43. Impact of JEFF-3.1.1 fission yields uncertainties on ^{239}Pu decay heat produced with the COCODRILO code (Monte Carlo approach with Gaussian sampling in the variances).

3.2. Impact of recent TAGS data on reactor antineutrino calculations

Reactor antineutrinos still suffer from several anomalies (the reactor anomaly [Mention, 2011] and the shape anomaly [An, 2017]) and the study of nuclear data could help solving these puzzles which have impact not only on fundamental neutrino physics but also on neutrino applied physics [INDC0786, 2019].

Detailed studies of the impact of TAGS (Total Absorption Gamma Spectroscopy) measurements on the reactor antineutrino spectra from $^{235,238}\text{U}$ and $^{239,241}\text{Pu}$ fuels have been performed as soon as 2012 in [Fallot, 2012]. In this paper was published an updated version of our summation calculations developed since 2008 for antineutrino energy spectra prediction in which we quantified the relative impact of 7 nuclei measured in 2007 [Algora, 2010] and corrected for Pandemonium effect [Hardy, 1977] on the spectra [Fallot, 2012]. The ratios of the antineutrino spectra computed with our model including the 7 nuclei Pandemonium free over the same calculation performed using older Nuclear DataBases (NDB) for those nuclei for the 4 fissile nuclei present in the reactor core exhibited a noticeable deviation from unity [Fallot, 2012]. And it was later shown that this behaviour is systematic, correcting for Pandemonium free data. The effect is to increase the spectra before 2-3 MeV and decreases it above in the energy region which dominates the flux. The limits of this systematic behaviour depends on the Q values of the nuclei involved.

So far, two TAGS experimental campaigns have been carried-out in 2009 and 2014 at IGISOL in Jyväskylä with main motivations decay heat and reactor antineutrino physics. For the first time, a total absorption spectrometer (TAS) has been coupled to a double Penning trap (JYFLTRAP) in order to obtain sources of very high isobaric purity. Two different TAS, both segmented, were used for those campaigns. In 2009, Rocinante has been used. It was made of 12 BaF_2 crystals of very good efficiency which was coupled with a silicon detector for β coincidences. In 2014, the DTAS was used for the first time. It was constituted of 16 to 18 NaI crystals and was coupled to a plastic detector for β coincidences. At the end of the day, roughly 30 nuclei were measured of first interest for reactor physics.

With respect to our predictions in 2012, we have then quantified the cumulative impact of the TAGS beta intensities of the other nuclei measured in these campaigns in [Estienne, 2019] and then in the frame of this European project in [Algora, 2021] and [Guadilla, 2022].

In [Estienne, 2019], was studied the absolute impact of a decade of TAGS measurements on the calculated antineutrino energy spectra updating our summation model. Among other modifications not commented here, we have step by step included in the calculations the nuclei of the campaigns 2009 and 2014 analyzed and published over 10 years. The total antineutrino inverse beta decay yields have then been computed for the different summation models called SM2012, SM2015, SM2017 and SM2018 (which stands for “Summation Model” followed by the year of publication of the TAGS decay data added in the calculations) as a function of the ^{239}Pu fraction of fission. The result is presented in Fig 2 from [Estienne, 2019]. We observed a systematic reduction of the detected flux correcting for pandemonium free data. And also a systematic reduction of the discrepancy with the Daya Bay results quoted in the figure with the small diamonds, reaching a 1.9% which does not leave much room for the reactor anomaly. We show in [Estienne, 2019] that the discrepancy will inevitably reduce with the inclusion of future TAGS data leaving less room for the reactor anomaly in flux.

In [Algora, 2021] have been computed the cumulative impact of the TAGS beta intensities of the nuclei measured with the Rocinante detector at Jyväskylä in 2009 on the antineutrino spectra generated after the thermal fission of ^{235}U , ^{239}Pu and ^{241}Pu , and fast fission of ^{238}U . It is presented in figure 44 with respect to the spectra built with the most recent NDB for the same nuclei and containing only TAGS data from [Greenwood, 1997]. The decrease of the 2 plutonium spectra above 1.5 MeV is remarkable, reaching 8%. The impact on the two uranium isotopes amounts to about 2% and 3.8% in the 3 to 4 MeV range in ^{235}U and ^{238}U respectively.

The cumulative impact of the nuclei measured in 2014 in Jyväskylä with the DTAS detector has been studied as well and presented in figure 45. It has shown an important deviation from unity in the energy range of interest for the shape anomaly. The consideration in the calculation of the 2 niobium $^{100,102}\text{Nb}$ in particular and their isomers corrected for Pandemonium bias implied a strong decrease of the spectra peaked at 4.5 MeV and a strong increase at 6.5 MeV, in the region of the shape distortion. However, it was not enough to fully explain the observed shape anomaly.

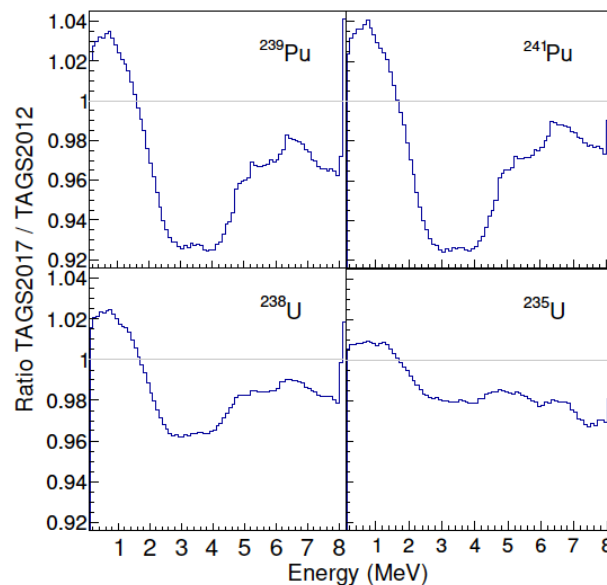


Figure 44. Impact of the TAGS measurements for $^{86-88}\text{Br}$ and $^{91,92,94}\text{Rb}$ from [Valencia, 2017][Rice, 2017] on the summation calculations for reactor antineutrino spectra based on the summation model from [Estienne, 2019]. Figure extracted from [Algora, 2021].

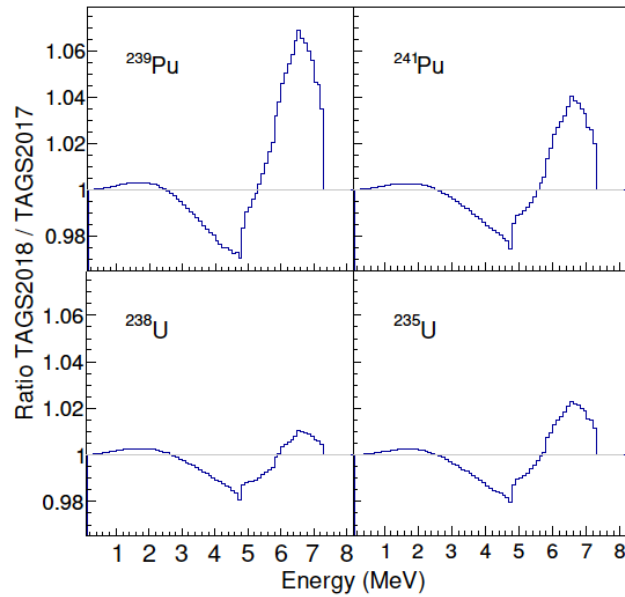


Figure 45. Impact of the TAGS measurements for 100,100m,102,102m Nb from [Guadilla, 2019] on the summation calculations for reactor antineutrino spectra based on the summation model from [Estienne, 2019].

More recently the impact of the new TAGS results from 96,96m Y measured in the second TAGS campaign in Jyvaskyla was studied and published in [Guadilla, 2022]. For several reasons the measurement of the decay of 96 Y ground state (gs) and isomer (m) is interesting :

For the decay heat first, the decays of both nuclei produce almost 5% of the DH around 10s after the thermal fission of 235 U. The ground state being of first priority for the IAEA experts in the case of U/Pu and Th/U fuels and the isomer being of priority 1 for Th/U fuel [Dimitriou, 2015].

Concerning reactor antineutrino spectra, the ground state of 96 Y is the second most important contributor to the spectra in the range of the bump.

Eventually, it has some interest for the study of the structure of the daughter 96 Zr which lies in a region of phase transition and emergence of shape-coexisting states.

The detailed description of the obtained new data is provided in the WP2 of the present project.

In this article, we report on the impact of the new measurement on the reactor antineutrino spectra. Only the data from 96m Y have been found to be suffering from the pandemonium effect. Its impact has been found to be small on antineutrino energy spectra calculation as it is a minor contributor in the 5-7 MeV range [Guadilla, 2022].

3.3. For fission yields on reactor antineutrino calculations

Estienne et al. collaborate with K.-H. Schmidt for several years with the purpose to use the GEF fission yields (FY) along with their uncertainties in order to perform the uncertainty propagation on summation calculations for reactor antineutrinos. First results have been obtained in the frame of this European project [Schmidt, 2021]. The main outcomes are:

- Antineutrinos are a very sensitive probe for fission yields. Indeed, the comparison of the first summation calculations performed with the GEF code that was tuned for decay heat calculations showed results very far from both the JEFF FY and integral antineutrino spectra as can be seen in figure 46.

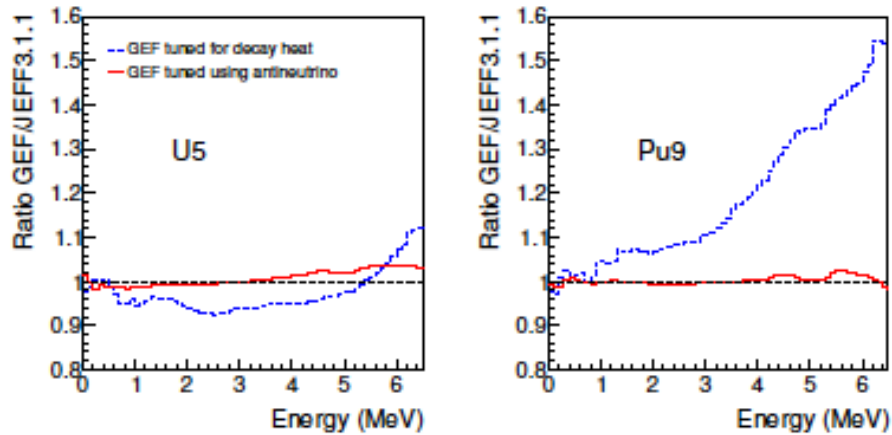


Figure 46. Relative ratios of reactor antineutrino spectra for ^{235}U and ^{239}Pu thermal fission obtained with the version of GEF tuned for the decay heat calculations (blue line), and then for reactor antineutrino calculations (red line) [Schmidt, 2021].

- A new version of the GEF code was obtained, improved thanks to the antineutrino spectral studies. The disagreement found above triggered a new careful and detailed study of the FY data for a large amount of fissioning systems [Schmidt, 2021]. It appeared that the antineutrino energy spectra are sensitive to some individual fission yields that influence less decay heat calculations. Both the decay heat and reactor antineutrino observables are thus complementary probes to test evaluated nuclear databases of FY.

An assessment of the experimentally available fission yields with the GEF model showed that the discrepancies between FY from JEFF3.1.1 and JEFF3.3 are not always understood as illustrated in figure 47 and 48. In figure 47, an example of comparison of the GEF mass FY with the JEFF3.3 FY for the ^{241}Pu thermal fission is displayed [Schmidt, 2021].

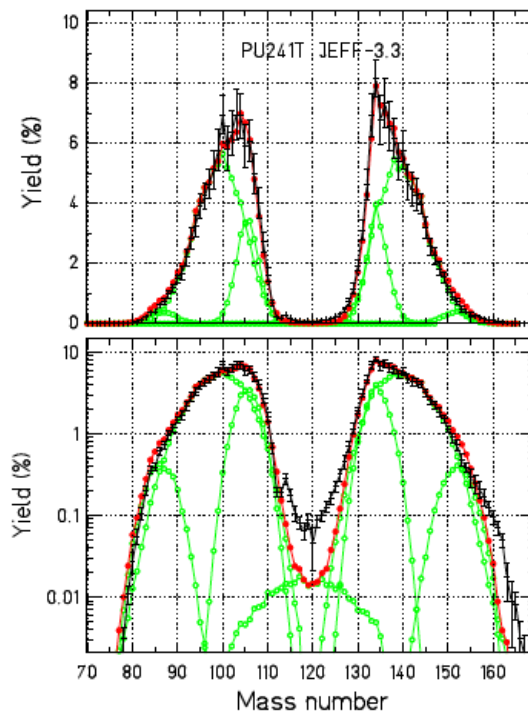


Figure 47. Mass yields of $^{241}\text{Pu}(n,f)$ in linear and logarithmic scale. GEF results are displayed with red points in comparison with JEFF-3.3 (black symbols) [Schmidt, 2021].

In **Figure 48**, the ratios between reactor antineutrino spectra computed with the JEFF3.1.1 (red) and JEFF3.3 (blue) FY over the GEF FY were studied and show discrepancies which are not well understood.

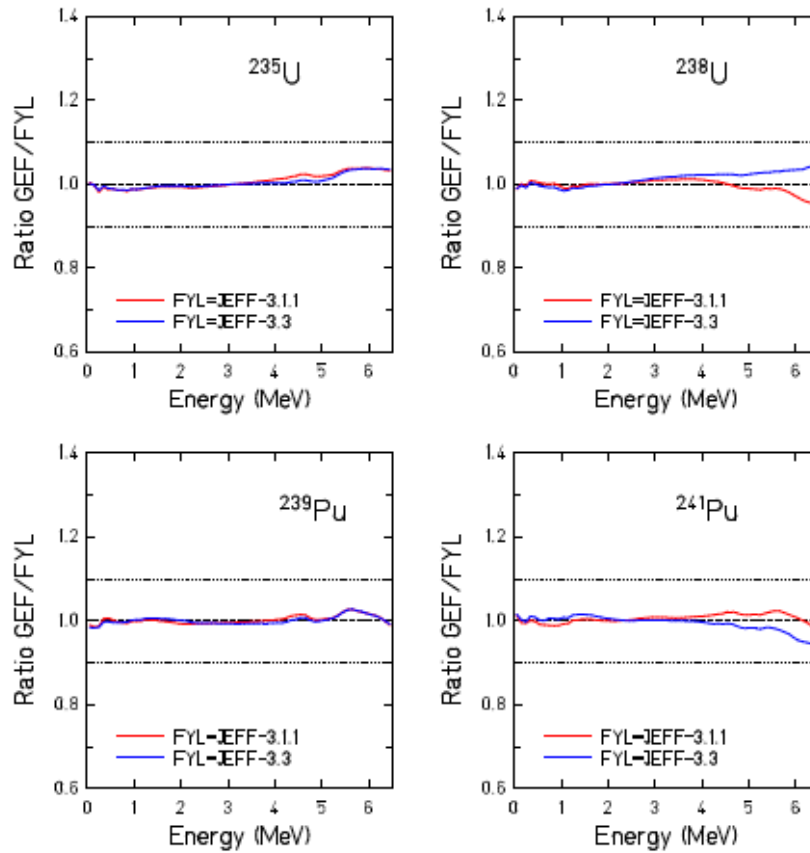


Figure 48. Relative ratios of reactor antineutrino spectra calculated with the JEFF3.1.1 (red) and JEFF3.3 (blue) fission yields over the one computed with the GEF fission yields [Schmidt2021].

- New predictions were obtained with the updated GEF version compared with the Daya Bay flux. The obtained agreement is now good enough to use the GEF code to propagate the FY uncertainties on the reactor antineutrino calculations.
- New predictions of actinide antineutrino spectra for Applications for thermal fissions were provided in [Schmidt2021].

3.4. For shielding applications on pulsed spheres

In this section, other important Benchmarks for nuclear data validation are studied, the LLNL pulsed spheres that are not yet in SINBAD database.

This sensitivity analysis undertaken provides further guidance on which nuclear data observables are contributing primarily to simulating pulsed-sphere spectra. The UPM work on sensitivity analysis in LLNL pulsed spheres³ is carried out with different techniques:

- MCSEN code [MCSEN,1996]:

³ Caution that not too strong conclusions should be drawn on the quality of nuclear data given the lack of UQ and Q&A on pulsed spheres

- MCSEN is able to operate on: cross-sections, nubar, CHI and MF4 and MF6
- Perturbation of cross-sections using FRENDY (cross-sections, nubar and CHI) and SANDY (cross-sections, nubar, CHI and MF4) codes
 - SANDY [**SANDY**]
 - SANDY perturbs either ENDF or PENDF files
 - Process ENDF/PENDF files into ACE format with NJOY
 - SANDY is able to operate on: cross-sections, nubar, CHI and MF4 (soon on MF6)
 - FRENDY [**FRENDY**]
 - FRENDY directly perturbs ACE files
 - FRENDY is able to operate on: cross-sections, nubar and CHI

This work has been presented in **WPEC/SG47 Meetings: [SG47, June 2019], [SG47, December 2020] and [SG47, May 2021]**.

An example of this work is the LLNL-235 pulsed sphere: U-235, 0.7 mfp, fwhm=2.0 ns, NE213-B bias=1.6, FP=945.54 cm, 26-deg (see **Figure 49**).

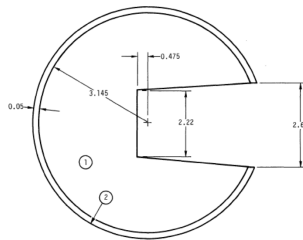


Figure 49. Dimensions of the small 235U solid spherical target ,Report: LLNL UCID-17332.

A short summary of the methodology is described as follows:

- This methodology can be applied for Pulsed Sphered Benchmarks for providing sensitivity profiles. ENDF/B-VII.1 is used to simulate sensitivity profiles. (Sensitivity profiles may not to change significantly from one library to another)
- FRENDY code is used for generating a perturbation set of the ACE formatted cross sections [**FRENDY/Perturb, 2019**]
 - “Types of reactions, energy ranges, and perturbation factor (multiplier) are provided as input to this capability in addition to the original (unperturbed) ACE file.”
In this work, a perturbation factor of +10% is used.
 - “A perturbed ACE file is generated on the basis of the input data. Note that multiple perturbations can be considered in the input file.”
In this work, multiple perturbation option is used to assess the impact of all discrete inelastic cross-sections (MT51 to MT90)
 - “The point-wise cross sections are uniformly perturbed within the specified energy range in input data.”
In this work, a 44-energy group structure is used for perturbed ACE files. Table 2 shows this energy structure.

- “The cross sections given as functions (number of neutrons generated per fission and fission spectrum) are perturbed after linearization and tabulation.”

In this work, number of neutrons generated per fission is assigned as MT452 (total nubar) and fission spectrum is assigned as MT1018.

- “Any nuclear reaction cross section, number of generated neutrons per fission and fission spectrum can be perturbed in the present capability.”

A list of reactions used in this work:

- MT1018 (PFNS),
- MT102 (n,gamma)
- MT103 (n,p)
- MT107 (n,alpha)
- MT18(n,fission)
- MT2(n,elastic)
- MT452 (nubar)
- MT4*(n, inelastic -only discrete levels)
- MT51 (n,inelastic-1st discrete level)
- MT91(n,inelastic-continuum)

- MCNP-6.1 is used for neutron transport calculations.

In this work, a comparison of sensitivity profiles calculated with MCSSEN code [MCSSEN, 1996] versus FRENDY is performed (see **Figure 50**).

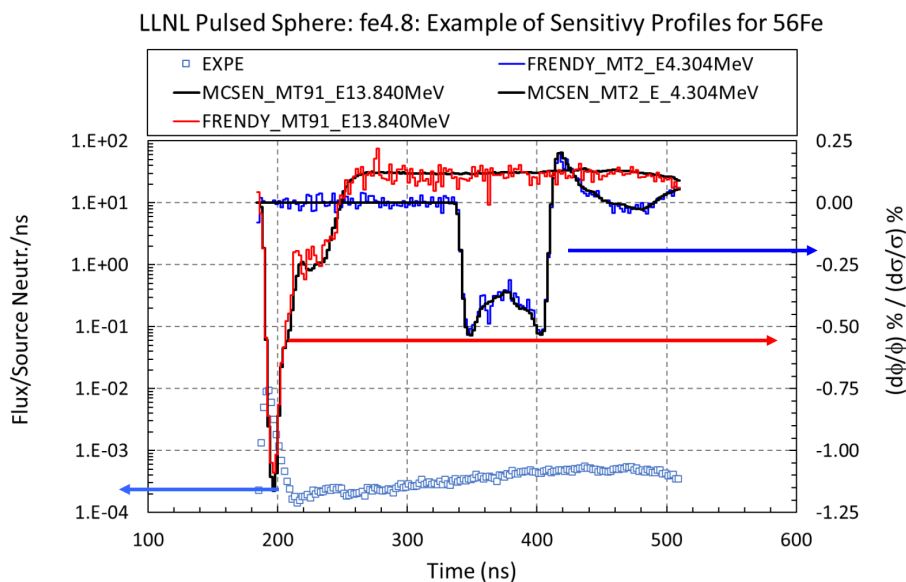


Figure 50. A comparison of sensitivity profiles calculated with MCSSEN code and FRENDY code for the iron-LLNL pulsed sphere with 56Fe (n,elastic) and (n,inelastic).

For LLNL pulsed spheres, sensitivity profiles of the spectra to nuclear data are calculated in order to understand in detail which isotopes, observables, and energy ranges of nuclear data contribute significantly to their simulation. Few selected spheres containing different materials, the neutron-leakage spectra is sensitive to:

- For spheres containing light elements (e.g. ^{16}O , ^{12}C) is mostly sensitive to elastic-and inelastic-scattering cross sections on discrete levels and corresponding angular distributions
- For spheres of structural materials (e.g. ^{56}Fe) are sensitive to elastic-and inelastic-scattering cross sections, including scattering on discrete levels and the continuum, and double-differential cross sections.
- For actinide spheres (e.g. ^{235}U , ^{239}Pu) are also strongly sensitive to the fission observables, in particular to the total-fission neutron spectrum (see **Figure 51**, **Figure 52** and **Figure 53**).

In regards of thickness:

- Thin spheres (in which neutrons experience on average less than one scatter) are mostly sensitive to data near the elastic peak, in the energy range from 12–15 MeV
- Thicker spheres can be sensitive to data at lower incident-neutron energies due to multiple-scattering effects

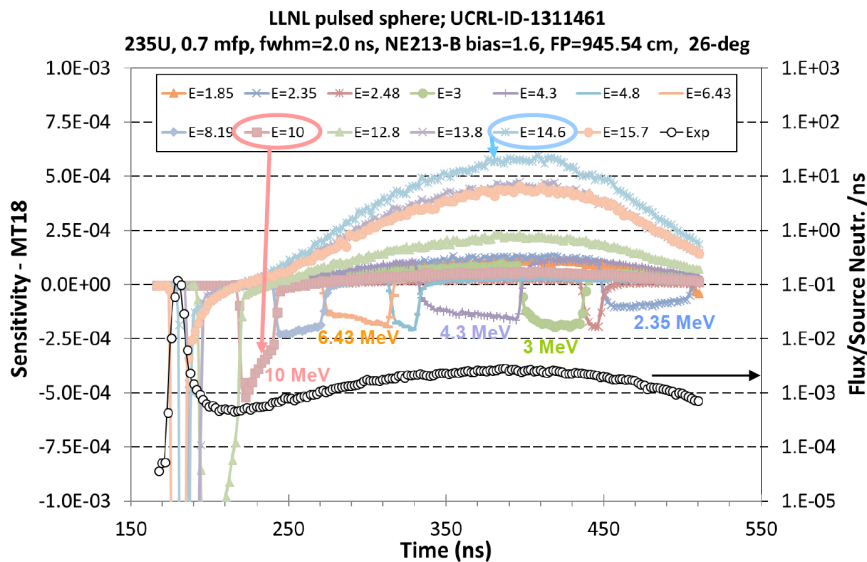


Figure 51. Sensitivity to $^{235}\text{U}(n,fission)$ in LLNL ^{235}U -pulsed sphere calculated with MCSSEN code [MCSSEN, 1996].

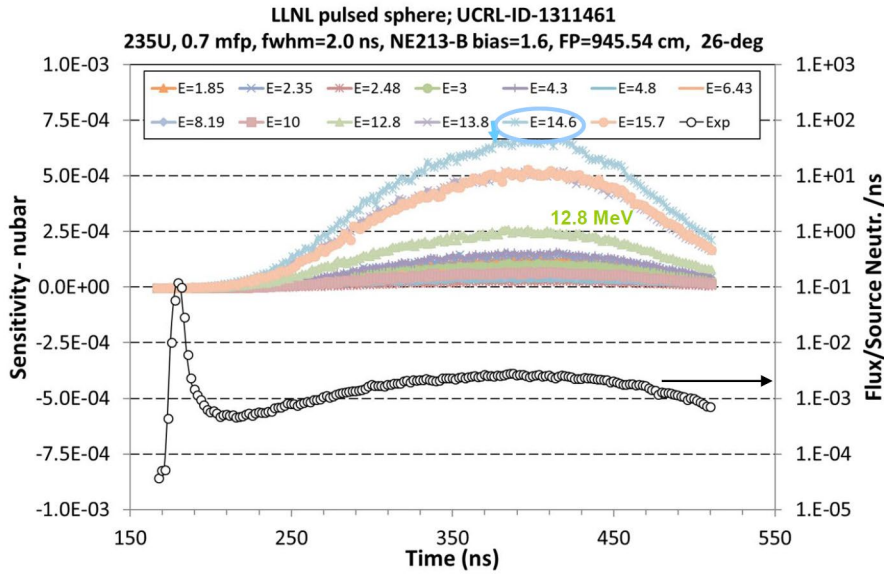


Figure 52. Sensitivity to $^{235}\text{U}(n,\bar{\nu})$ in LLNL ^{235}U -pulsed sphere calculated with MCSEN code [MCSEN, 1996].

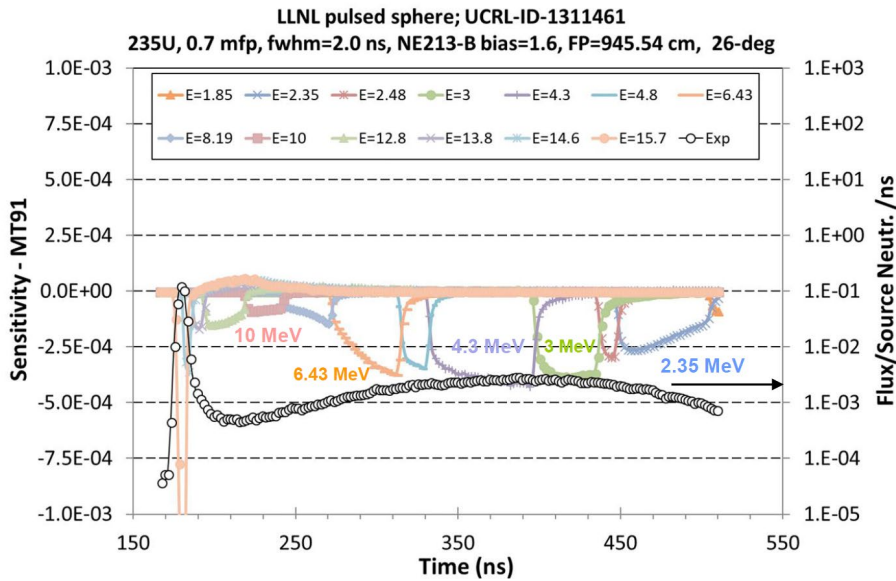


Figure 53. Sensitivity to $^{235}\text{U}(n,\text{inelastic-MT91})$ in LLNL ^{235}U -pulsed sphere calculated with MCSEN code [MCSEN, 1996].

It can be seen that the sensitivity of pulsed-sphere neutron-leakage spectra to PFNS (see **Figure 54**) is larger than to the nubar and (n,fission) (see **Figure 55**).

Figure 54 and **Figure 55** are calculated with FRENDY perturbation technique [JEF/DOC-2015, 2020].

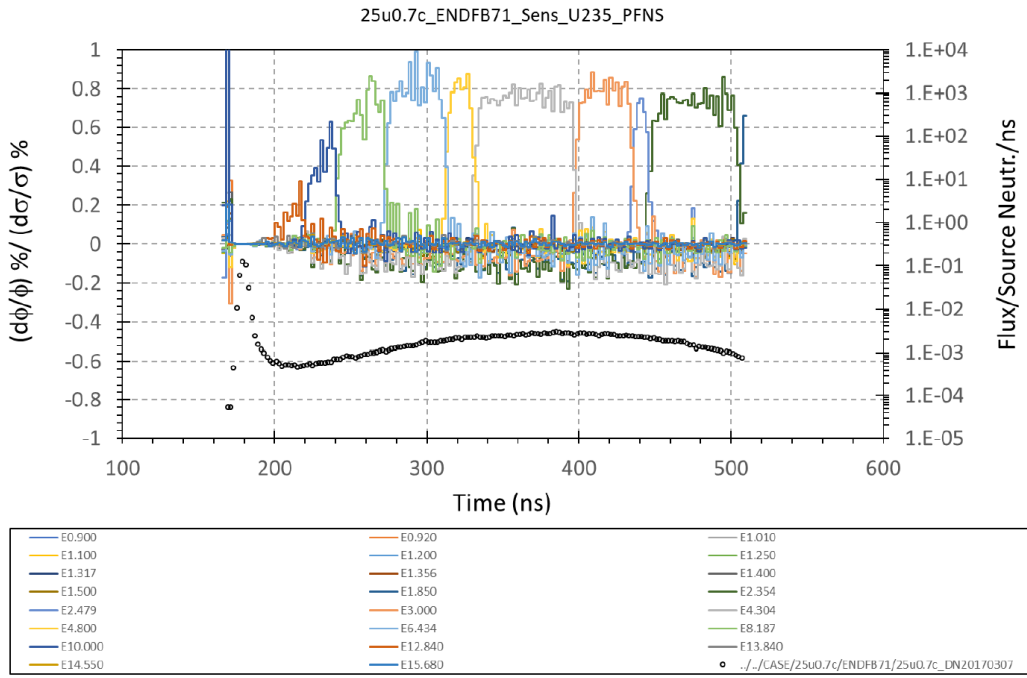


Figure 54. Sensitivity to ^{235}U (PFNS) in LLNL ^{235}U -pulsed sphere.

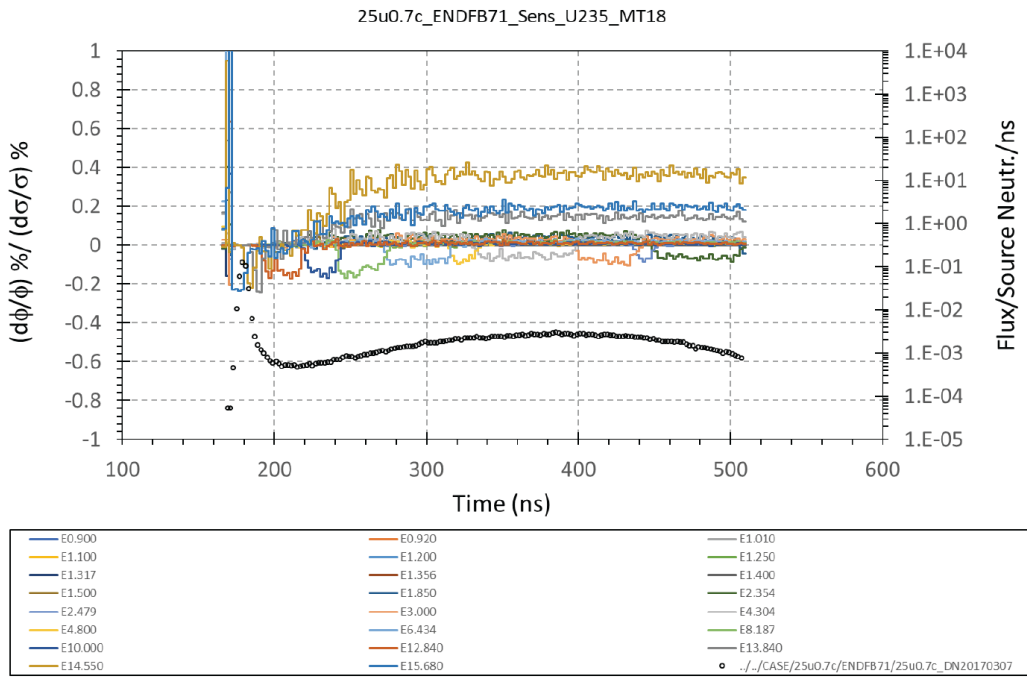


Figure 55. Sensitivity to ^{235}U (n,fission) in LLNL ^{235}U -pulsed sphere.

3.5. For transmission experiments

In this section, the IPPE neutron transmission experiments in ^{235}U material: FUND-JINR-1/E-MULT-TRANS-001/Vol.IX/ICSBEP are analysed. In these experiments, the explicit product of the experiments was the measurement of the energy-dependent self-shielded total and fission cross sections, as characterized by various self-shielded and unshielded total neutron count rates as well as self-shielded and unshielded fission rates performed using the time-of-flight technique. Self-shielding was varied systematically through the use of samples of different thicknesses [JEF/DOC-2015, 2020], [IAEA/INDEN-Actinides, 2020].

Results are shown in:

- Case 1 are shown in **Figure 56** and **Figure 57**
- Case 2 are shown in **Figure 58**
- Case 5 are shown in **Figure 59** and **Figure 60**
- Case 7 are shown in **Figure 61** and **Figure 62**

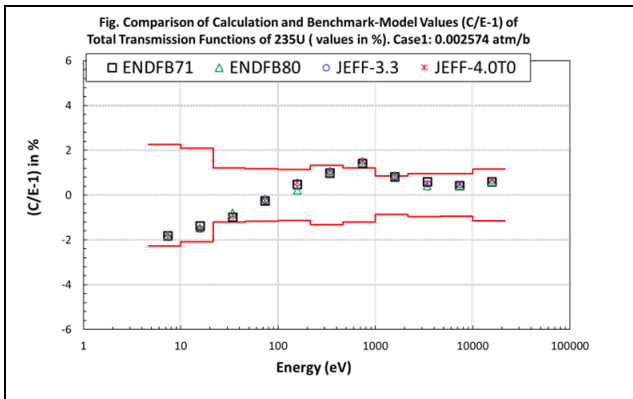


Figure 56. Values $(C/E-1)$ in % of ^{235}U -Total Transmission Function for sample 1(0.002574 atm/b)

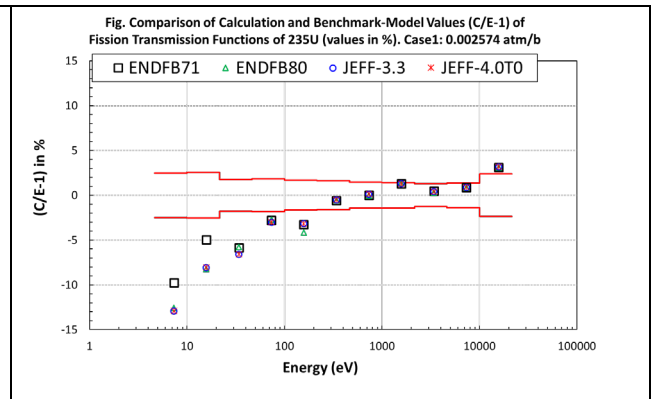


Figure 57. Values $(C/E-1)$ in % of ^{235}U -fission Transmission Function for sample 1(0.002574 atm/b)

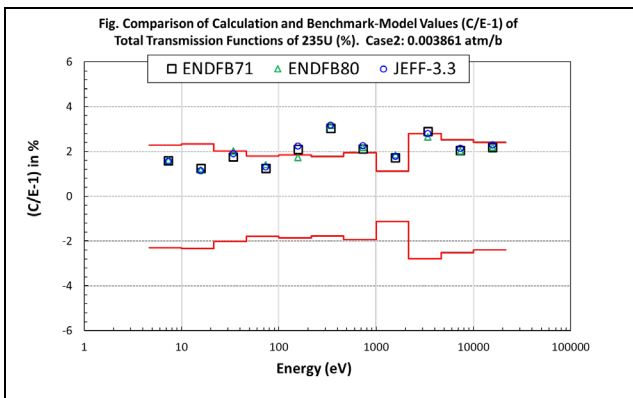


Figure 58. Values $(C/E-1)$ in % of ^{235}U -Total Transmission Function for sample 2(0.003861 atm/b)

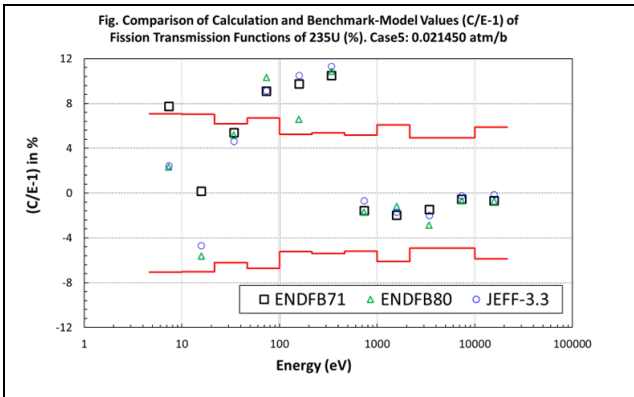


Figure 59. Values $(C/E-1)$ in % of ^{235}U -Total Transmission Function for sample 5(0.021450 atm/b)

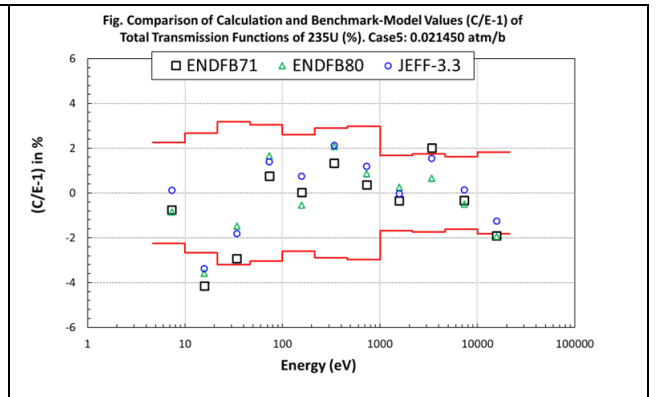


Figure 60. Values $(C/E-1)$ in % of ^{235}U -fission Transmission Function for sample 5(0.021450 atm/b)

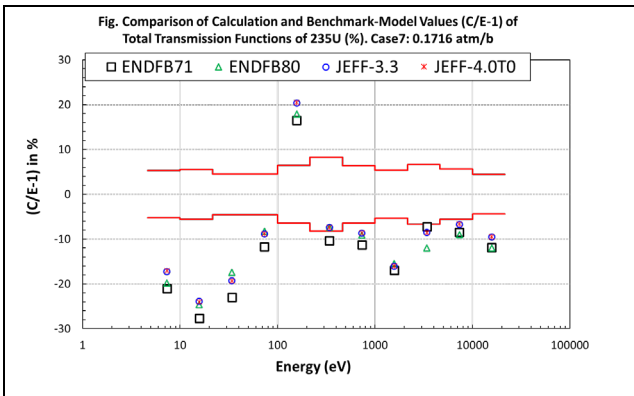


Figure 61. Values $(C/E-1)$ in % of ^{235}U -Total Transmission Function for sample 7(0.17160 atm/b)

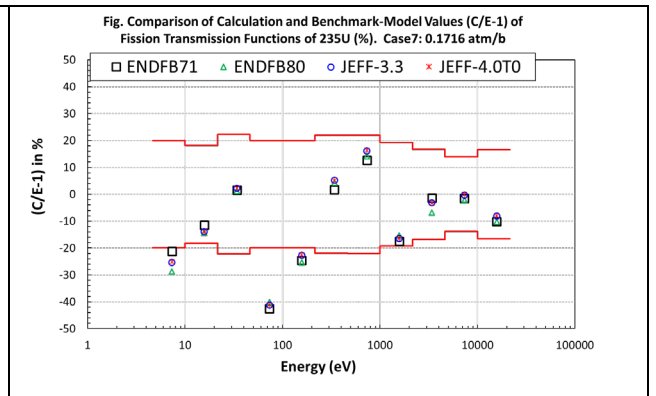


Figure 62. Values $(C/E-1)$ in % of ^{235}U -fission Transmission Function for sample 7(0.17160 atm/b)

The same procedure, based on perturbations of cross-sections using FRENDY, was used to provide sensitivities in the IPPE neutron transmission experiments.

Results are shown in:

- **Figure 63 to Figure 66** show the sensitivity profiles due to $^{235}\text{U}(n,\text{fission})$ and $^{235}\text{U}(n,\text{gamma})$ for this Sample 1.
- **Figure 67 to Figure 70** show the sensitivity profiles due to $^{235}\text{U}(n,\text{fission})$ and $^{235}\text{U}(n,\text{gamma})$ for this Sample 7.

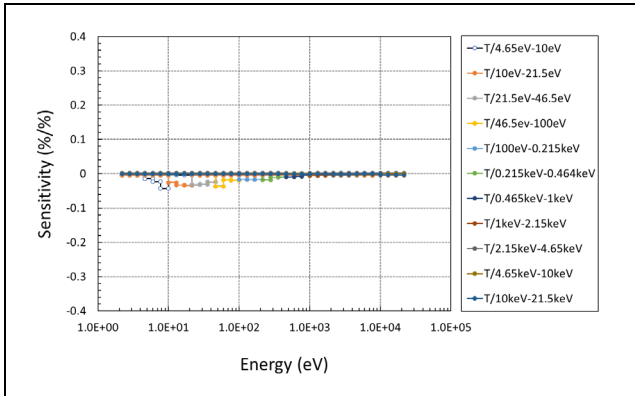


Figure 63. $^{235}\text{U}(n,\text{fission})$ -Sensitivity (%/%) to ^{235}U -Total Transmission Function in Sample 1.

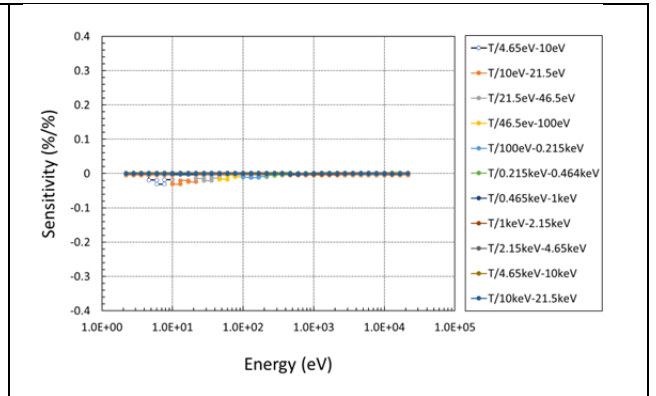


Figure 64. $^{235}\text{U}(n,\text{gamma})$ -Sensitivity (%/%) to ^{235}U -Total Transmission Function in Sample 1.

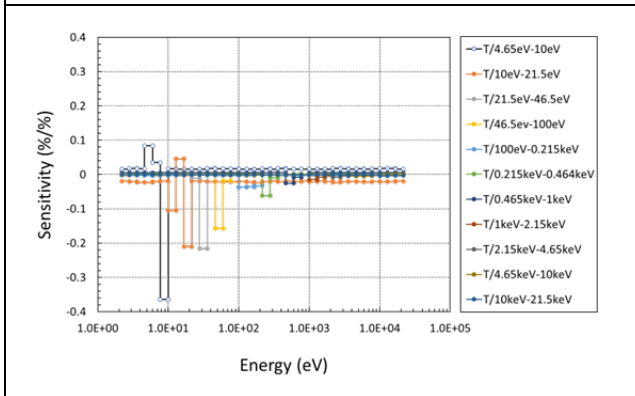


Figure 65. $^{235}\text{U}(n,\text{fission})$ -Sensitivity (%/%) to ^{235}U -fission Transmission Function in Sample 1.

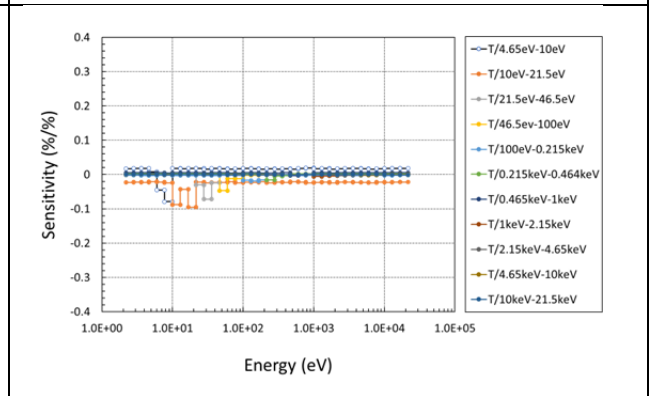


Figure 66. $^{235}\text{U}(n,\text{gamma})$ -Sensitivity (%/%) to ^{235}U -fission Transmission Function in Sample 1.

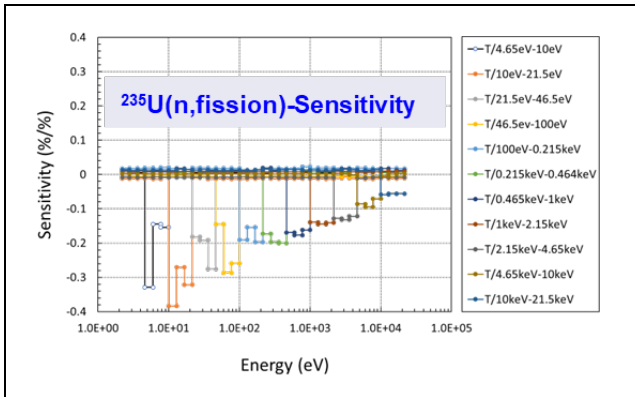


Figure 67. $^{235}\text{U}(n,\text{fission})$ -Sensitivity (%/%) to ^{235}U -Total Transmission Function in Sample 7.

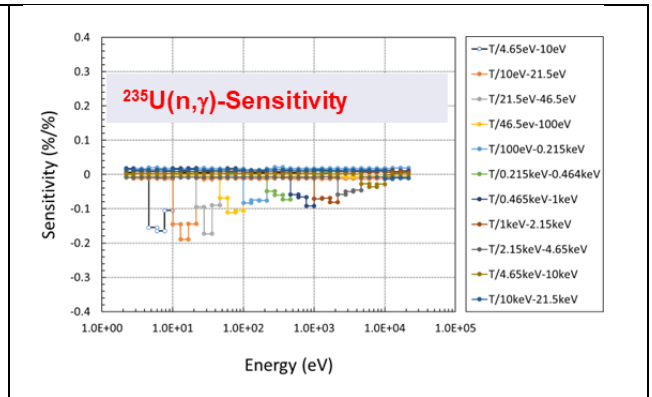


Figure 68. $^{235}\text{U}(n,\gamma)$ -Sensitivity (%/%) to ^{235}U -Total Transmission Function in Sample 7.

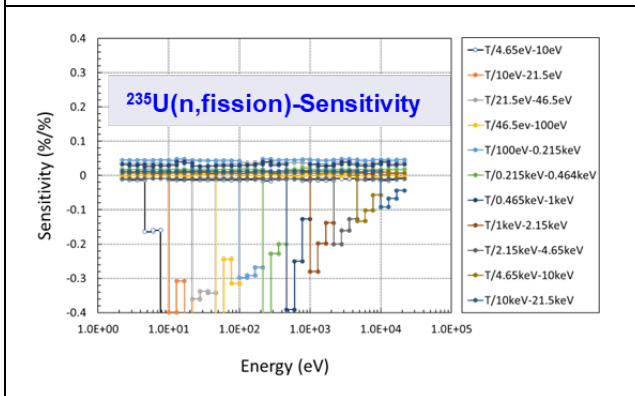


Figure 69. $^{235}\text{U}(n,\text{fission})$ -Sensitivity (%/%) to ^{235}U -fission Transmission Function in Sample 7.

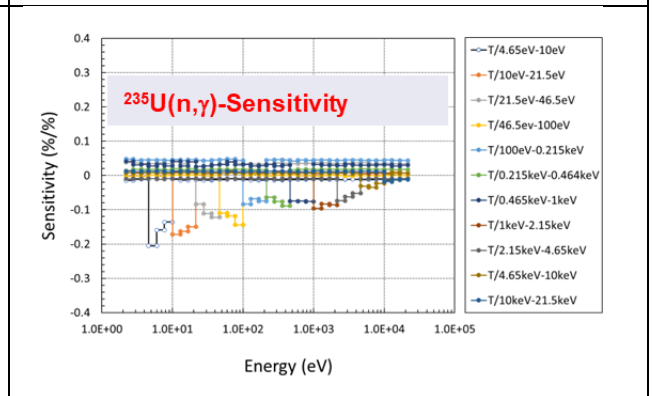


Figure 70. $^{235}\text{U}(n,\gamma)$ -Sensitivity (%/%) to ^{235}U -fission Transmission Function in Sample 7.

3.6. For burnup calculations

Sensitivities for a typical PWR-Westinghouse fuel assembly (4.8%wo) depleted up to 60 GWD/MT were performed using SANDY/FRENDY sampling of nuclear data for 239Pu and 238U [JEF/DOC-2015, 2020] , [IAEA/INDEN-Actinides, 2020], [JEF/DOC-2111, 2021].

The specifications for this sensitivity analyses are as follows:

- Depletion PWR-Westinghouse Fuel Assembly 17x17 – 4.8wt%
- Hot Full Power (HFP)
- Boron concentration= 500ppm
- Calculations with WIMSD5 code in 69 energy groups
- Sensitivity profiles calculated using FRENDY code which is used to perturb nuclear data in JEFF-3.3.
 - Sensitivity profiles are obtained for: (n,fission), (n,gamma) and nubar were calculated in 69 energy groups of WIMSD code.
 - Two types of sensitivities were calculated:
 - Direct term (only changes in nuclear data) with no changes in the isotopic inventory.
 - Direct+Indirect: here, changes in nuclear data will provoke changes in the isotopic inventory along depletion. Both terms are calculated jointly.

Figure 71, Figure 73 and Figure 75 show Pu239 sensitivity coefficients due to (n,fission), (n,gamma) and nubar at 32 GWd/MTU. In addition, these Figures show the relative perturbation in keff due to (n,fission), (n,gamma) and nubar between ENDF/B-VIII.0 and JEFF-3.3 at 32 GWd/MTU.

Figure 72, Figure 74 and Figure 76 show Pu239 sensitivity coefficients due to (n,fission), (n,gamma) and nubar at 32 GWd/MTU. In addition, these Figures show the relative perturbation in keff due to (n,fission), (n,gamma) and nubar between ENDF/B-VII.1 and JEFF-3.3 at 32 GWd/MTU.

Sensitivity analysis in burnup provide different insights for nuclear data:

- Large differences for “Direct” + “Indirect” depending on reaction, burnup and wt
- Depletion provides different sensitivities to keff

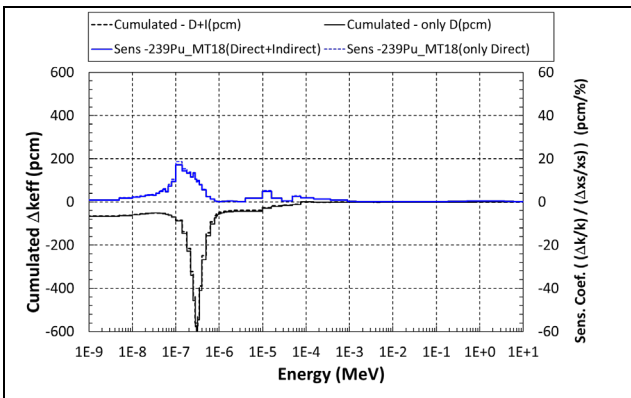


Figure 71. Pu239 sensitivity coefficients and relative perturbation in keff to (n,fission) between ENDF/B-VIII.0 and JEFF-3.3 at 32 GWd/MTU

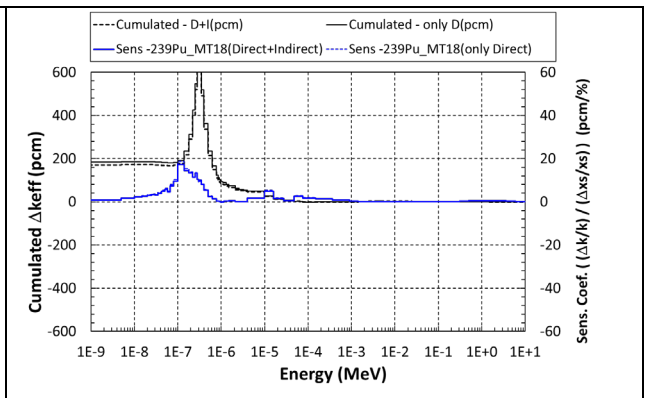


Figure 72. Pu239 sensitivity coefficients and relative perturbation in keff to (n,fission) between ENDF/B-VII.1 and JEFF-3.3 at 32 GWd/MTU.

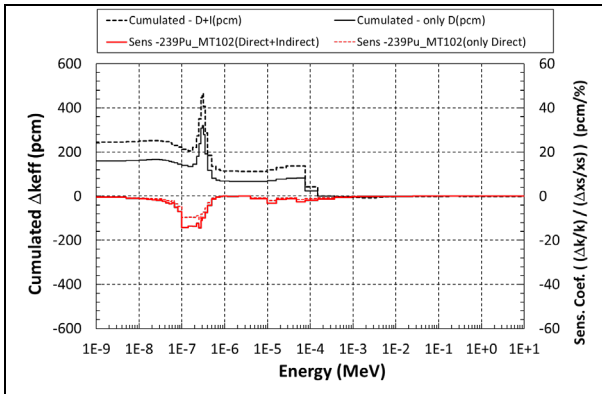


Figure 73. Pu239 sensitivity coefficients and relative perturbation in keff to (n,gamma) between ENDF/B-VIII.0 and JEFF-3.3 at 32 GWd/MTU.

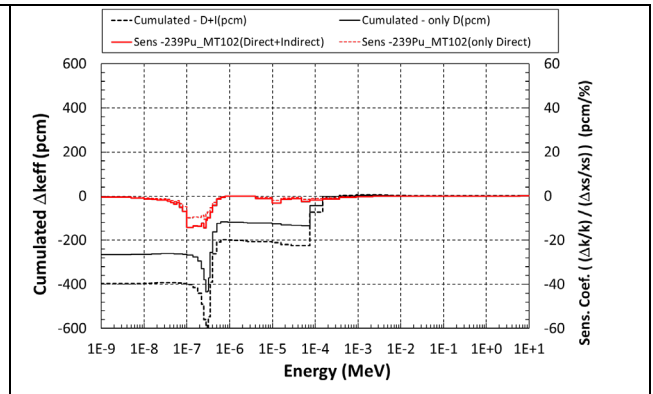


Figure 74. Pu239 sensitivity coefficients and relative perturbation in keff to (n,gamma) between ENDF/B-VII.1 and JEFF-3.3 at 32 GWd/MTU.

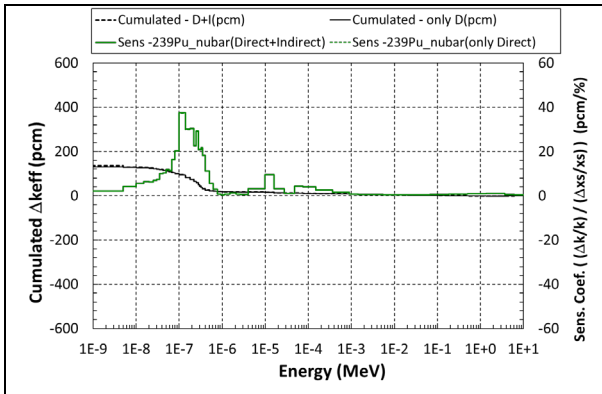


Figure 75. Pu239 sensitivity coefficients and relative perturbation in keff to (n,nubar) between ENDF/B-VIII.0 and JEFF-3.3 at 32 GWd/MTU

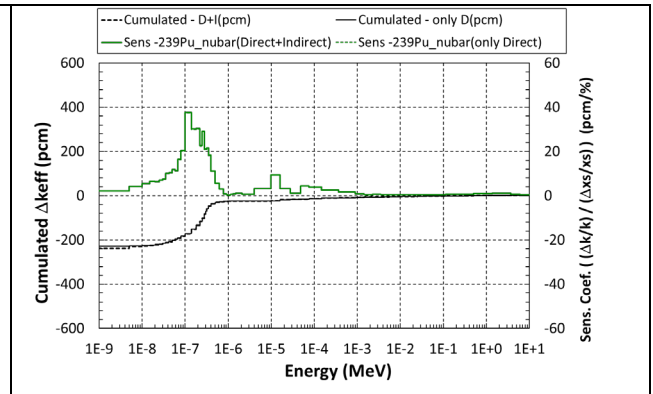


Figure 76. Pu239 sensitivity coefficients and relative perturbation in keff to (n,nubar) between ENDF/B-VII.1 and JEFF-3.3 at 32 GWd/MTU

Figure 77 and Figure 78 show Pu239 sensitivity coefficients due to (n,gamma) at two different burnup steps: 0.150 GWd/MTU and 32 GWd/MTU. In addition, these Figures show the relative perturbation in keff due to (n,gamma) between ENDF/B-VII.1 and JEFF-3.3 at 32 GWd/MTU.

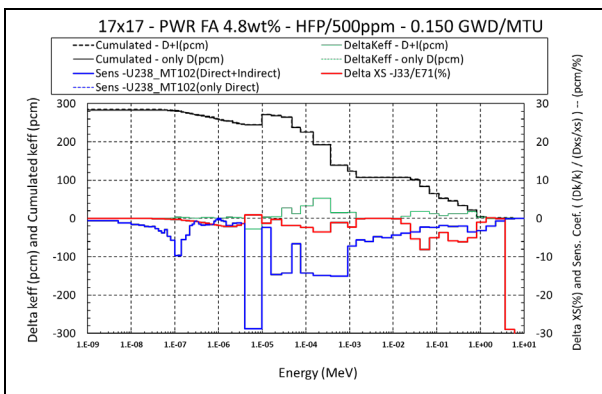


Figure 77. U238 sensitivity coefficients and relative perturbation in keff to (n,gamma) between ENDF/B-VII.1 and JEFF-3.3 at 0.150GWd/MTU

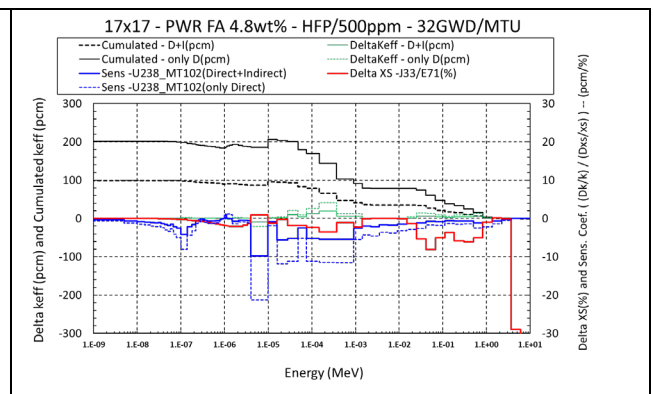


Figure 78. U238 sensitivity coefficients and relative perturbation in keff to (n,gamma) between ENDF/B-VII.1 and JEFF-3.3 at 32GWd/MTU

Figure 79 and Figure 80 show Pu239 sensitivity coefficients due to (n,gamma) at two different w/o enrichments, 4.8% and 3.1% at 32 GWd/MTU. In addition, these Figures show the relative perturbation in keff due to (n,gamma) between ENDF/B-VII.1 and JEFF-3.3 at 32 GWd/MTU.

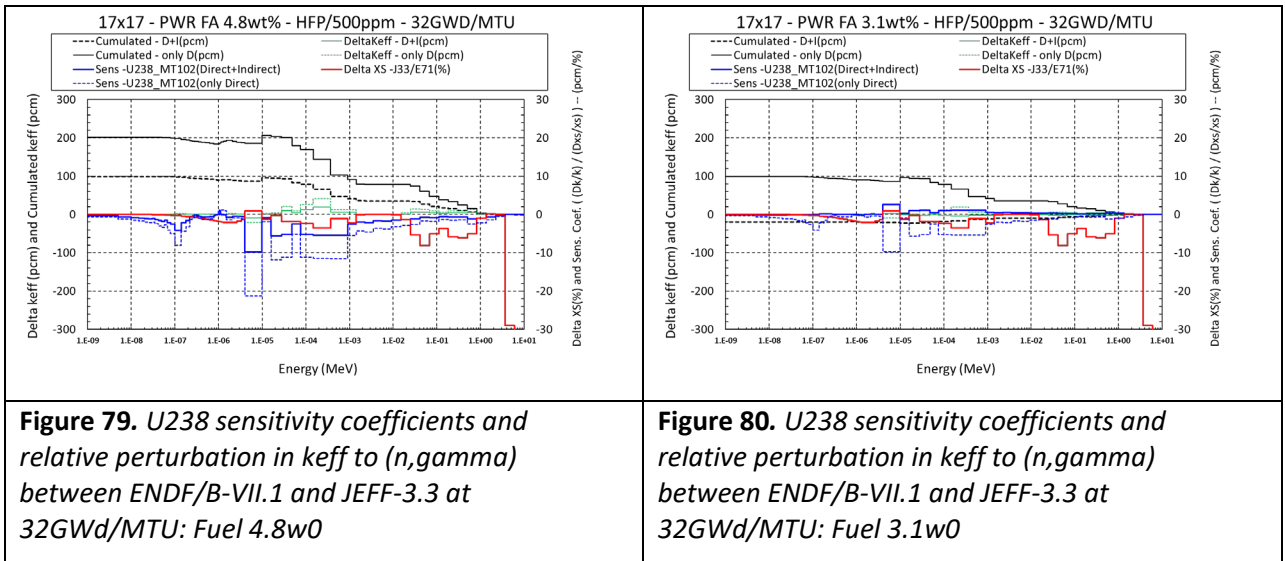
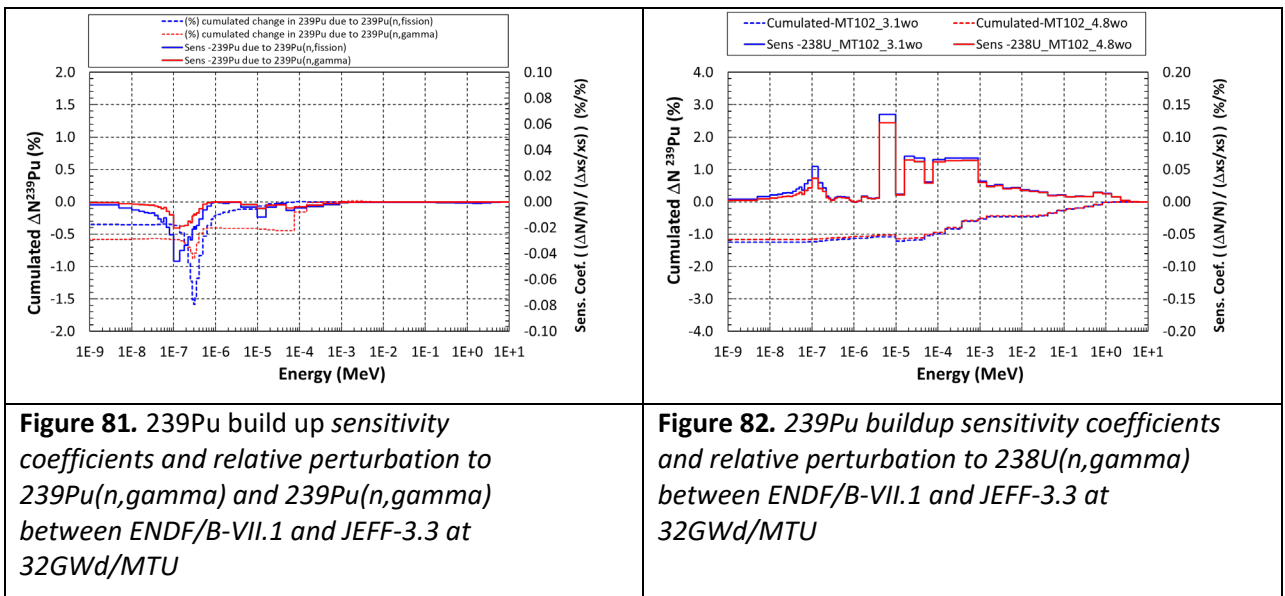


Figure 81 shows Pu239 build-up sensitivity coefficients due to 239Pu(n,gamma) and 239Pu(n,fission) for 4.8wo at 32 GWd/MTU. In addition, **Figure 81** shows the relative perturbation in 239Pu due to these 239Pu cross-sections between ENDF/B-VII.1 and JEFF-3.3.

Figure 82 shows Pu239 build-up sensitivity coefficients due to 238U(n,gamma) for two different enrichments, 4.8wo and 3.1wo, at 32 GWd/MTU. In addition, **Figure 82** shows the relative perturbation in 239Pu due to the differences in 238U(n,gamma) between ENDF/B-VII.1 and JEFF-3.3.



Sensitivity profiles can be downloaded in NDaST code which is able to predict the change in keff due to different perturbations. The ratio ENDF/B-VIII.0 over JEFF-3.3 will be used in the perturbation formula to predict the change in any nuclear reaction. Ratio of weighted cross-section in 69 energy groups is used in NDaST with a constant spectrum as weighting function (see **Figure 83 and Figure 84**).

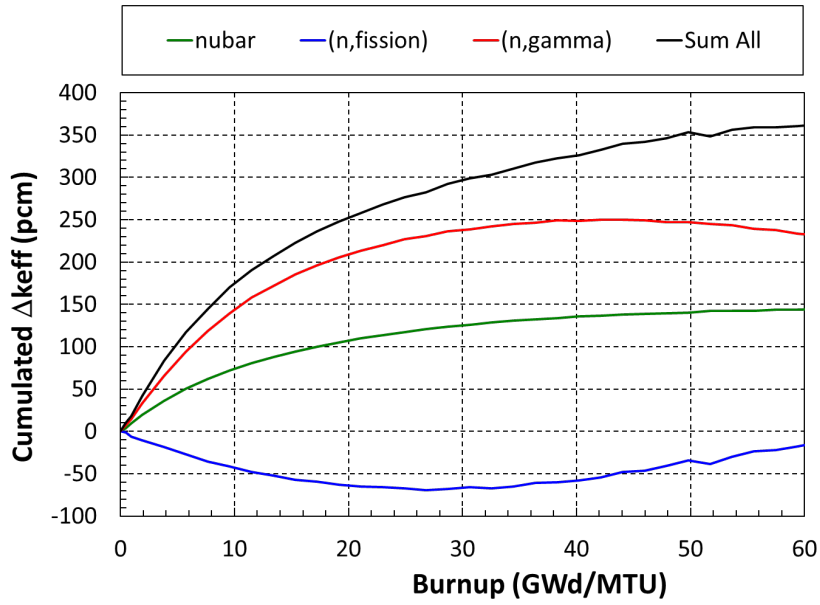


Figure 83. Modification in Δk_{eff} in a PWR 17x17 - 4.8wt% as a function of burnup due to ^{239}Pu nuclear data changes between ENDF/B-VIII.0 and JEFF-3.3

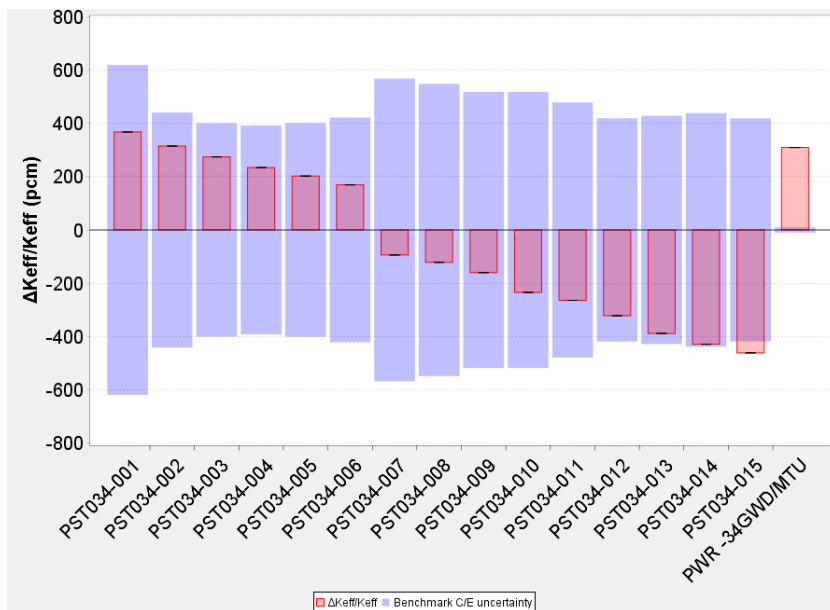


Figure 84. Modification in Δk_{eff} for PST-034 cases and a PWR 17x17-4.8wt% at 34GWd/MTU calculated as a perturbation of Pu239 (nubar, (n,fission) and (n,g) between ENDF/B-VIII.0 and JEFF-3.3

In addition, a new code COCONUST was developed at CNRS per A. Laureau to generate random cross sections according to covariance matrices. The sampled cross sections contained in different ACE files can be used in independent transport calculations for uncertainty propagation or as a prior cross sections set usable for Bayesian Monte Carlo assimilation. Generating random cross sections from covariance matrices will allow to use libraries such as ENDF/B-VIII.0 or JEFF-3.3 in the future. The COCONUST code is a python wrapper which embeds NJOY21 [NJOY 21] and the Serpent2 depletion code [Leppänen, 2015]. From the nuclear data libraries provided in the ENDF6 format, ACE cross sections files and covariance matrices are generated with the NJOY21 code. Then the COCONUST code is used for the sampling of the cross sections. Specific corrections have been implemented for non-positive semidefinite matrices, and to avoid negative cross section values using a gamma distribution or a truncated normal distribution. Cross sections of ^{240}Pu with a relative standard deviation close to 100% in the low energy range (fission reaction) and high energy range (inelastic and capture reactions) are good candidates to see the impact of the gamma correction (switch from a normal distribution to a gamma distribution for distributions close to zero). **Figure 85** presents an example of sampled ^{240}Pu cross sections with the COCONUST code with a gamma correction. The developed tool for the sampling and the covariance matrix fixing is generic and can also be used with external covariance matrices produced per other codes.

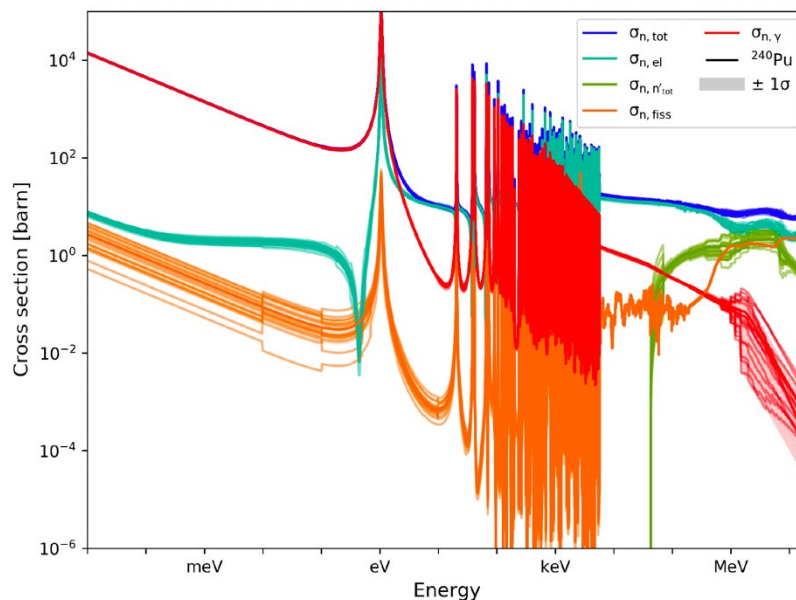


Figure 85. ^{240}Pu cross sampled cross sections (8 samplings) produced with the COCONUST code.

In order to check the uncertainty propagation in burnup calculations based on cross-section random sampling, a two-dimensional fuel pin representative of the PWR TMI-1 was modelled with reflective boundary conditions and at Hot Full Power conditions. This PWR burnup pin cell is part of Phase I of the OECD LWR Uncertainty Analysis in Modelling (UAM) benchmarks [Ivanov, 2013]. This benchmark has been chosen in order to compare the COCONUST calculations performed at SUBATECH per L. Giot with the results published in [Park, 2012, Park, 2018] using an uncertainty propagation method of nuclear data in a Monte Carlo burnup calculation performed with the McCARD code [Park, 2012]. First, a static calculation was performed on the reactivity uncertainty due to the cross-section covariance data for a fresh fuel. The McCARD code was coupled to the ENDF/B-VII.1 library and their 44-group covariance data, and to the SCALE6.1/COVA-44G cross-section covariance data, with 10^7 neutrons per calculation. The same library ENDF/B-VII.1 was chosen with a set of 512 random cross-sections generated per MT at the ACE format with probability tables in the unresolved energy range and then propagated using the Monte Carlo code Serpent2. Table 21 presents the nuclear data component of the uncertainty propagation for ^{235}U and ^{238}U cross-sections obtained for 10^6 neutrons and 10^7 neutrons per calculation. The McCARD results are presented in Table 22 for the comparison. We can see a good overall agreement. Some differences can be noticed, for example on the ^{238}U capture with 383 ± 2 pcm in this work and 417

pcm with McCARD and ENDF/B-VII. This difference might come from the energy binning of the matrices (728 groups from ENDF6 file in this work and 44 groups with McCard) even if the order of magnitude is very good and the difference between ENDF/B-VII and SCALE6.1 with McCARD is equivalent. Results are very similar between 10^6 and 10^7 simulated neutrons. A difference is visible on elastic and inelastic cross-sections for ^{235}U : the two results are compatible but the total statistics is 10 times bigger and then the confidence interval size is reduced. For this reason, depletion calculations with the MT numbers perturbed all together can be performed with 10^6 neutrons per burnup step thanks to the large nuclear data component on the standard deviation.

Table 21. Reactivity effect in pcm of the ^{235}U and ^{238}U cross-section perturbation (512 samples) for different reaction numbers (MT) and numbers of neutrons per simulation with COCONUST code. With 10^6 and 10^7 neutrons the pure statistical standard deviations are respectively 61 and 20 pcm. The average multiplication factor is 1.41063.

iso	^{235}U		^{238}U	
	10^6 neut.	10^7 neut.	10^6 neut.	10^7 neut.
2	10 ± 10	0 ± 2.7	47.1 ± 3.9	50.7 ± 1.8
4	6.9 ± 8.6	3.3 ± 3.0	157.0 ± 5.7	165.0 ± 5.3
18	106.3 ± 4.4	107.9 ± 3.4	22.1 ± 5.7	22.8 ± 1.2
102	279.7 ± 9.2	281.8 ± 8.9	410 ± 13	383 ± 12
452	888 ± 28	898 ± 28	117.8 ± 4.7	118.4 ± 3.9

Table 22. Reactivity effect in pcm of the ^{235}U and ^{238}U cross-section perturbation for different reaction numbers calculated with McCARD using ENDF/B-VII.1 and SCALE6.1 libraries, values are coming from paper [Park, 2012]. The average multiplication factor is 1.41701.

iso	^{235}U		^{238}U	
	B-VII.1	SCALE6.1	B-VII.1	SCALE6.1
4	1	3	147	15
18	115	106	23	21
102	306	299	417	373
452	856	374	101	99

Some burnup calculations taking with some propagation of the cross-section uncertainties were also compared between the COCONUST and McCARD codes. The reactivity uncertainty as a function of the fuel burnup was also calculated taking into account the cross-section covariance matrices of ENDF/B-VII.1 for the two following isotopes: ^{235}U and ^{238}U . The following MT codes were perturbed: 4, 18, 102 and 452. A specific power of 33.58 kW/kgU was taken for the Serpent2 depletion calculation with 10^7 neutrons per burnup step. The McCARD calculations were taken from [Park, 2018] were obtained with 200 active cycles with 10^4 neutrons per cycle. **Figure 86** shows the reactivity effect of these cross-section perturbations (300 samples per cross-section) as a function of the burnup steps for both calculations. A good agreement is obtained between the McCARD results and this work. The initial nuclear data uncertainty at the beginning of the depletion is around 1000 pcm and then reduces down to 330 pcm. Compared to McCARD results, the global agreement is good, the order of magnitude is very similar for the whole burnup range.

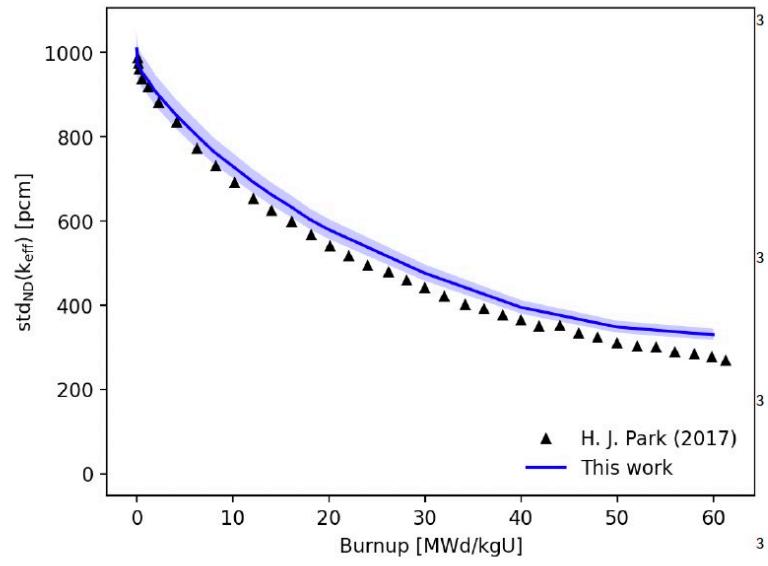


Figure 86. Nuclear data uncertainty propagation due to mt reaction numbers 4,18,102 and 452 for ^{235}U and ^{238}U using McCARD in black and COCONUST results in blue.

3.7. For reaction rates

The use of different integral benchmarks (with different sensitivities) may avoid compensating effects in the evaluation. **Figure 87 to Figure 90** show the energy dependent sensitivity profiles of keff and different spectral indexes with respect to 238U cross-sections in IEU-MET-FAST-007/Big-10 benchmark [JEF/DOC-2015, 2020], [IAEA/INDEN-Actinides, 2020].

Reaction rates/spectral indexes should be used in B&V to identify potential compensations in criticality benchmarks: sensitivities differ from criticality.

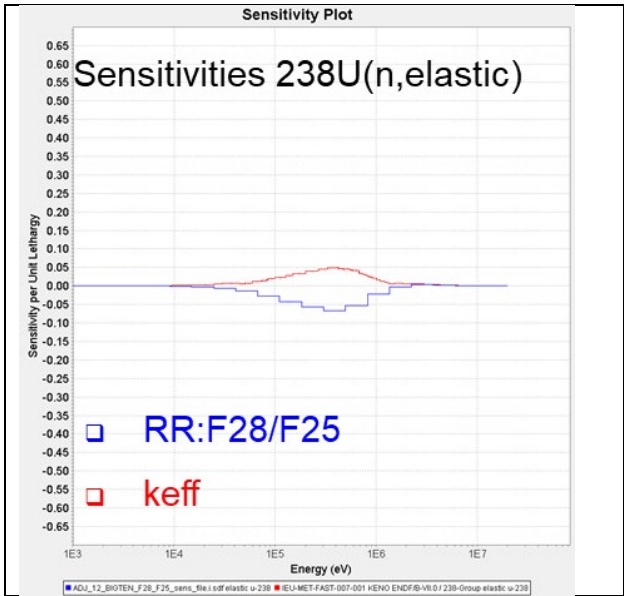


Figure 87. Sensitivity profiles of keff and F28/F25 with respect to 238U(n,elastic) in Big-10.

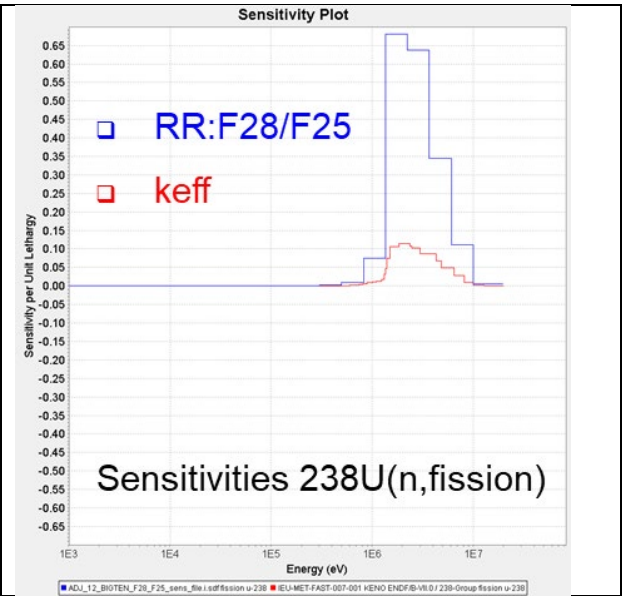


Figure 88. Sensitivity profiles of keff and F28/F25 with respect to 238U(n,fission) in Big-10.

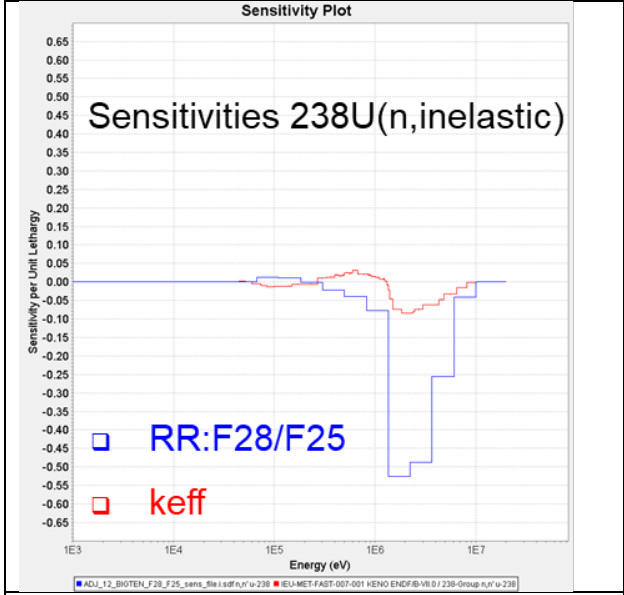


Figure 89. Sensitivity profiles of keff and F28/F25 with respect to 238U(n,inelastic) in Big-10.

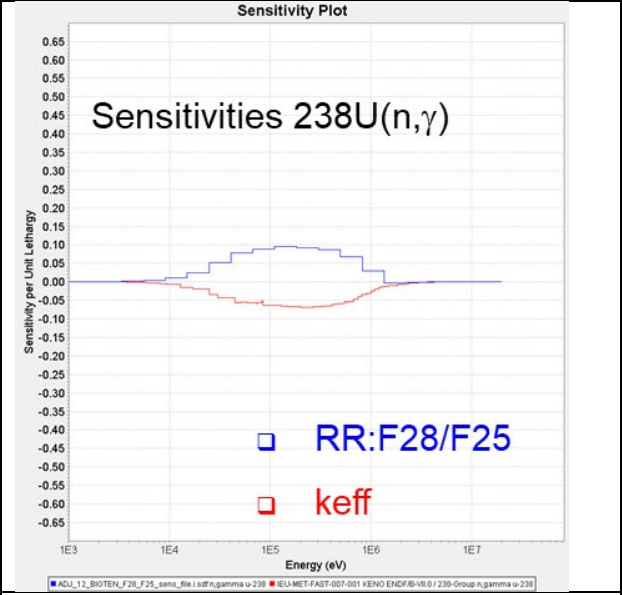


Figure 90. Sensitivity profiles of keff and F28/F25 with respect to 238U(n,gamma) in Big-10.

3.8. For criticality Benchmarks: PST34 criticality benchmarks

In this section, we study the PU-SOL-THERM-034 benchmarks, that is, 15 cases consisting of a plutonium nitrate solution with gadolinium in a water-reflected cylinder with a 24-inch diameter compiled as a part of the International Criticality Safety Benchmark Evaluation Project (ICSBEP). PST34 benchmarks have shown large sensitivity profiles (see **Figure 91**) to the ^{239}Pu cross sections and fission neutron multiplicity in the range 0.01eV-1eV [**JEF/DOC-2015, 2020**].

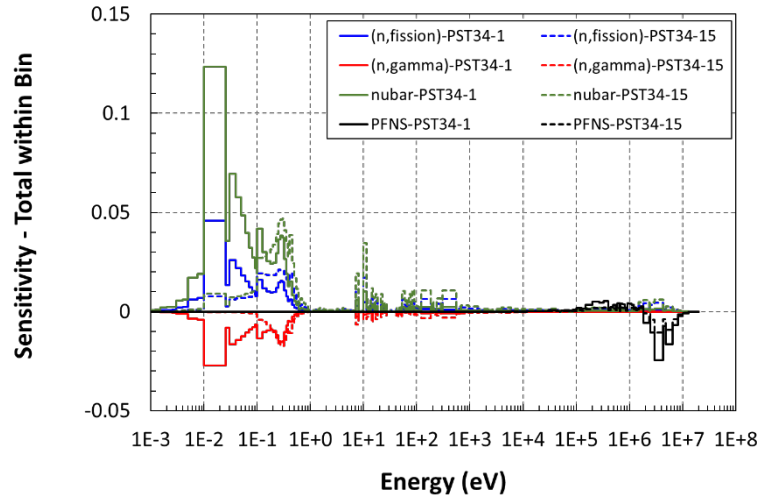


Figure 91. ^{239}Pu sensitivity coefficients (Total within bin) for PST34-001 and 015 benchmarks.

PST34s will be very useful to show the impact of the large differences between ENDF/B-VIII.0 and JEFF-3.3 (see **Figure 92**), for Pu239 in the energy range 0.1eV-1.0eV are found.

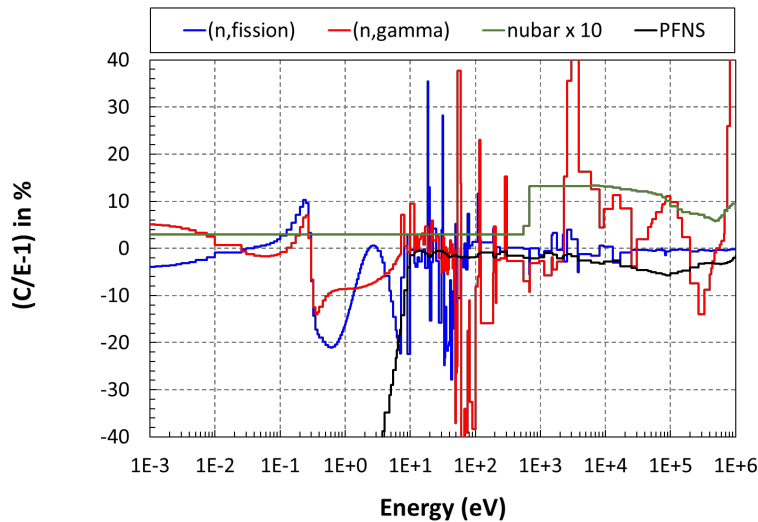


Figure 92. Differences in Pu239 nuclear data (E80/J33-1) in %

We define the cumulated change is the cumulative change from high ($g=G$) to thermal energy ($g=1$):

$$\Delta k_{eff}^i = \sum_{g=G}^1 S_g^i \cdot \Delta \sigma_g^i$$

Figure 93 shows the cumulative change due to the perturbation of ^{239}Pu cross-sections between ENDF/B-VIII.0 and JEFF-3.3. Approximately. 80% of the change in k_{eff} occurs between 0.1eV-1eV.

- aprox. 20% of Δk_{eff} change is between 1eV-10eV for (n,fission)
- aprox. 80% is in the first resonance for (n,fission)

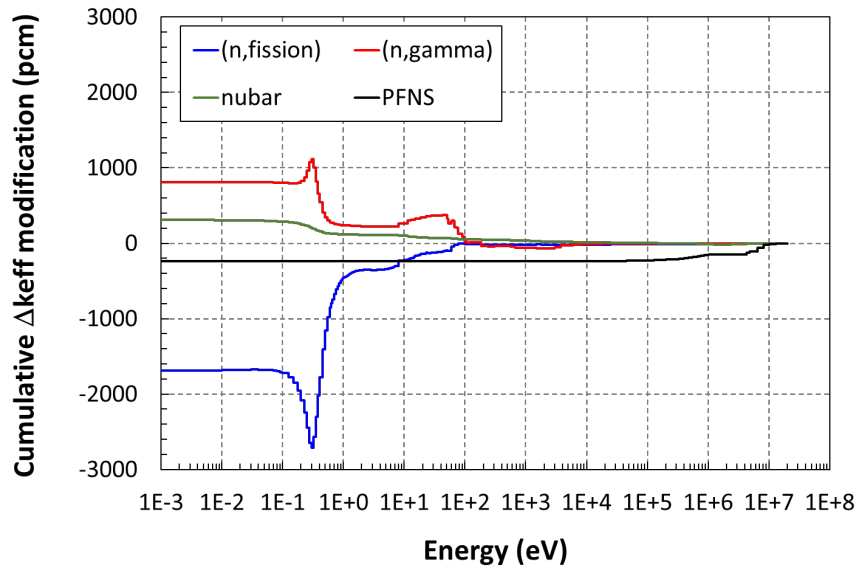


Figure 93. Cumulated change in Δk_{eff} (in pcm) for PST34-015 case due to changes in ^{239}Pu . Calculations performed with NDaST code.

(1) Uncertainty quantification

An uncertainty quantification is performed in PST34 benchmarks [IAEA/INDEN-Actinides, 2020]. It can be seen that:

- k_{eff} experimental uncertainties are lower than predicted uncertainties due to nuclear data uncertainties (see **Table 23**)
- Pu239 is the most important contributor to the total uncertainty (see **Table 24**)

Table 23. k_{eff} uncertainty (in pcm) prediction for PST-034 benchmarks calculated with NDaST software and ENDF/B-VIII.0 covariance data.

PST Benchmarks	Exp. uncertainty	All isotopes	^1H	^{16}O	Cr	Fe	Ni	Gd	Pu
PST-034-001	620	1408	288	38	15	68	7	0	1376
PST-034-002	440	1348	208	36	10	39	4	308	1294
PST-034-003	400	1349	148	34	6	24	3	476	1253
PST-034-004	390	1358	103	31	4	13	2	566	1229
PST-034-005	400	1374	76	28	2	7	1	629	1219
PST-034-006	420	1379	69	25	1	3	0	657	1210
PST-034-007	570	1292	119	41	7	21	3	274	1256
PST-034-008	550	1293	104	41	6	19	2	289	1255
PST-034-009	520	1288	93	42	6	16	2	300	1248
PST-034-010	520	1279	77	40	5	13	2	311	1238
PST-034-011	480	1278	65	39	4	10	1	318	1235
PST-034-012	420	1277	54	37	3	7	1	324	1234
PST-034-013	430	1273	46	36	2	5	1	326	1229
PST-034-014	440	1270	40	34	2	4	1	330	1225
PST-034-015	420	1270	41	35	1	3	0	332	1225

Table 24. *keff* uncertainty (in pcm) prediction for PST-034 benchmarks and a PWR – 17x17 4.8wt% at 34 GWd/MTU calculated with NDaST software and ENDF/B-VIII.0 covariance data.

PST Benchmarks	²³⁹ Pu						
	²³⁹ Pu	(n,eI)	(n,inel)	(n,fission)	(n,g)	nubar	CHI
PST-034-001	1374	2	12	467	1167	312	424
PST-034-002	1292	2	11	571	1038	312	362
PST-034-003	1251	2	11	643	955	312	312
PST-034-004	1228	2	10	698	895	313	267
PST-034-005	1217	2	8	738	857	313	227
PST-034-006	1208	1	7	773	822	313	181
PST-034-007	1254	8	37	640	962	304	311
PST-034-008	1254	7	37	659	947	304	309
PST-034-009	1246	8	37	668	935	304	301
PST-034-010	1236	8	35	693	911	304	276
PST-034-011	1234	8	34	704	902	304	263
PST-034-012	1232	8	33	720	890	304	253
PST-034-013	1227	7	31	739	874	303	233
PST-034-014	1223	7	28	748	867	303	205
PST-034-015	1223	7	28	755	861	303	201
PWR-34GWD/MTU	-	-	267	639	134	-	-

(2) Similarities

Ck-values can be used to estimate the correlation between PWR and PST34 cases for Pu239 nuclear data (see **Table 25**). In particular, similarities up to 95% were calculated between the neutron multiplication factor of the PWR fuel assembly case analysed in this study, and the PU-SOL-THERM-034 benchmarks [JEF/DOC-2015, 2020], [IAEA/INDEN-Actinides, 2020].

Table 25. Representative ck-values for PST-034 benchmarks and a PWR – 17x17 4.8wt% at 34GWD/MTU.

#\#	01	02	03	04	05	06	07	08	09	10	11	12	13	14	015	PWR
PST34-001	1.00	0.99	0.98	0.96	0.94	0.93	0.93	0.92	0.92	0.90	0.90	0.89	0.88	0.87	0.86	0.95
PST34-002	0.99	1.00	1.00	0.99	0.98	0.96	0.95	0.94	0.94	0.93	0.92	0.92	0.91	0.90	0.90	0.95
PST34-003	0.98	1.00	1.00	1.00	0.99	0.98	0.95	0.95	0.95	0.94	0.94	0.93	0.92	0.92	0.92	0.95
PST34-004	0.96	0.99	1.00	1.00	1.00	0.99	0.95	0.95	0.95	0.94	0.94	0.94	0.93	0.93	0.92	0.94
PST34-005	0.94	0.98	0.99	1.00	1.00	1.00	0.95	0.94	0.94	0.94	0.94	0.94	0.93	0.93	0.92	0.93
PST34-006	0.93	0.96	0.98	0.99	1.00	1.00	0.94	0.94	0.94	0.94	0.94	0.94	0.93	0.93	0.92	0.93
PST34-007	0.93	0.95	0.95	0.95	0.95	0.94	1.00	1.00	1.00	1.00	1.00	0.99	0.99	0.99	0.99	0.89
PST34-008	0.92	0.94	0.95	0.95	0.94	0.94	1.00	1.00	1.00	1.00	1.00	1.00	0.99	0.99	0.99	0.88
PST34-009	0.92	0.94	0.95	0.95	0.94	0.94	1.00	1.00	1.00	1.00	1.00	1.00	1.00	0.99	0.99	0.88
PST34-010	0.90	0.93	0.94	0.94	0.94	0.94	1.00	1.00	1.00	1.00	1.00	1.00	1.00	1.00	1.00	0.87
PST34-011	0.90	0.92	0.94	0.94	0.94	0.94	1.00	1.00	1.00	1.00	1.00	1.00	1.00	1.00	1.00	0.87
PST34-012	0.89	0.92	0.93	0.94	0.94	0.94	0.99	1.00	1.00	1.00	1.00	1.00	1.00	1.00	1.00	0.86
PST34-013	0.88	0.91	0.92	0.93	0.93	0.93	0.99	0.99	1.00	1.00	1.00	1.00	1.00	1.00	1.00	0.85
PST34-014	0.87	0.90	0.92	0.93	0.93	0.93	0.99	0.99	0.99	1.00	1.00	1.00	1.00	1.00	1.00	0.85
PST34-015	0.86	0.90	0.92	0.92	0.92	0.92	0.99	0.99	0.99	1.00	1.00	1.00	1.00	1.00	1.00	0.85
PWR 34GWD/MTU	0.95	0.95	0.95	0.94	0.93	0.93	0.89	0.88	0.88	0.87	0.87	0.86	0.85	0.85	0.85	1.00

4. Summary and conclusions

- **Review Processing Tools**

- Processing and Verification (P&V) is an important step of nuclear data activities
- JEFF Processing & Verification (P&V) Working Group activities: reconstruction, processing and internal consistency diagnosis of evaluated files using different codes such as NJOY, PREPRO, AMPX, FRENDY,...
- This P&V job depends of end-user needs: MCNP, SCALE... and sometimes relying on end-user capabilities.
- A close collaboration with end-users leads a double benefit for the ND community
 - Feedback/diagnosis of evaluated files
 - Feedback for code's developers
- Warnings/Errors found in P&V activities can be solved in constructive ways
 - Examples of updating JEFF-3.3 evaluation using FRENDY warnings/errors
- Finally, the current status of processing activities on the reconstruction of the angular differential cross-sections (MF4) from resonance parameters (RPs) of the Reich-More Limited format (LRF=7) using NJOY code is reviewed. The main conclusion is that additional methods development would be needed:
 - a rigorous methodology to Doppler broaden for these distributions
 - thinning of the dense energy grid, before there can be routine use of this capability
 - sampling of these many distributions during transport calculations

Ref.: UPM report: 2022-12-20/WP4-D4.5/R2, "UPM contribution to D4.5: Review Processing Tools". O. Cabellos

- **Processing of JEFF nuclear data libraries using AMPX code for the SCALE Code System and testing with criticality benchmark experiments**

- JEFF-3.3 neutron cross section library, including TSLs, has been successfully processed with AMPX using the most recent SCALE release. The CE library has been created for its use with SCALE neutron transport tools.
- This work is a step further on the interaction between AMPX and JEFF libraries, identifying remaining issues towards a more efficient procedure. During the testing and benchmarking phases, relevant improvements have been highlighted concerning the treatment of Be-9. On the other hand, several W isotopes require a more specific analysis in order to adjust potential inconsistencies. Nonetheless, the CE library performs adequately for the set of 120 benchmarks and according to all the verification activities already carried out.
- Associated covariances have been also generated using different energy group structures and verified against NJOY-processed files.
- Finally, it is worth mentioning that these libraries (along with JEFF-3.1.1 CE library) are currently distributed through the NEA/CPS aiming to expand the user's group of JEFF nuclear data libraries in the frame of the widely used SCALE Code System (see Appendix I and Appendix 2). This will also contribute to a more extensive verification and validation capabilities of the current JEFF-3.3, targeting future releases: JEFF-4.

Ref.: UPM report: 2022-12-20/WP4-D4.5/R1 , “UPM contribution to D4.5: Processing of JEFF nuclear data libraries using AMPX code for the SCALE Code System and testing with criticality benchmark experiments“. O. Cabellos, A. Jiménez-Carrascosa, N. García-Herranz

- **Processing Covariances**

- This work summarized the processing and verification activities for the covariance data in major nuclear data evaluations (e.g. JEFF-3.3 and ENDF/B-VIII.0) using NJOY code.
 - Examples of processing for MF31, MF32/MF33, MF34 and MF35 are given and provided in 7 energy groups for the WPEC/SG46 framework.
- A review of keff-uncertainties of a set of criticality benchmarks using JEFF-3.3 covariance data is also performed. This work has served to identify potential cross-sections to be improved.

Ref.: UPM report: 2022-12-20/WP4-D4.5/R5, “UPM contribution to D4.5: Processing Covariances“. O. Cabellos

- **Processing and Verification (P&V)**

- The 123-Mosteller’s suite is still useful for an overall performance of nuclear data libraries
 - Easily identifying potential issues in the evaluations: W and Ni in JEFF-4T0
- Necessity of extended ICSBEP criticality suites to identify trends in ND evaluations
 - Example of PST-034: Joint evaluation... 239Pu-16O-TSL/H2O is needed!
- Reaction Rates (RRs) should be used in B&V to identify potential compensations in criticality benchmark
 - RRs Sensitivities differ from criticality
- LWR/KRITZ Benchmarks at room and elevated temperatures
 - For KRITZ-LWR-RESR-001, 2 and 3
 - UO2 cases: Good performance for JEFF-3.3
 - MOX case: large biases at room and elevated temperatures both for JEFF-3.3 and ENDF/B-VIII.0
 - For KRITZ-LWR-RESR-004 smaller calculation biases, particularly for JEFF-3.3
 - The trend with temperature becomes stronger for series 4, in particular for JEFF-3.3
 - This strong trend may indicate **remaining nuclear data biases**: $^{235}\text{U}(n,fission) \sim 0.01 \text{ eV} - 1\text{eV} ?$

Ref.: UPM report: 2022-12-20/WP4-D4.5/R4, “UPM contribution to D4.5: Processing and Verification (P&V)“. O. Cabellos, A. Jiménez-Carrascosa, N. García-Herranz

- **Sensitivity Analysis (SA) and Uncertainty Quantification (UQ)**

- Necessity of extended ICSBEP criticality suites to identify trends in ND evaluations
 - Example of PST-034: Joint evaluation... 239Pu-16O-TSL/H2O is needed!
- Reaction Rates should be used in B&V to identify potential compensations in criticality benchmarks
 - Sensitivities differ from criticality
- Using transmission and shielding benchmarks in V&V can give us insight to different ND trends
 - Sensitivities differ from criticality
- Using depletion benchmarks in V&V can give us insight to different ND trends
 - Sensitivities for isotopic prediction might differ from criticality
 - Sensitivities & correlations change over time.

Ref.: UPM report: 2022-12-20/WP4-D4.5/R3, “Sensitivity Analysis (SA) and Uncertainty Quantification (UQ). O. Cabellos

5. Acknowledgements

MCNP 6.2 has been obtained through RSICC.

AMPX 6 code has been provided by OECD-NEA Computer Program Services, as part of the SCALE 6.2.3 code package.

SERPENT-v2 has been provided by OECD-NEA Computer Program Services.

6. References

- [Algora, 2010] A. Algora et al., Phys. Rev. Lett. 105, 202501 (2010).
- [Algora, 2021] A. Algora, J. L. Tain, B. Rubio, M. Fallot and W. Gelletly, Eur. Phys. J. A 57, 85 (2021).
- [AMPX, 21016] D. Wiarda, M. E. Dunn, N. M. Greene, M. L. Williams, C. Celik, L. M. Petrie, AMPX-6: A Modular Code System for Processing ENDF/B, ORNL/TM-2016/43, (April 2016)
- [An, 2017] F. P. An et al. (Daya Bay Collaboration), Phys. Rev. Lett. 118, 251801 (2017).
- [Bécares 2020a] V. Bécares et al., Unresolved resonance treatment with AMPX and NJOY. CIEMAT report DFN/IN-03/II-20 (2020).
- [Bécares 2020b] V. Bécares et al., Processing the unresolved resonances of neutron cross sections with the AMPX and NJOY codes. In virtual meeting of the Spanish Nuclear Society, 16-19 November 2020.
- [Bondarenko 1964] I. I. Bondarenko, Group Constants for Nuclear Reactor Calculations. Consultants Bureau, 1964.
- [Chadwick 2011] M. B. Chadwick et al., ENDF/B-VII.1 Nuclear Data for Science and Technology: Cross Sections, Covariances, Fission Product Yields and Decay Data. Nucl. Data Sheets 112 (2011) 2887-2996. DOI: 10.1016/j.nds.2011.11.002.
- [CoNDERC, 2021] CoNDERC: Compilation of Nuclear Data Experiments for Radiation Characterisation (2019). URL <http://www-nds.iaea.org/conderc/>.
- [Conlin 2019] J. L. Conlin and P. Romano, Compact ENDF (ACE) Format Specification, Los Alamos National Laboratory Report LA-UR-19-29016 (2019).
- [Diez, 2016] C.J. Díez et al., Eur. Phys. J. Web of Conferences 111, 06003 (2016)
- [Dimitriou, 2015] P. Dimitriou and A. L. Nichols, "IAEA Report No. INDC(NDS)-0676, IAEA, Vienna, Austria," (2015).
- [Dunn 2002] M. E. Dunn and L. C. Leal, Calculating probability tables for the unresolved resonance region using Monte Carlo methods. PHYSOR 2002, Seoul (Korea) 7-10 October 2002.
- [Estienne, 2019] M. Estienne et al., Phys. Rev. Lett. 123, 022502 (2019).
- [Fallot, 2012] M. Fallot et al., Phys. Rev. Lett. 109, 202504 (2012).
- [FRENDY, 2017] K. Tada, Y. Nagaya, S. Kunieda, K. Suyama, T. Fukahori, "Development and verification of a new nuclear data processing system FRENDY," J. Nucl. Sci. Technol., 54, pp.806-817 (2017).
- [FRENDY/Perturb, 2019] R. KONDO, T. ENDO, A. YAMAMOTO, K. TADA. "Implementation of Random Sampling for ACE-Format Cross-Sections Using FRENDY and Application to Uncertainty Reduction". Proceedings MC2019, pp.1493-1502.(2019)
- [FRENDY] https://rpg.jaea.go.jp/main/en/program_frendy/
- [Greenwood, 1997] R. C. Greenwood et al., Nuclear Instruments and Methods in Physics Research A 390, 95 (1997).
- [Guadilla, 2019] V. Guadilla et al., Phys. Rev. Lett. 122, 4, 42502 (2019) DOI 10.1103/PhysRevLett.122.042502.
- [Guadilla, 2022] V. Guadilla et al., Phys. Rev. C 106, 014306 (2022).
- [Hardy, 1977] J. C. Hardy et al., Phys. Lett. 71B, 307 (1977).
- [Herman, 2012] M. Herman, A. Trkov, Data Formats and Procedures for the Evaluated Nuclear Data File ENDF/V-VI and ENDF/B-VII, CSEWG BNL-90365-2009 (2012)
- [Hursin, 2022] M. Hursin, O. Cabellos, G. Palmiotti, Status of the WPEC/SG46: Efficient and Effective Use of Integral Experiments for Nuclear Data Validation, in Proceedings of the International Conference on Physics of Reactors, PHYSOR, 15-20 May 2022, Pittsburgh, USA (2022)

- [IAEA/INDEN-Actinides, 2020] O. Cabellos, “Indications from integral benchmarks on U-235, U-238 and Pu-239 evaluations”, IAEA CM of the INDEN on Actinide Evaluation in the Resonance Region, 17-19 Nov 2020 (Video-conference)
- [IAEA/TM/Processing, 2019] O. Cabellos, Current activities on Processing and Verification(P&V) at Universidad Politécnica de Madrid (UPM), Technical Meeting on Nuclear Data Processing, IAEA Headquarters, Vienna, Austria. September 23-26, 2019.
- [IAEA/TM/Processing, 2022] O. Cabellos, Processing files with LRF7 option for the reconstruction of the MF4, pros and cons.- User’s point of view -IAEA Technical Meeting on ND Processing - November 29-December 2, 2022 (video-conference)
- [ICSBEP, 2019] Nuclear Energy Agency, ICSBEP Handbook 2019, Technical Report OECD/NEA (2019)
- [INDC0786, 2019] M. Fallot, B. Littlejohn and P. Dimitriou, IAEA Headquarters, Vienna, Austria 23-26 April 2019, INDC(NDS)- 0786.
- [Ivanov, 2013] K. Ivanov, M. Avramova, S. Kamerow, I. Kodeli, E. Sartori, E. Ivanov, O. Cabellos, Benchmarks for Uncertainty Analysis in Modelling (UAM) for the Design, Operation and Safety Analysis of LWRs-Volume I: Specification and Support Data for Neutronics Cases (Phase I), Tech. rep., NEA-NSC-DOC 2013-7, Nuclear Energy Agency of the OECD (2013).
- [JEF/DOC-2015, 2020] O. Cabellos, M. García-Hormigos, B. Moreno and S. Sánchez-Fernández, “The importance of using different integral benchmarks to provide valuable feedbacks to the evaluation process”, JEFF Nuclear Data Week - Nov 24-27,2020. JEF/DOC-2015 (video-conference)
- [JEF/DOC-2111, 2021] O.Cabellos, “Comparison of Burnup Calculations for ND Validation Activities”, JEFF Nuclear data week, - Depletion Session, November 25, 2021. JEF/DOC-2111 (in-person)
- [JEF/DOC-2211, 2022] O. Cabellos, “Processing files with LRF7 option for the reconstruction of the MF4, pros and cons”, JEFF Nuclear Data Week, November 24, 2022 NEA Headquarters, Boulogne-Billancourt, France (in-person)
- [JEF-CG/Nov. 2020] O. Cabellos, “Criticality Benchmarking: JEFF-4.0T0”, NEA Headquarters (Nov 27-30,2018), JEFF CG, November 2022
- [JEFDOC-1904, 2017] O. Cabellos, and F. Michel-Sendis, JEFF-3.3 criticality benchmarks, OECD/NEA JEFFDOC-1904 (2017).
- [JEFDOC-1987, 2019] O. Cabellos, “P&V of JEFF-3.3 by using FRENDY code”, JEFF Nuclear Data Week – Nov 2019. NEA Headquarters, Boulogne-Billancourt, France. November 23-26, 2019. JEFDOC-1987
- [JEFDOC-1991] O. Cabellos, “Feedbacks on JEFF-3.3 Evaluation: Uncertainty in keff for some ICSBEP Outliers, PWR Critical Boron Letdown Curve and Additional integral data testing using reaction rates in critical assemblies”, JEFF Meeting, April 2020. JEFDOC-1991 (video-conference)
- [JEFDOC-2015] O. Cabellos, M. García-Hormigos, B. Moreno and S. Sánchez-Fernández, “The importance of using different integral benchmarks to provide valuable feedbacks to the evaluation process “JEFF Meeting and JEFF-CG, Nov 2020. JEFDOC-2015 (video-conference).
- [JEFDOC-2041] O. Cabellos, Overview of Processing, Verification and Benchmarking activities at UPM, JEFF Nuclear Data Week, April 28, 2021, JEFDOC-2041 (video -conference)
- [JEFDOC-2091, 2021] O. Cabellos et al., Testing of the JEFF-3.3 with IRPhEP/LWR KRITZ Benchmarks, OECD/NEA JEFFDOC-2091 (2021)
- [JEFDOC-2091] O. Cabellos, A. Jiménez-Carrascosa, N. García-Herranz, G. de Alcázar, Overview of Processing, Testing of the JEFF-3.3 with IRPhEP/LWR KRITZ Benchmarks, JEFF Nuclear Data Week, November 24, 2021, JEFDOC-2091 (in-person)
- [JEFDOC-2097, 2021] A. Jiménez-Carrascosa et al., Impact of Doppler calculations in SEFOR benchmark due to the differences between JEFF-3.3 and JEFF-3.1.1, OECD/NEA JEFFDOC-2097 (2021)

- [JEFDOC-2144, 2022] A. Jiménez-Carrascosa et al., Processing and benchmarking of JEFF-4T1 library in the frame of the SCALE Code System, OECD/NEA JEFDOC-2144 (2022)
- [JEFFDOC-1991] O. Cabellos, “Feedbacks on JEFF-3.3 Evaluation: Uncertainty in keff for some ICSBEP Outliers, PWR Critical Boron Letdown Curve and Additional integral data testing using reaction rates in critical assemblies”, JEFF Meeting, April 2020. JEFDOC-1991 (video-conference)
- [JEFFDOC-2062] O. Cabellos, WPEC/SG46 TAR exercise: Preliminary Results, JEFF Nuclear Data Week, November 22, 2021, JEFDOC-2062 (in-person)
- [JEFFDOC-2109] O. Cabellos, Processing covariances for WPEC/SG46 TAR Exercise, JEFF Nuclear Data Week, November 22, 2021, JEFDOC-2109 (in-person)
- [JEFF-JENDL, 2019] O. Cabellos, “First feedback on using FRENDY for processing of JEFF-3.3.”, April 24, 2019. JEFF-JENDL Bilateral Meeting, NEA Headquarters.
- [Jiménez-Carrascosa 2019] A. Jiménez-Carrascosa et al., About the impact of the Unresolved Resonance Region in Monte Carlo simulations of Sodium Fast Reactors. ICAPP-2019, Juan-les-Pins (France) 12-15 May 2019.
- [Kim, 2019] K.S. Kim et al., *Ann. Nucl. Energy* 132, 161-171 (2019)
- [Kodeli, 2009] Kodeli et al, Analysis of the KRITZ Critical Benchmark Experiments, NENE2009
- [L.Leal, 2016] Luiz Leal, Evgeny Ivanov, Gilles Noguère, Arjan Plompen, and Stefan Kopecky, “Resonance parameter and covariance evaluation for ¹⁶O up to 6 MeV”, *EPJ Nuclear Sci. Technol.* 2, 43 (2016)
- [Leppänen, 2015] J. Leppänen, M. Pusa, T. Viitanen, V. Valtavirta, T. Kaltiaisenaho, The Serpent Monte Carlo code: Status, development and applications in 2013, *Annals of Nuclear Energy* 82 (2015) 142-150.
- [Leppänen, 2015] J. Leppänen, M. Pusa, T. Viitanen, V. Valtavirta, T. Kaltiaisenaho, The Serpent Monte Carlo code: Status, development and applications in 2013, *Annals of Nuclear Energy* 82 (2015) 142-150.
- [MCSEN, 1996] R.L. Perel, J.J. Wagschal, Y. Yeivin, “Monte Carlo Calculation of Point-Detector Sensitivities to Material Parameters”, *Nuclear Science and Engineering*, 124 (1), 197–209 (1996)
- [Mennerdahl, 2020] D. Mennerdahl, KRITZ-1-MK Critical Measurements at temperatures from 20 °C to 250 °C, *PHYSOR2020* (2021)
- [Mention, 2011] G. Mention et al., *Phys. Rev. D* 83, 073006 (2011).
- [ND2022/TAR, 2022] Oscar Cabellos, Mathieu Hursin, and Pino Palmiotti on behalf SG46 members, WPEC/SG46 Exercise on Target Accuracy Requirement, 15th International Conference on Nuclear Data for Science and Technology (ND2022), 25-30 July 2022 (to be published in EPJ Web of Conferences) (video - conference)
- [Nichols, 2023] A. L. Nichols et al., Improving Fission-product Decay Data for Reactor Applications: Part I -Decay Heat, accepted in *Eur. Phys. J. A* (2023).
- [NJOY 21] NJOY21—NJOY for the 21st Century. <https://www.njoy21.io>. (accessed on 28 September 2022).
- [NJOY, 2016] D. W. Muir, R.M. Boicourt, A.C. Kahler, J.L. Conlin, W. Haeck, “The NJOY Nuclear Data Processing System - Version 2016,” LA-UR-17-20093, pp. 1-816, <https://github.com/njoy/NJOY2016-manual/raw/master/njoy16.pdf>, 2019.
- [NJOY, 2016] D. W. Muir, R.M. Boicourt, A.C. Kahler, J.L. Conlin, W. Haeck, “The NJOY Nuclear Data Processing System - Version 2016,” LA-UR-17-20093, pp. 1-816, <https://github.com/njoy/NJOY2016-manual/raw/master/njoy16.pdf>, 2019.
- [Park, 2012] H. J. Park, H. J. Shim, C. H. Kim, Uncertainty Propagation Analysis for PWR Burnup Pin-Cell Benchmark by Monte Carlo Code McCARD, *Science and Technology of Nuclear Installations* 2012 (616253) (2012).

- [Park, 2018] H. J. Park, Validation of Uncertainty Propagation Formulation in Monte Carlo Burnup Analysis by Direct Stochastic Sampling Method, Transactions of the Korean Nuclear Society Virtual Autumn Meeting (December 17-18).
- [Plompen, 2020] A. Plompen et al., The joint evaluated fission and fusion nuclear data library, JEFF-3.3, Eur. Phys. J. A 56, 181 (2020)
- [Rearden, 2018] B.T. Rearden, M.A. Jesse, SCALE Code System Version 6.2.3, ORNL/TM-2005/39 (2018)
- [Rice, 2017] S. Rice et al., Phys. Rev. C 96, 014320 (2017).
- [SANDY] <https://github.com/luca-fiorito-11/sandy>
- [SCALE, 2020] W. A. Wieselquist, R. A. Lefebvre, M. A. Jessee, Editors: SCALE Code System, ORNL/TM-2005/39, Version 6.2.4 (April 2020)
- [Schmidt, 2021] K.-H. Schmidt, M. Estienne, M. Fallot et al. Nuclear Data Sheets Volume 173, (2021), Pages 54-117, <https://doi.org/10.1016/j.nds.2021.04.004>
- [SG46/Cov, December 2021] O. Cabellos, Processing covariances for WPEC/SG46 TAR Exercise, WPEC/SG46 Meeting, December 7, 2021 (video - conference)
- [SG46/CSEWG, November 2021] O. Cabellos, WPEC/SG46 TAR exercise: Preliminary Results, virtual meeting CSEWG - Covariance Session, November 15, 2021 (video -conference)
- [SG46/TAR, December 2021] O. Cabellos, WPEC/SG46 TAR exercise: Preliminary Results, WPEC/SG46 Meeting, December 7, 2021 (video - conference)
- [SG47, December 2020] O. Cabellos, Remarks on LLNL pulsed sphere work, WPEC/SG47 December 7, 2020, (video - conference)
- [SG47, June 2019] O. Cabellos, UPM contribution to WPEC/SG47, WPEC/SG47 June 24, 2019. OECD/NEA Headquarters, Boulogne-Billancourt, France (in-person)
- [SG47, May 2021] O. Cabellos, Remarks on LLNL pulsed sphere work (part II), WPEC/SG47 May 11, 2021 (video - conference)
- [Valencia, 2017] E. Valencia et al., Phys. Rev. C 95, 024320 (2017)
- [Werner 2017] C. J. Werner (Ed.), MCNP User's Manual. Code Version 6.2. Los Alamos National Laboratory Report LA-UR-17-29981 (2017).
- [Wiarda, 2016] D. Wiarda et al., AMPX-6: A Modular Code System for Processing ENDF/B, ORNL/TM-2016/43 (2016)

Appendix 1. Presentations/Contributions related to AMPX Processing

Spanish Annual Meeting -SNE2021

- [1] [Bécares 2020b] V. Bécares et al., Processing the unresolved resonances of neutron cross sections with the AMPX and NJOY codes. In virtual meeting of the Spanish Nuclear Society, 16-19 November 2020.
- [2] [SNE 2021] A. Jiménez-Carrascosa, O. Cabellos, C.J. Díez, N. García-Herranz, Processing of JEFF nuclear data libraries for the SCALE Code System, 46ª Reunión Anual Sociedad Nuclear Española, October 6-8, 2021 **(in -person)**
- [3] [Bécares 2020b] V. Bécares et al., Processing the unresolved resonances of neutron cross sections with the AMPX and NJOY codes. In virtual meeting of the Spanish Nuclear Society, 16-19 November 2020.

JEFF Meetings in JEFF Nuclear Data Week

- [4] [JEFDOC-2107] A. Jiménez-Carrascosa, O. Cabellos, C.J. Díez, N. García-Herranz, Processing of JEFF nuclear data libraries for the SCALE Code System, JEFF Nuclear Data Week, November 22-26, 2021, JEFDOC-2107 **(video - conference)**
- [5] [JEFDOC-2144] A. Jiménez-Carrascosa, O. Cabellos, N. García-Herranz, C.J. Díez. Processing and benchmarking of JEFF-4T1 library in the frame of the SCALE Code System, JEFF Nuclear Data Week, April 25-29, 2022, JEFDOC-2144 **(video - conference)**
- [6] [JEFDOC-2091] O. Cabellos et al., *Testing of the JEFF-3.3 with IRPhEP/LWR KRITZ Benchmarks*, OECD/NEA JEFDOC-2091 (2021) **(in-person)**
- [7] [JEFDOC-2097] A. Jiménez-Carrascosa et al., *Impact of Doppler calculations in SEFOR benchmark due to the differences between JEFF-3.3 and JEFF-3.1.1*, OECD/NEA JEFDOC-2097 (2021) **(video - conference)**

International Conference - ND2022

- [8] [ND2022/AMPX, 2022] A. Jiménez-Carrascosa, O. Cabellos, C.J. Díez, N. García-Herranz, Processing of JEFF nuclear data libraries for the SCALE Code System and testing with criticality benchmark experiments, 15th International Conference on Nuclear Data for Science and Technology (ND2022), 25-30 July 2022 (to be published in EPJ Web of Conferences) **(video - conference)**

Dissemination Activities

- [9] [AMPX/Revista SNE, 2021] A. Jiménez-Carrascosa, N. García-Herranz, O. Cabellos, Capacidades del Sistema de Códigos SCALE para el Análisis de Reactores Rápidos Avanzados, Revista Nuclear España, December 2021 **(this paper explicitly mentioned the work performed in SANDA for processing librarires in AMPX format)**
<https://www.revistanuclear.es/wp-content/uploads/2021/12/Art.-UPM.pdf>

NEA DATA BANK COMPUTER PROGRAM SERVICE

- [10] NEA-1927 ZZ-AMPXJEFF3.1.1-UPM
Z-AMPX-JEFF3.1.1UPM, AMPX-formatted Neutron Cross Section Library and Covariances based on JEFF-3.1.1 (<https://www.oecd-nea.org/tools/abstract/detail/nea-1927/>), which contains a continuous energy neutron cross-section data library based on the JEFF-3.1.1 evaluated nuclear data file for the Monte Carlo codes distributed within SCALE Code System (AMPX format);
- [11] NEA-1928 ZZ-AMPXJEFF3.3-UPM.
ZZ-AMPX-JEFF3.3-UPM, AMPX-formatted Neutron Cross Section Library and Covariances based on JEFF-3.3 (<https://www.oecd-nea.org/tools/abstract/detail/nea-1928/>), which contains the continuous energy neutron cross-section data library based on the JEFF-3.3 evaluated nuclear data file for the Monte Carlo codes distributed within SCALE Code System (AMPX format) and the covariance matrices based on JEFF-3.3 collapsed into two group structures (33- and 7-group) using a weighting spectrum optimised for fast spectrum systems (COVERX format).

Appendix 2. Presentations/Contributions related to Review of Processing Tools

JEFF Meetings in JEFF Nuclear Data Week

- [1] O. Cabellos, “First feedback on using FRENDY for processing of JEFF-3.3.”, April 24, 2019. JEFF-JENDL Bilateral Meeting, NEA Headquarters,
- [2] [JEFDOC-1987] O. Cabellos, “P&V of JEFF-3.3 by using FRENDY code”, JEFF Nuclear Data Week – Nov 2019. NEA Headquarters, Boulogne-Billancourt, France. November 23-26, 2019. JEFDOC-1987 **(in-person)**
- [3] [JEF-CG/Nov. 2020] O. Cabellos, “Criticality Benchmarking: JEFF-4.0T0”, NEA Headquarters (Nov 27-30,2018), JEFF CG, November 2020 **(vide-conference)**
- [4] [JEF/DOC-2041] “JEFF P&V, B&V meeting: Introduction”, O. Cabellos, NEA Headquarters (Nov 27-30,2018), JEFF Meeting, April 29, 2021. JEF/DOC-2041 **(vide-conference)**
- [5] [JEF/DOC-2211, 2022] O. Cabellos, “Processing files with LRF7 option for the reconstruction of the MF4, pros and cons”, JEFF Meeting, November 21-24, 2022 JEF/DOC-2211 **(in-person)**
- [6] [JEF/DOC-2239, 2023] M. Astigarraga, O. Cabellos, “Benchmarking and Validation with JEFF-4T2.2”, JEFF Meeting, April 25-28, 2023 JEF/DOC-2239 **(in-person)**
- [7] [JEF/DOC-2224, 2023] M. González-Torre, O. Cabellos, “Feedbacks on Processing and Verification for JEFF-4T2.2”, JEFF Meeting, April 25-28, 2023 JEF/DOC-2224 **(in-person)**

IAEA Meetings

- [8] [IAEA/TM/Processing, 2019] O. Cabellos, Current activities on Processing and Verification(P&V) at Universidad Politécnica de Madrid (UPM), Technical Meeting on Nuclear Data Processing, IAEA Headquarters, Vienna, Austria. September 23-26, 2019.
- [9] [IAEA/TM/Processing, 2022] O. Cabellos, Processing files with LRF7 option for the reconstruction of the MF4, pros and cons. - User’s point of view –, IAEA Technical Meeting on ND Processing - November 29-December 2, 2022. O. Cabellos (UPM)

Appendix 3. Presentations/Contributions related to Processing and Verification

JEFF Meetings in JEFF Nuclear Data Week

- [1] [JEFDOC-1991] O. Cabellos, “Feedbacks on JEFF-3.3 Evaluation: Uncertainty in keff for some ICSBEP Outliers, PWR Critical Boron Letdown Curve and Additional integral data testing using reaction rates in critical assemblies”, JEFF Meeting, April 2020. JEFDOC-1991 **(video-conference)**
- [2] [JEFDOC-2015] O. Cabellos, M. García-Hormigos, B. Moreno and S. Sánchez-Fernández, “The importance of using different integral benchmarks to provide valuable feedbacks to the evaluation process “JEFF Meeting and JEFF-CG, Nov 2020. JEFDOC-2015 **(video-conference)**.
- [3] [JEFDOC-2041] O. Cabellos, Overview of Processing, Verification and Benchmarking activities at UPM, JEFF Nuclear Data Week, April 28, 2021, JEFDOC-2041 **(video -conference)**
- [4] [JEFDOC-2091] O. Cabellos, A. Jiménez-Carrascosa, N. García-Herranz, G. de Alcázar, Overview of Processing, Testing of the JEFF-3.3 with IRPhEP/LWR KRITZ Benchmarks, JEFF Nuclear Data Week, November 24, 2021, JEFDOC-2091 **(in-person)**

Appendix 4. Presentations/Contributions related to SA and UQ

JEFF Meetings in JEFF Nuclear Data Week

- [1] [JEFDOC-2015] O. Cabellos, M. García-Hormigos, B. Moreno and S. Sánchez-Fernández, “The importance of using different integral benchmarks to provide valuable feedbacks to the evaluation process “JEFF Meeting and JEFF-CG, Nov 2020. JEFDOC-2015 **(video-conference)**.
- [2] [JEF/DOC-2111, 2021] O.Cabellos, “Comparison of Burnup Calculations for ND Validation Activities”, JEFF Nuclear data week, - Depletion Session, November 25, 2021. JEF/DOC-2111 (in-person)

WPEC Meetings

- [3] [SG47, June2019] O. Cabellos, “UPM contribution to WPEC/SG47”, WPEC/SG47, June 24, 2019. OECD/NEA Headquarters, Boulogne-Billancourt, France **(in-person)**
- [4] [SG47, December 2020] O. Cabellos, Remarks on LLNL pulsed sphere work, WPEC/SG47 December 7, 2020 **(video - conference)**
- [5] [SG47, May 2021] O. Cabellos, Remarks on LLNL pulsed sphere work (part II), WPEC/SG47 May 11, 2021 (video - conference)

IAEA Meetings

- [6] [IAEA/INDEN-Actinides, 2020] O. Cabellos, “Indications from integral benchmarks on U-235, U-238 and Pu-239 evaluations”, IAEA CM of the INDEN on Actinide Evaluation in the Resonance Region, 17-19 Nov 2020 (Video-conference)

Appendix 5. Presentations/Contributions related to Processing Covariances

JEFF Meetings in JEFF Nuclear Data Week

- [1] [JEFFDOC-1991] O. Cabellos, “Feedbacks on JEFF-3.3 Evaluation: Uncertainty in keff for some ICSBEP Outliers, PWR Critical Boron Letdown Curve and Additional integral data testing using reaction rates in critical assemblies”, JEFF Meeting, April 2020. JEFFDOC-1991 **(video-conference)**
- [2] [JEFFDOC-2015] O.Cabellos, M. García-Hormigos, B. Moreno and S. Sánchez-Fernández, “The importance of using different integral benchmarks to provide valuable feedbacks to the evaluation process “JEFF Meeting and JEFF-CG, Nov 2020. JEFFDOC-2015 **(video-conference)**
- [3] [JEFFDOC-2062] O. Cabellos, WPEC/SG46 TAR exercise: Preliminary Results, JEFF Nuclear Data Week, November 22, 2021, JEFFDOC-2062 **(in-person)**
- [4] [JEFFDOC-2109] O. Cabellos, Processing covariances for WPEC/SG46 TAR Exercise, JEFF Nuclear Data Week, November 22, 2021, JEFFDOC-2109 **(in-person)**

WPEC Meetings

- [5] [SG46/CSEWG, November 2021] O. Cabellos, WPEC/SG46 TAR exercise: Preliminary Results, virtual meeting CSEWG - Covariance Session, November 15, 2021 **(video -conference)**
- [6] [SG46/Cov, December 2021] O. Cabellos, Processing covariances for WPEC/SG46 TAR Exercise, WPEC/SG46 Meeting, December 7, 2021 **(video - conference)**
- [7] [SG46/TAR, December 2021] O. Cabellos, WPEC/SG46 TAR exercise: Preliminary Results, WPEC/SG46 Meeting, December 7, 2021 **(video - conference)**

International Conference - ND2022

- [8] [ND2022/TAR, 2022] Oscar Cabellos, Mathieu Hursin, and Pino Palmiotti on behalf SG46 members, WPEC/SG46 Exercise on Target Accuracy Requirement, 15th International Conference on Nuclear Data for Science and Technology (ND2022), 25-30 July 2022 (to be published in EPJ Web of Conferences) **(video - conference)**